Theses and Dissertations | 1. Thesis and Dissertation Collection, all items

2009-12

Development of a laboratory-scale test facility to investigate armor solutions against buried explosive threats

GarciÌa, Felipe.

Monterey, California: Naval Postgraduate School

http://hdl.handle.net/10945/4453

NAVAL
# POSTGRADUATE
SCHOOL

MONTEREY, CALIFORNIA

THESIS

DEVELOPMENT OF A LABORATORY-SCALE TEST FACILITY TO INVESTIGATE ARMOR SOLUTIONS AGAINST BURIED EXPLOSIVE THREATS

by

Felipe Garcia
December 2009

Thesis Advisor:	Jose O. Sinibaldi
Co-Advisor:	Robert S. Hixson

Approved for public release; distribution is unlimited

THIS PAGE INTENTIONALLY LEFT BLANK

REPORT DOCUMENTATION PAGE			*Form Approved OMB No. 0704-0188*
Public reporting burden for this collection of information is estimated to average 1 hour per response, including the time for reviewing instruction, searching existing data sources, gathering and maintaining the data needed, and completing and reviewing the collection of information. Send comments regarding this burden estimate or any other aspect of this collection of information, including suggestions for reducing this burden, to Washington Headquarters Services, Directorate for Information Operations and Reports, 1215 Jefferson Davis Highway, Suite 1204, Arlington, VA 22202-4302, and to the Office of Management and Budget, Paperwork Reduction Project (0704-0188) Washington DC 20503.			
1. AGENCY USE ONLY	**2. REPORT DATE** December 2009	**3. REPORT TYPE AND DATES COVERED** Master's Thesis	
4. TITLE AND SUBTITLE: Development of a Laboratory-scale Test Facility to Investigate Armor Solutions against Buried Explosive Threats.		**5. FUNDING NUMBERS**	
6. AUTHOR(S) Garcia, Felipe			
7. PERFORMING ORGANIZATION NAME(S) AND ADDRESS(ES) Naval Postgraduate School Monterey, CA 93943-5000		**8. PERFORMING ORGANIZATION REPORT NUMBER**	
9. SPONSORING /MONITORING AGENCY NAME(S) AND ADDRESS(ES) N/A		**10. SPONSORING/MONITORING AGENCY REPORT NUMBER**	
11. SUPPLEMENTARY NOTES The views expressed in this thesis are those of the author and do not reflect the official policy or position of the Department of Defense or the U.S. Government.			
12a. DISTRIBUTION / AVAILABILITY STATEMENT Approved for public release; distribution is unlimited		**12b. DISTRIBUTION CODE A**	

13. ABSTRACT (200 words)

The purpose of this study was to drive a planar shock wave into a layer of sand for use in armor effectiveness studies.

We proposed to use an explosively-driven flyer plate to impact the sand layer and launch a shock wave. In detail our concept is to use a slanted flyer plate, with an explosive layer underneath it, and accelerate the flyer plate by detonating the explosive. As the resulting detonation wave runs through the explosive layer, it pushes the flyer plate. If all the geometry is carefully designed and the flyer plate/explosive layers are precisely positioned, we will produce a flat flyer plate that travels on the order of 1 to 2 km/s towards a layer of sand. The subsequent impact will generate a shock wave within the sand that will eventually accelerate the sand with a flat top profile towards the intended target, thus achieving a flat sand-loading profile on the target.

Success in these experiments will allow us to be able to test various armor designs for effectiveness in mitigating this threat. Since our experiments are done on a laboratory scale, armor testing can be done in a timely and cost-effective manner.

14. SUBJECT TERMS Flyer plate, Nitromethane, blast wave, loading profile.			**15. NUMBER OF PAGES** 141
			16. PRICE CODE
17. SECURITY CLASSIFICATION OF REPORT Unclassified	**18. SECURITY CLASSIFICATION OF THIS PAGE** Unclassified	**19. SECURITY CLASSIFICATION OF ABSTRACT** Unclassified	**20. LIMITATION OF ABSTRACT** UU

NSN 7540-01-280-5500

Standard Form 298 (Rev. 2-89)
Prescribed by ANSI Std. 239-18

THIS PAGE INTENTIONALLY LEFT BLANK

**DEVELOPMENT OF A LABORATORY-SCALE TEST FACILITY
TO INVESTIGATE ARMOR SOLUTIONS AGAINST
BURIED EXPLOSIVE THREATS**

Felipe García
Lieutenant Commander, Mexican Navy
B.S., Mexican Naval Academy, 1991

Submitted in partial fulfillment of the
requirements for the degree of

MASTER OF SCIENCE IN APPLIED PHYSICS

from the

**NAVAL POSTGRADUATE SCHOOL
December 2009**

Author: Felipe Garcia

Approved by: Jose O. Sinibaldi
                Thesis Advisor

                Robert S. Hixson
                Co-Advisor

                Andres Larraza
                Chairman, Department of Physics

THIS PAGE INTENTIONALLY LEFT BLANK

ABSTRACT

The purpose of this study was to drive a planar shock wave into a layer of sand for use in armor effectiveness studies.

We proposed to use an explosively-driven flyer plate to impact the sand layer and launch a shock wave. In detail, our concept is to use a slanted flyer plate, with an explosive layer underneath it, and accelerate the flyer plate by detonating the explosive. As the resulting *detonation* wave runs through the explosive layer, it pushes the flyer plate. If all the geometry is carefully designed and the flyer plate/explosive layers are precisely positioned, we will produce a flat flyer plate that travels on the order of 1 to 2 km/s toward a layer of sand. The subsequent impact will generate a shock wave within the sand that will eventually accelerate the sand with a flat top profile toward the intended target, thus achieving a flat sand-loading profile on the target.

Success in these experiments will allow us to be able to test various armor designs for effectiveness in mitigating this threat. Since our experiments are done on a laboratory scale, armor testing can be done in a timely and cost-effective manner.

THIS PAGE INTENTIONALLY LEFT BLANK

TABLE OF CONTENTS

LIST OF FIGURES

LIST OF TABLES

THIS PAGE INTENTIONALLY LEFT BLANK

LIST OF ACRONYMS AND ABBREVIATIONS

LSTF	Laboratory-scale Test Facility
CC	Conical Charge
FP	Flyer Plate
HVSB	High Velocity Sand Blast
HE	High Explosive
NM	Nitromethane
DETA	Diethylenetriamine
COTS	Commercial off-the-shelf
RPG	Rocket Propelled Grenade
EVD	Explosive Vehicle Device
IED	Improvised Explosive Device
TBI	Traumatic Brain Injuries
GTV	Ground Tactical Vehicle
Kg	Kilogram
gr	Gram
Km	Kilometer
m	Meter
mm	Millimeter
in	Inches
s	Second
µs	Microsecond
mL.	Milliliter
Km/s	Kilometers per Second

m/s	Meters per seconds
g/cc	Grams per cubic centimeter
GPa	Giga Pascal
J	Joules
CAD	Computer-aided Design
FEM	Finite Element Method
FDM	Finite Difference Method
EOS	Equation of State
2D	Two Dimensional
3D	Three Dimensional
fps	Frames per second
V	Volts
SOP	Standard Operation Procedure
STP	Standard Temperature and Pressure
CMOS	Complementary metal–oxide–semiconductor

ACKNOWLEDGMENTS

THIS PAGE INTENTIONALLY LEFT BLANK

EXECUTIVE SUMMARY

Design and validation of various structures against ballistic impacts and blast loads are important for modern society to protect and secure its citizens. Since it is difficult, expensive and often impossible to validate and optimize protective structures or vital infrastructure against blast loads using full-scale experimental tests, we have to turn our attention towards the development of a Laboratory-scale Test Facility (LSTF).

This thesis summarizes the design of a laboratory-scale explosive device as a valuable tool for armor design optimization. Examples are presented showing a good agreement between computational and experimental results addressing the effects of High Velocity Sand Blast (HVSB).

This work is based on fundamental shock physics theory aided by software based on hydrodynamic codes (commercial off-the-shelf [COTS] software AUTODYN [1]) to simulate the explosive detonation and flyer plate projectile. This computer code was used to design and optimize computationally the experimental setup. Once the experimental designs were optimized, several experimental setups were fabricated and tested to measure plate velocities and resulting sand-loading profiles.

Success in this small-scale testing approach will allow more cost-effective testing of advanced armor concepts against simulated buried explosive threats. This will in turn provide essential data for validation for numerical codes used to perform optimization of novel armor designs at relatively low cost.

The LSTF reduces the complexity and cost of this kind of experimentation, and allows the use of COTS components. Additionally, the shorter construction timeline is ideal for educational institutions where students can also participate in the design, construction and testing, thus obtaining the full educational experience.

THIS PAGE INTENTIONALLY LEFT BLANK

I.   INTRODUCTION

In Operation Iraqi Freedom and Operation Enduring Freedom in Afghanistan, Rocket Propelled Grenades (RPG), buried mines, Improvised Explosive Devices (IEDs), and small arms fire have been responsible for over 30% of Marine Corps Traumatic Brain Injuries (TBI) level III and IV casualties [2].

Of particular concern are the dynamic phenomena that occur in a land mine blast and the interactions between the detonation products and sand (soil). This causes sand ejecta to impact armor on vehicles, and so mine survivability is an important subject related to the design and manufacture of Ground Tactical Vehicles (GTV). Such interactions have resulted in vehicle damage/destruction through mechanisms that are currently poorly understood. Normally, enhanced mine survivability of the GTVs is attained through the use of heavier armor.

Existing GTVs have been shown not to have the survivability required to support and sustain operations on the modern battlefield. This has led to efforts to redesign the armor protection systems on existing vehicles, or to design new vehicles. The development of effective mine protection systems for armored vehicles requires a comprehensive understanding of two distinct groups of phenomena:

- Detonation of high-energy explosive mines buried in soil, and the resulting vertical acceleration of the emplacement soil/sand.

- Interaction of the ejected soil with the target (armor).

Recent experiences show that the main damage mechanism for GTVs is not the shock wave overpressure in air, but rather the high velocity sand particles impacting the vehicle armor. A single grain of sand would not cause much damage, but when 5,000,000 grains are hurled at high velocity against a surface, the effect is noticeable.

The Laboratory-scale Test Facility (LSTF) gives us the opportunity to investigate different armor loading conditions and measure damage in a reproducible way.

Since personnel safety is crucial in operations where buried mines and IEDs pose a threat, the insights gained in this work will help a better understanding of how to develop better protection systems.

A.   LSTF CONCEPT AND RESEARCH GOAL

Detonation of an explosive device buried in soil is typically considered to consist of three different phases:

1.   The detonation wave/soil interaction phase;

2.   The gaseous detonation products expansion phase;

3.   The detonation-products/vehicle and soil-ejecta/vehicle interaction phase.

This work is focused on the last phase where High Velocity Sand Blast (HVSB) creates two main dynamic loading mechanisms, which are typically considered as: (a) short-duration concentrated impact loading resulting from the interaction of the ejected soil plug and the air blast wave against the target structure; and (b) long duration distributed dynamic loading dominated by the interactions between later time soil ejecta and the target structure [3].

This LSTF will address the effects of HVSB and allow the use of a flat sand-loading profile as required for code validation purposes. The areas to be specifically investigated are shock propagation through sand and the resultant sand dispersion.

The goal of this thesis research is focused on the development of a LSTF to investigate how the HVSB conditions can be reproduced in a safe environment. The ultimate goal is to develop the LSTF as a tool for generating well-defined sand impacts upon various materials in a reproducible and

controllable manner. It is important to mention that the use of the LSTF was appealing because of the simplicity of equipment required.

B.   BENEFITS OF THE THESIS STUDY

The LSTF reduces the complexity and cost of this kind of experimentation by use of a simple and direct experimental design that uses many off the shelf components. Additionally, this approach allows for a shorter construction timeline, which is ideal for educational institutions and allows students to participate in the design, construction, and testing.

The data in turn will be used to constrain new physics models that in turn will be used to design new protection systems for GTVs.

C.   OBJECTIVES AND OVERALL TECHNICAL APPROACH

This LSTF provides a simple way to constrain numerical computer codes that will be used to perform optimization of novel armor designs at relatively low cost. Because there is a clear need for this kind of data, our work supports future research efforts in this area.

The purpose of developing a LSTF to study HVSB:

- HVSBs can be a serious hazard for all vehicles, but especially GTVs.

- This research helps to assess the risk of high-speed debris impacting GTVs.

- Developing new materials and designs from HVSB data will ultimately allow better armor systems to be developed to protect tactical vehicles from the HVSB in the war environment.

Researchers working in this area have a need for a cost effective and simple experimental platform such as the LSTF to provide critical data. Our initial research objectives are:

3

- Design an LSTF to reproduce HVSB conditions in a safe environment.

- Create a database of sand impact velocity vs. damage for future impact studies.

- Develop a framework using computational dynamics to gain more insight into the complex phenomena accompanying detonation of a buried mine or IED.

- Provide high fidelity measurements of the dynamic parameters required for calibration and development of numerical models for sand ejected by an explosive device.

- Use the resulting computational models to allow the future design of higher performance armor systems made out of advanced composite structures.

D.   THESIS OVERVIEW

This research was based on fundamental shock physics concepts to simulate soil ejected from a buried explosive device. Initial calculations indicated that the concept was feasible. Detailed numerical simulations were then done and, lastly, experimentation studies were performed to provide the data required to validate modeling efforts. Our results will be described as follows:

Chapter II provides a description, background and concept of the LSTF and Conical Charge (CC). It also outlines specifications required to select components for their design.

Chapter III contains an explanation of the design and construction of the computational simulations.

Chapter IV describes the design and construction of the LSTF and CC.

Chapter V documents the experimental setup and procedure.

Chapter VI gives predictions using hydrocodes, which will be compared against experiments.

Chapter VII provides thesis recommendations and conclusions.

The last section consists of appendices containing information that supports the technical discussion presented in the aforementioned chapters.

THIS PAGE INTENTIONALLY LEFT BLANK

II. LABORATORY-SCALE TEST FACILITY BACKGROUND AND CONCEPT

The goal of this study is the development of an experimental technique capable of "efficiently" generating a flat-loading profile "cloud" of high velocity sand onto intended targets. The techniques considered include a) to use a Flyer Plate (FP) that is explosively driven using the minimum possible amount of energetic material, and b) to use a Conical Charge (CC) at the expense of using larger amounts of energetic material and compare flatness of sand profiles between these two approaches.

Research on blasts from buried explosives is important for understanding the interaction between sand ejected and target and, also, for the development and optimization of blast-resistant materials (armor). Typically, explosive blast tests are conducted on full-scale models to determine the actual material response. Even the smallest of these full-scale tests can require 5–100 kg explosive charges at distances of up to 100 m from the test device, forcing these tests outdoors into relatively uncontrolled environments. At this scale, costs are driven up and time required for tests increases. This research presents a new method for conducting High Velocity Sand Blast (HVSB) experiments in a laboratory-scale test facility (LSTF) in a relatively safe and controlled environment.

A. PROJECT DESIGN

Operational considerations for these tests include keeping the design simple for ease of setup, keeping the amount of High Explosive material (HE) at a minimum to be carried on preferably in an indoor facility, and adjustability to vary flyer plate velocity at impact. The LSTF design can be carried out by any of the two following approaches:

- Computational simulation.

- Empirical methods (experiments).

We have chosen to use a combination of these two approaches.

The design of GTVs with mine survivability characteristics requires the ability to understand and quantify the impulsive loads from land mines and/or IEDs buried in different soil media and the ability to model the response of structures of interest. It is not practical or cost-effective, however, to carry out experimental tests of the response of all kind of targets to buried charges of all sizes in a variety of terrains. Recent advances in numerical analysis (computational simulation capabilities), particularly the coupling of Eulerian solvers (used to model gaseous detonation products and air) and Lagrangian solvers (used to represent vehicles/platforms and soil), have allowed simulations to provide insight into complex loading created by the mine blast event. This means that if we can get the physics in the codes right, we can use simulations to guide a smaller number of experiments.

This study use numerical simulations to obtain the solution of the equations governing the complex interactions between energy release from explosives and shock and blast interactions with the soil. The latter is based on the utilization of numerical codes (hydrocodes) that employ either the Finite Element Method (FEM) or the Finite Difference Method (FDM).

This approach provides large amounts of information and it is widely used for armor design optimization since high-capacity and high-speed computer systems are easily available. Often the use of numerical codes requires dynamic testing of materials involved to derive fundamental constitutive equations to supply to the code. At the end, integral blast testing is required to validate the design.

A quantified understanding of the relevant blast phenomena and through computer modeling, however, is still not complete. This is because of the fact that a planar shock-wave profile and a planar sand-loading profile are needed to properly characterize the codes under development with the currently available materials models to realistically represent the response of panels to HVSB. In

particular, the sand response and its dependence on the sand composition, water content, microstructure, and their self interactions and interactions with targets are poorly understood [4].

Optimum design of LSTF and CC can be achieved by a clever combination of the methods mentioned above. Figure 1 is a rough sketch of the methodology proposed for the first design: the flyer plate technique. Numerical modeling may be effectively useful to obtain a close approximation to the solution, discriminating between a large numbers of variables: materials selection, angles' thicknesses, etc.
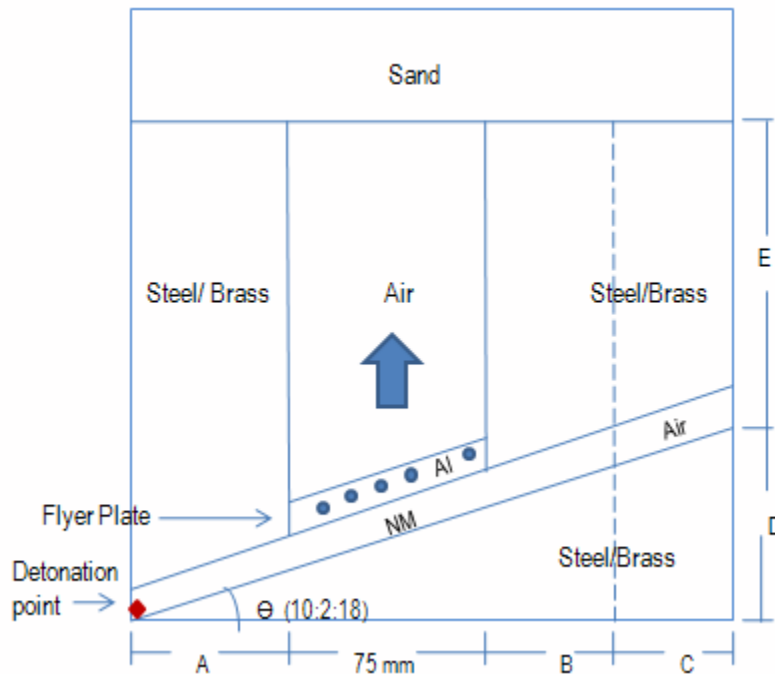
Figure 1.   Flyer plate concept—the LSTF.

Because there is no guarantee that the flyer plate approach would be successful, we worked in parallel on a second approach. Thus, a conical shaped charge (CC) was designed to directly drive the sand. The initial 2D drawing considers the axial symmetry advantage of the computational simulation, as shown in Figure 2.
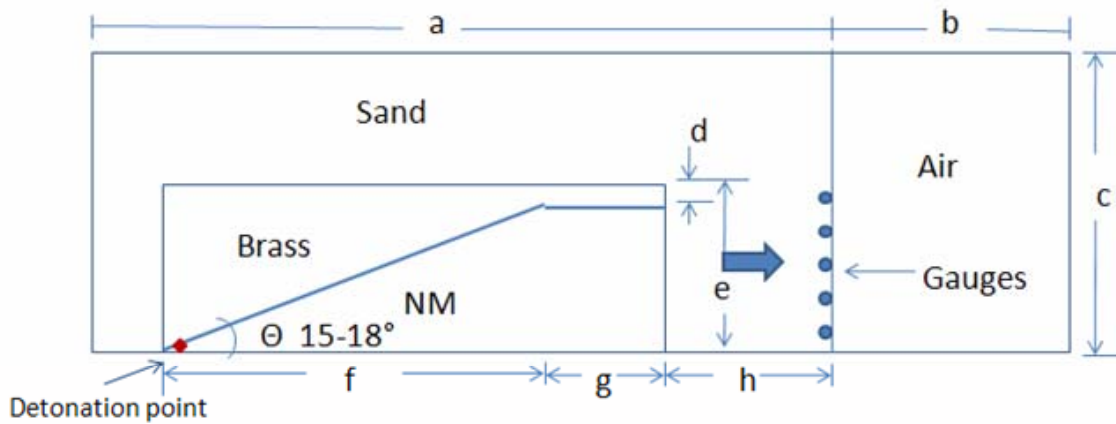
Figure 2.   Conical shaped charge concept.

Conducting blast loading research, even with small explosive systems, requires controlled surroundings. For this reason, we constructed a test chamber design to contain the main detonation event, as shown below in Figure 3. This design has an opening at the top to allow the ejected sand to interact with target plates and vertical pendulum systems or other sensor devices.
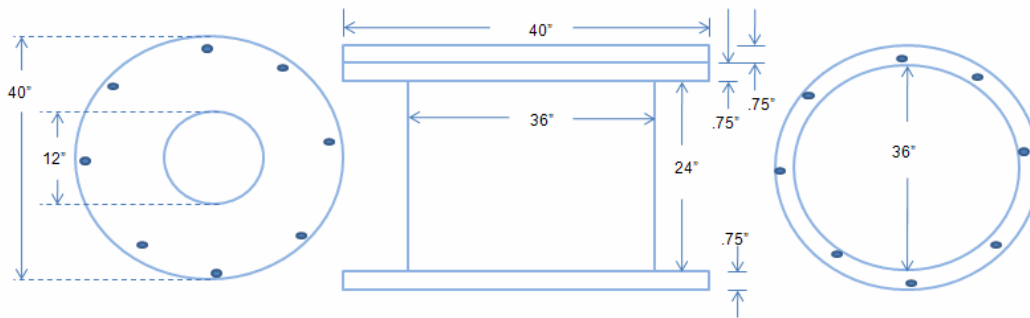
Figure 3.   Test chamber design.

After an overview of the LSTF is presented in this chapter. Chapter III gives an overview of LSTF Computational Simulation considering both: 1) flyer plate and 2) conical charge designs.

III. COMPUTATIONAL SIMULATION

This work, based on fundamental shock physics theory, was aided by hydrodynamic computer codes. The computational simulations performed were very helpful in predicting experimental results prior to testing the flyer plate and conical charge experimental techniques. This, in turn, allows the proper set-up of high-speed diagnostics to be done in advance.

Appendix A summarizes the Equation of State (EOS), strength model, failure model, and erosion criteria for the materials used in the simulations.

Numerical simulation analyses and experimentation were conducted to be able to assess critical aspects of the proposed concept. Approaches used in this work are reported in Section A and results are reported in Section B.

A. SIMULATION TECHNICAL APPROACH

The computer simulations will yield deformation contours for both kinds of experimental assemblies. Both computational simulations were done using the AUTODYN® hydrocode. The resulting pressure and/or velocity contours will be compared with deformation contours derived directly from experimental tests. In the LSTF tests, a steel-flyer plate was used for most tests, but a limited number of other materials were also used. Steel was preferred, however, due to its high density. For CC tests, brass was chosen for container material and Teflon® for the cap material on simulations.

AUTODYN® Lagrange and Euler Processors[1] are part of a multi-dimensional multi-material finite difference code. It was developed by Century Dynamics Inc., and used in this research. AUTODYN® is an engineering and scientific tool for solving complex non-linear dynamic problems, such as shock and blast waves, detonations, impact and penetration, and solid, fluid and gas dynamics. It offers many finite-difference solvers, such as Lagrange, Euler,

---

[1] The description of the AUTODYN Code is taken from instructional notes and documentation furnished by Century Dynamics.

Arbitrary Lagrange Euler and a mesh-free Smooth Particle Hydrodynamics (SPH) capability and coupling between these techniques and material physics. This type of program is sometimes referred to as a "hydrocode."

The 2D axial symmetric simulation setup is the simplest form that can be used to model problems in which there is cylindrical symmetry. Models are symmetrical about a single axis thus giving it a cylindrical symmetry. This form of setup also causes the simulation to be computed in a shorter time period when compared to fully 3D cases.

The Eulerian processor was selected because it is more ideally suited for handling large deformations and fluid flow. It is more difficult, however, to track free surfaces, material interfaces, and history-dependant material behavior. The Lagrange solver is well suited for the description of solid materials. It produces a mesh grid that overlays and moves with the material. In this case, the grid is continually deformed and refined during the simulation. Differing zoning setups can affect the fidelity of the numerical results. Coarser zoning causes lower fidelity results, but finer zoning causes longer computational times. There is a natural trade off: More zones per millimeter allow for higher fidelity simulations, but this is at the expense of very long computation time and memory usage. Coarse zoning may cause some fine details to be lost.

Gauges, set with predetermined fixed points within a particular computation space, measure and record the data that moves over the gauges. The use of gauges allows particular points in the materials used to be closely examined for stress, strain, and other relevant dynamic properties. In this simulation, gauges were used to obtain the velocity and pressure of the shock waves propagating through the target. The information obtained from these gauges was used to keep track of wave propagation and attenuation.

Geometric symmetries were exploited to decrease computational times as mentioned above. Material models for the flyer plate, air, sand (soil) and nitromethane (the energetic material) are defined in Appendix A.

12

1. **Flyer Plate Design**

The formulation of this computational problem deals with the detonation products, flyer plate (FP) and soil ejecta (all resulting from the explosion of the Nitromethane (NM) slanted case). Results are presented in this section.

a. Simulation Setup

- A progressive set of simulations were performed varying parameters that affect the sand profile:

- FP initial angle: This problem was overcome by slanting the ramp at many different angles, but the best results were obtained with a 14.5° ramp.

- FP construction material: Lightweight construction materials such as aluminum responded well to the expanding drive gases, but deformed substantially when hitting the walls. Simulations using steel 1006 were also considered with better behavior and less deformation, however, with a 30% reduction on flyer plate velocity. The best results were obtained by using steel 4340

- Thickness of the adjacent walls: Not only the thickness, but the shape of the walls made a big difference between simulations: the initial gases expanding made the design of the left wall difficult and played a big role in preserving the flat shape of the flyer plate.

- Material of the adjacent walls: Using low density materials provided less confinement; thus, results showed lower flyer plate velocities. In addition, these walls tended to "catch" the flyer plate and ruined the flat profile.

- Hydraulic and/or pneumatic dampers: Compressed gases bouncing inside the exhaust tunnel (see Figures 7, 8, and 9) help in some simulations to maintain the desired shape of the ends of the plate. The control of the center portion, however, was not affected much.

- Gases exhaust tunnel for pressure release: Heavy plates run slower and the drive pressure behind them stays relatively high, causing premature deformation (before reaching their high velocity). The solution was to build an exhaust port to allow gases to escape (expand) in a direction away from the flyer plate, thus keeping pressures lower behind the flyer plate and preventing undesired deformation (see Figures 9, 14, 15, and 16).

- Detonation point: By moving the detonation point along the layer of NM, different responses of the FP were obtained. The impact on the final profile was so small that the position of the detonation point was moved to the most practical location (see Figures 9, 10, 11, 12, 13, and 14).

Out-flow boundary conditions were applied to the up and side free faces of the Euler domain except for the down face (base). Several gauge points were defined within the FP and sand (upper and lower layers), which allowed monitoring of data such as pressure and velocity.

At the beginning of the simulation, the detonation point is exploded. The (rectangular shape) NM case was detonated on its left side at the beginning of the simulation.

b.   *Modeling Approaches*

The main objective of the simulations was to produce a flat flyer plate impacting a sand layer creating a HVSB with flat profile at velocities around 500-600 m/s. The ultimate aim was to be able to use the final results from the simulations and compare it with data from experimental tests. Therefore this work will be able to calibrate the models used in the hydrocodes to properly simulate target plate (armor) response to impacts with high velocity projectiles (sand debris).

Large sets of simulations were performed to optimize the parameters that affect the desired shape (flat). The FP simulations were performed using Eulerian solvers. The components of the simulation can be identified by the following color code:

- Cyan color indicates air at STP.

- Purple indicates steel 4340 or brass for the inertial confinement structure.

- Green color identifies NM-DETA explosive mixture as energetic material.

- Silver shows steel flyer plate (75 mm square, 5 mm thick).

- Pink was set for sand layer target.
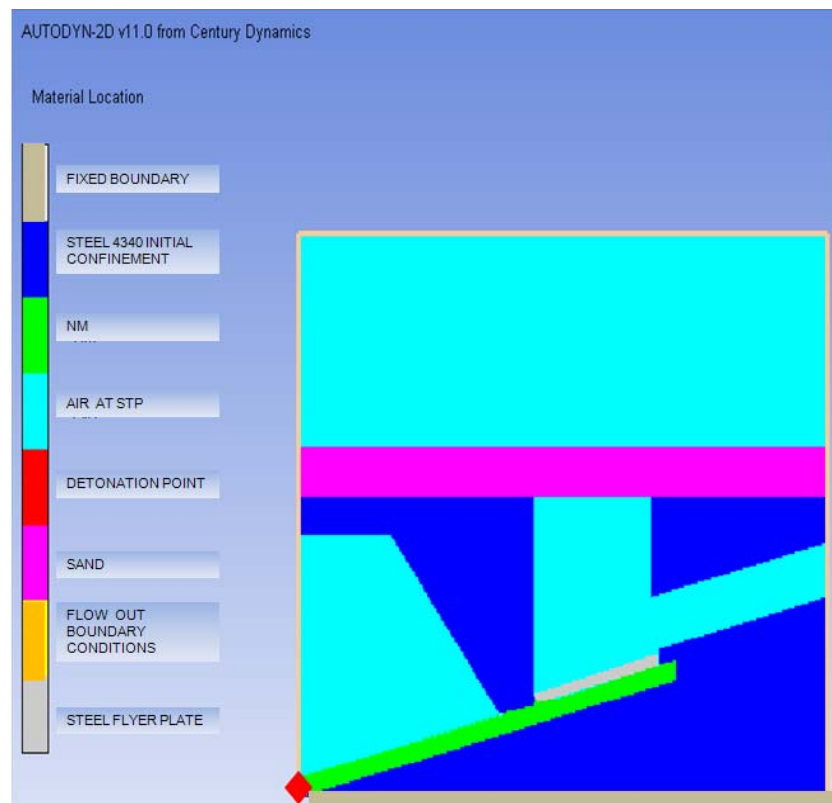
Figure 4.   Laboratory-scale test facility simulation setup and color code as follow: Cyan color indicates air at STP, Purple indicates steel 4340 or brass for the inertial confinement structure, Green color identifies NM-DETA explosive mixture as energetic material, Silver shows steel flyer plate, Pink was set for sand layer target.

2.   Conical Charge Design

In the previous section, we found that some aspects of the LSTF simulation allowed us to be able to better model the CC design.

Our experience with the LSTF simulations served to guide the CC modeling approach successfully.

a.   *Simulation Setup*

The first CC simulations were done with a void at the end of the cone that allowed the HE product gasses to expand easily. The idea was to use this design to also push a flyer plate, which would impact the sand layer and cause it to be accelerated. However, a new design was conceived in which we abandoned the flyer plate approach for this assembly, and instead used the HE product gasses to directly push the sand. We used a progressive set of simulations to determine the correct angle to obtain the most flat sand profile possible.

The new design was arrived at as follows:

- Initial simulations used a FP to impact the sand layer.

- Thickness of the container: the critical part was on the upper edge of the CC.

- Material chosen for the cone: brass, due to its high density, which provides confinement.

- Wall height: it depends mainly on the angle of the CC.

- Detonation point: fixed at the bottom part of the CC.

As shown in Figure 5, the out-flow boundary conditions were applied to the top, left and right sides of the drawing. Several gauge points were defined within the sand, which allowed pressure and velocity to be monitored.

b. Modeling Approaches

Results of the simulations predict that a flat sand profile at velocities around 600-800 m/s will be obtained. The ultimate aim was to be able to use the results from these simulations to compare with data from LSTF tests. Using the results of this comparison, differences between sand flatness and velocity profile can be assessed.

The CC simulation was performed using 2D with axial symmetry. In every simulation, the components on the simulation can be identified by the following color code:

- Cyan color indicated air at STP.

- Purple indicated fixed boundary condition.

- Red showed brass CC container to be filled with explosive.

- Green color identifies NM-DETA explosive mixture as energetic material.

- Beige indicated flow out boundary condition.

- Pink was set for sand layer target.

- Blue showed steel flyer plate.
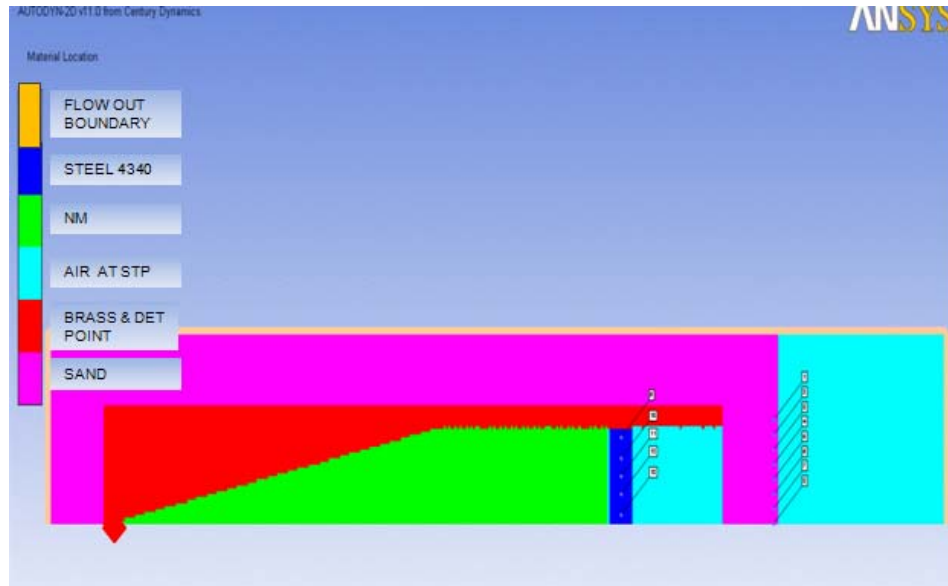
Figure 5. Conical charge simulation setup and color code: Cyan color indicated air at STP, Purple indicated fixed boundary condition, Red showed brass CC container to be filled with explosive, Green color identifies NM-DETA explosive mixture as energetic material, Beige indicated flow out boundary condition, Pink was set for sand layer target, Blue showed steel flyer plate.

B. SIMULATION RESULTS

The computational simulations shown in Figures 6–33 represent part of the different stages of the process to obtain a flat final profile, the circle and the cross inserted were used to the verify the improvement of the flyer plate geometrical shape during the different simulations.

1. Flyer Plate Technique–LSTF

The first set of simulations was conducted using an aluminum flyer plate and a steel 4340 internal confinement. They had exhaust tunnels for gases on expansion to observe the behavior of the FP and calibrate the variables.
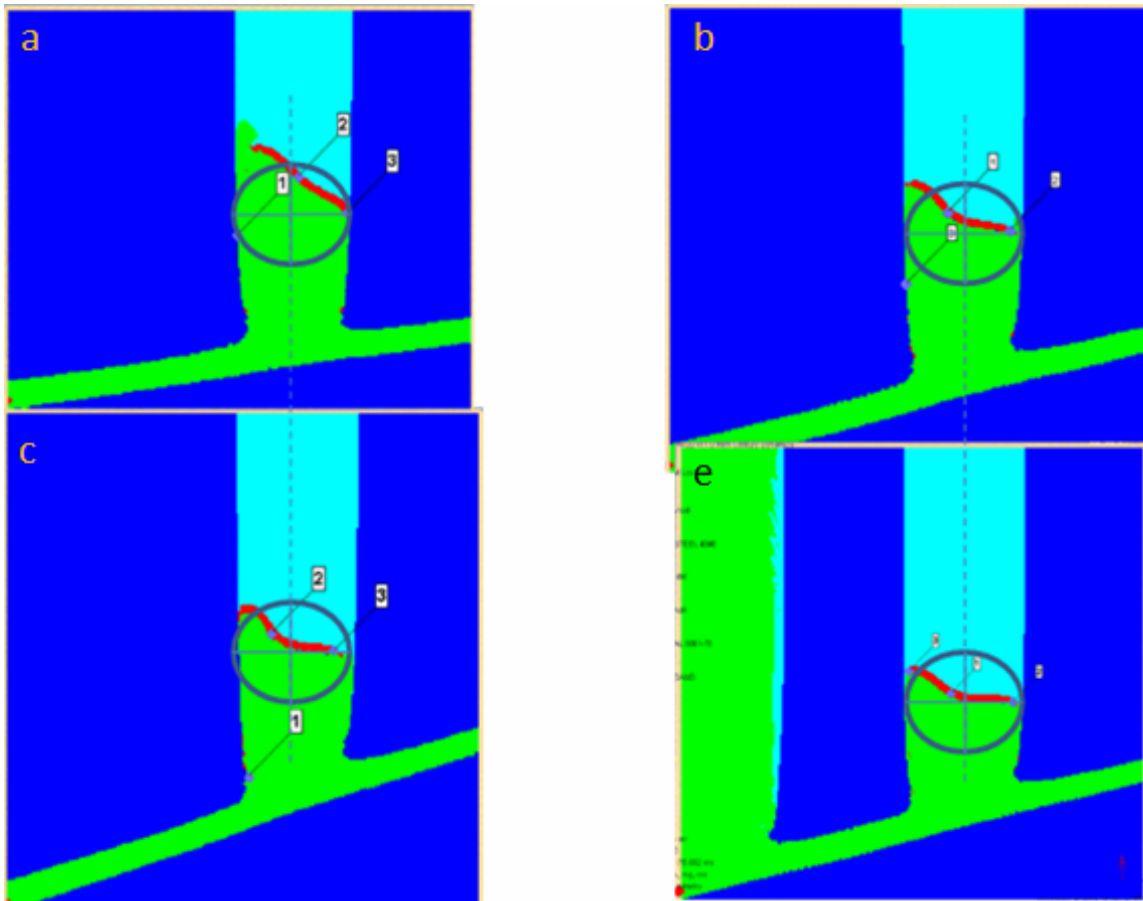
Figure 6.   Initial simulations at different angles of inclination: (a): 08°, (b): 10°, (c): 18°, (d): 14°.

After some failed attempts, an inclination of 14° ramp looked like the best option. Subsequent work was performed using this slope and varying new parameters. Improvements were found. Results are shown in Figure 6.
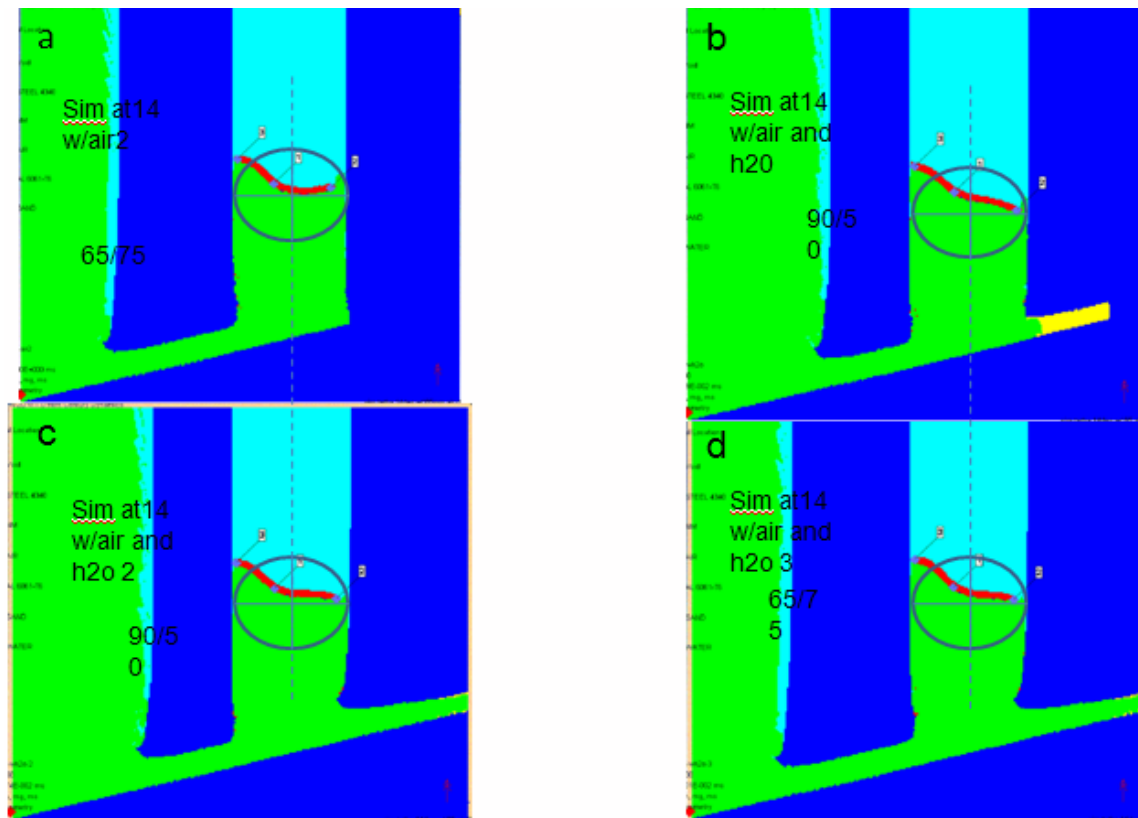
Figure 7.   Simulations changing the walls' thickness: (a): 75 mm,
(b): 50 mm with hydraulic damper, (c): 50 mm,
(d): 75 mm with hydraulic damper.

The hydraulic damper, shown in yellow in Figure 7b, helped control the right tip, but left one still uncontrollable. This damper is simply a column of water used to attenuate the propagating shockwave. Nonetheless, this was not enough to solve the problem completely. The solution was to use a combination of hydraulic and pneumatic damper to lower the left tip of the flyer and obtain a flat flyer plate. The pneumatic damper is shown in light blue in Figure 8d. This damper was made of an air column.
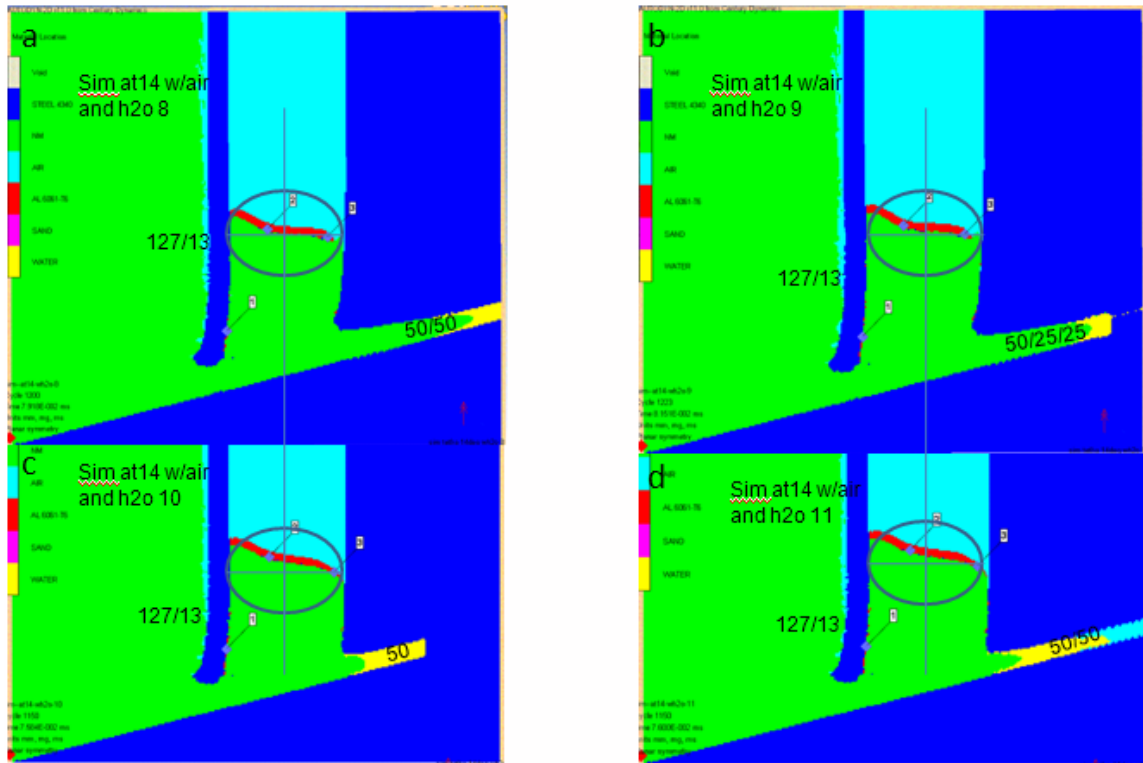
Figure 8.   Simulations adding a combination of dampers (left wall
thickness 13 mm): (a): 50/50 pneumatic-hydraulic,
(b): 25/25 pneumatic-hydraulic, (c): 50/00 hydraulic-pneumatic,
(d): 50/50 hydraulic-pneumatic.

At this stage, the FP left tip was moving in the right direction (lower), but not as much as was required. Therefore, we varied the detonation point next, as shown in Figure 9.
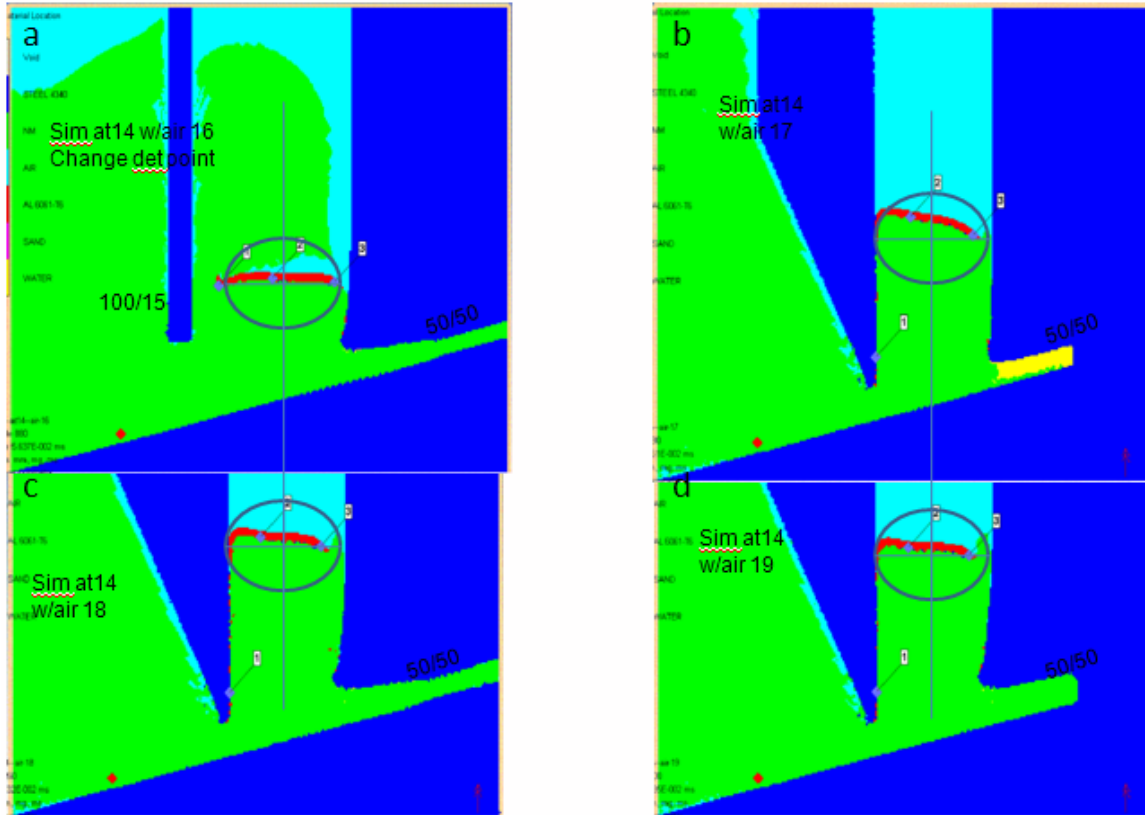
Figure 9.   Simulations varying detonation point (in red) position and combined with different kinds of dampers and wall shape changes: (a): wall thickness 15 mm, 50 mm pneumatic damper with exhaust tunnel, (b): indistinct inclination angle on wall shape and 50 mm hydraulic damper, (c): 50mm hydraulic damper with exhaust tunnel, (d): 50 mm pneumatic damper.

Improved flyer plate shape was obtained, but now we saw a significant deformation in the center of the flyer plate. This also changed the wall inclination angle and thickness. The next option was to vary the ramp slant angle, as shown in Figure 10.

22
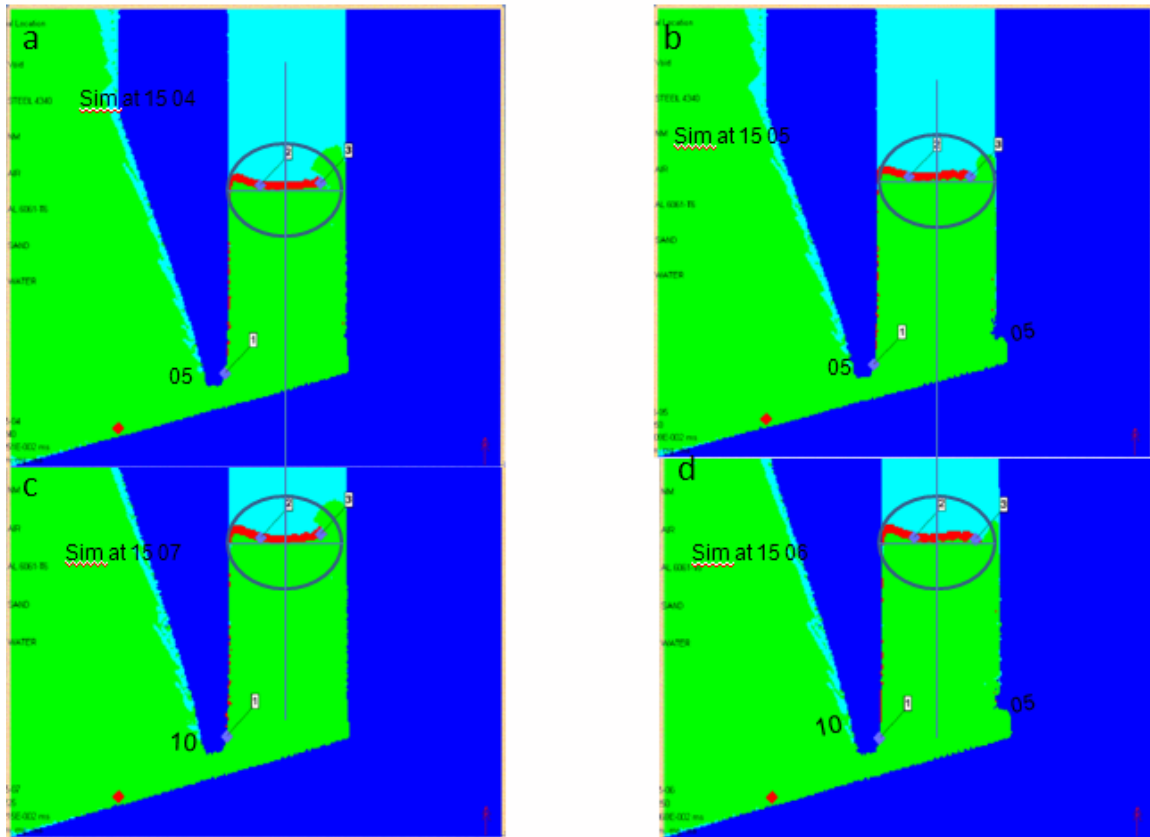
Figure 10.   Simulations without dampers, detonation point same place as before, but slanted angle is now 15°: (a): wall thickness 5 mm with indifferent inclination, (b): same configuration in general but added more space for NM layer, (c): wall thickness 10 mm and no extra NM, (d): 10 mm wall and extra space for NM.

The desired profile is now almost obtained. The plate left tip, however, was still too high and the complete flyer plate was displaced to the left, which caused it to impact the wall and deform. The solution found to correct the problem was to vary the slope of the ramp to 14.5°.
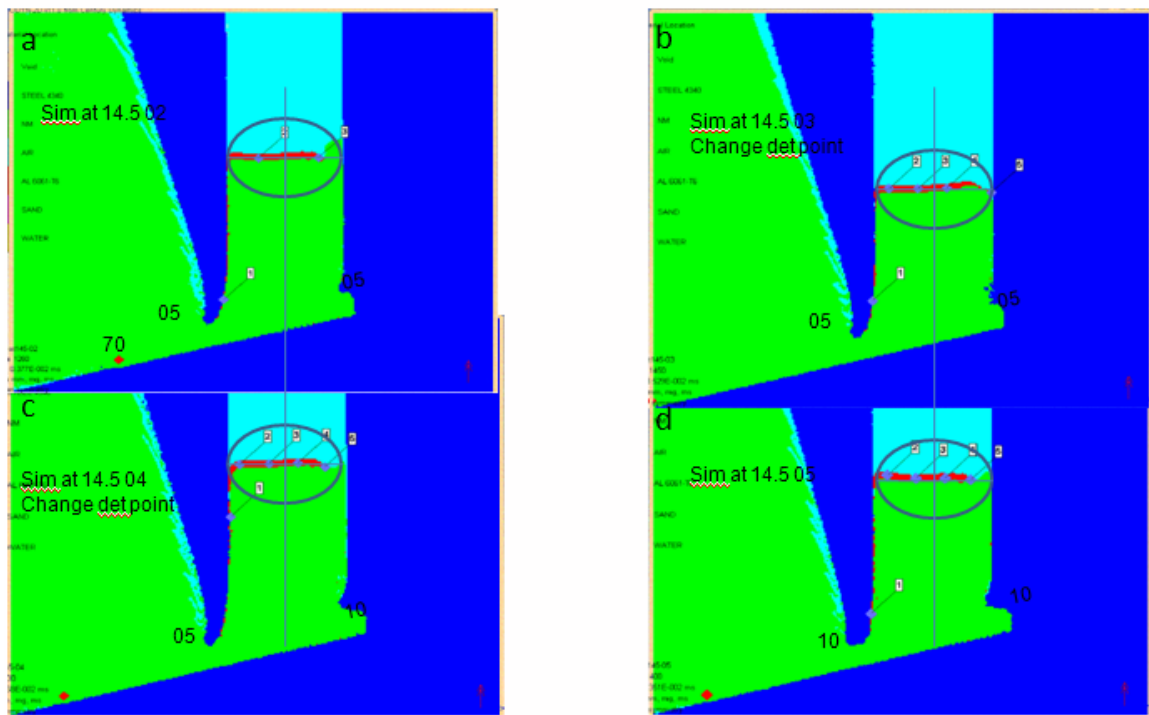
Figure 11.   Simulation with same parameters, but moving detonation point: (a): at 70 mm from origin, (b): at origin, (c): at 35 mm from origin and 10 mm extra space for NM, (d): 10 mm wall and extra space for NM.

A flat flyer plate profile was now obtained, but still with the flyer plate impacted the left containment wall. Using the configuration shown in Figure 11-c, a change of material (and initial density) for the walls was done to look for improved FP behavior.
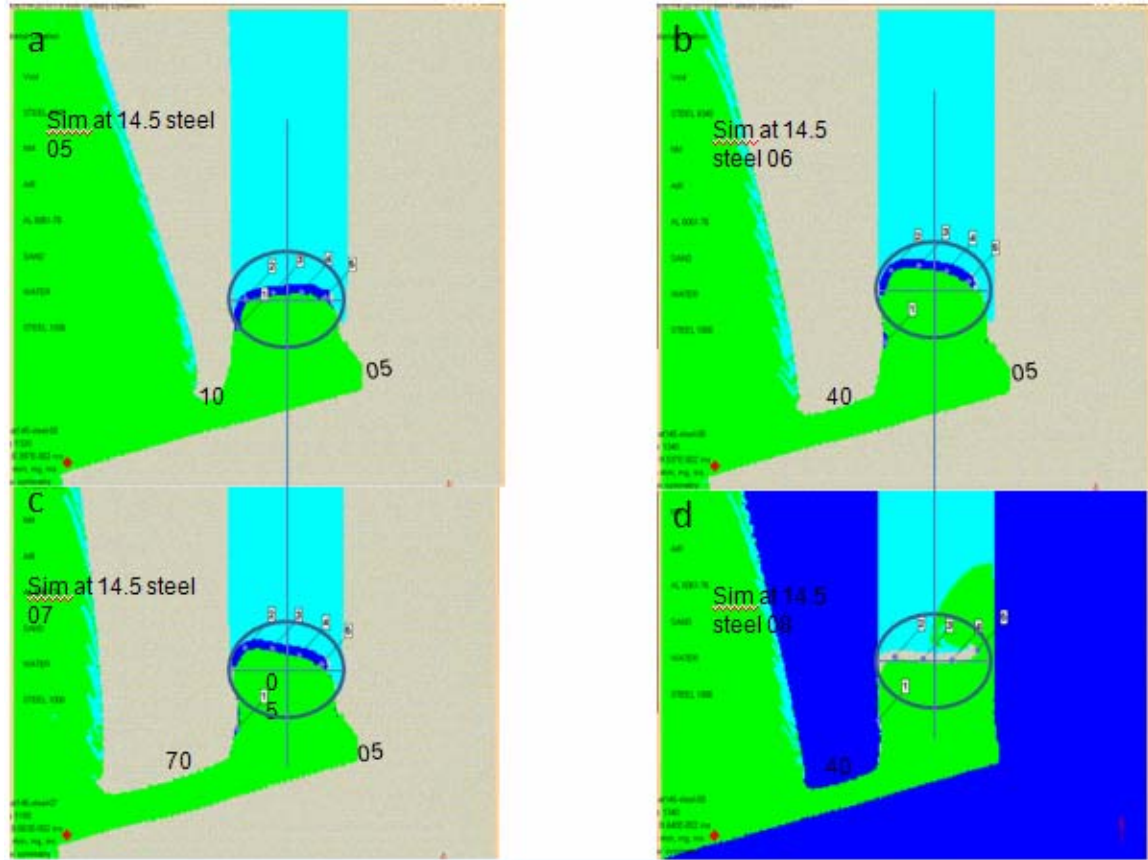
Figure 12.   Simulations changing material density in the internal confinement: (a): steel 4340 FP, (b): increase thickness to 40 mm on left wall, (c): 70 mm thickness, (d): best result switching steel 4340 and steel 1006.

With a slope ramp of 14.5°, walls made of steel 4340 and flyer plate on steel 1006, there was an almost flat flyer plate profile. However, the simulation still shows gases escaping on the FP right tip. The solution found to control this end was to vary the thickness of the left wall and increase the thickness of the NM layer on the right. This is shown in Figure 13.
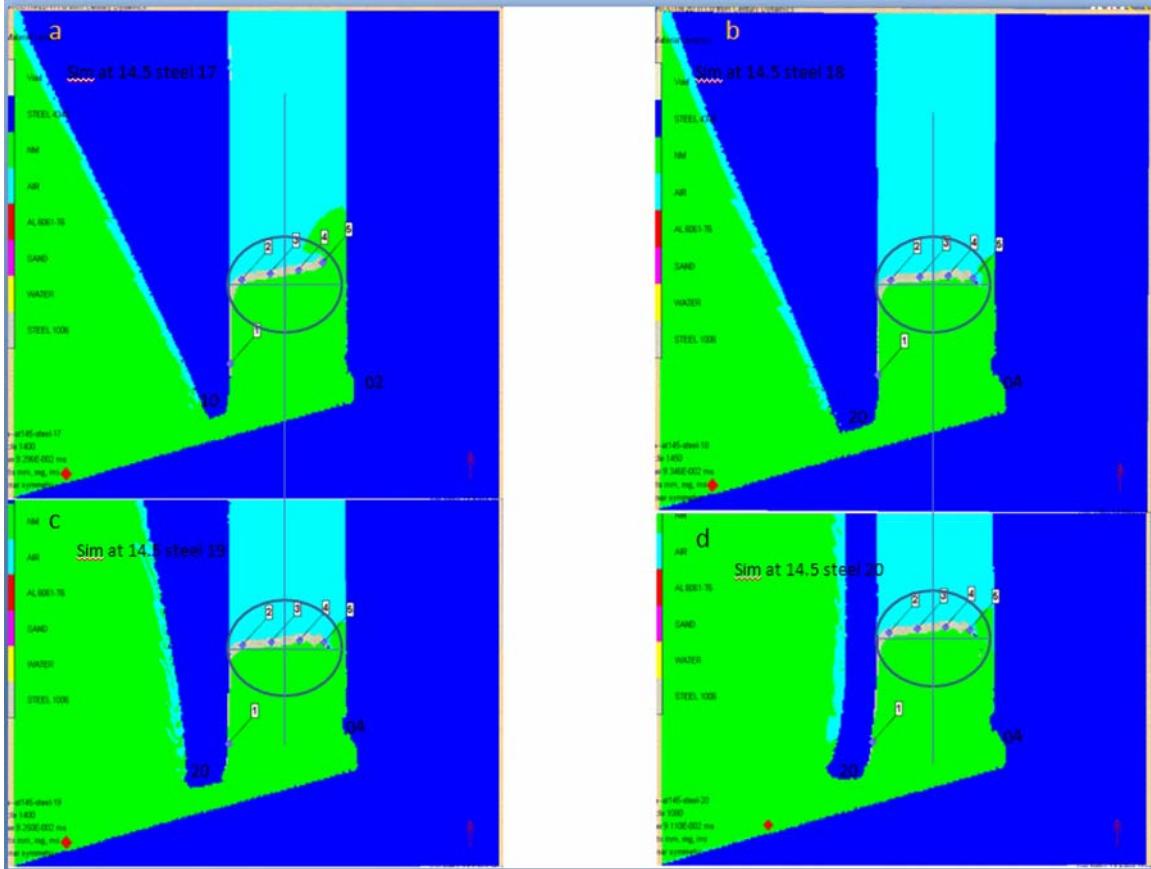
Figure 13.   Simulations changing shape and thickness on the internal confinement: (a): 10 mm left wall tip, (b): increase thickness to 20 mm on left wall, (c): 20 mm thickness, different shape (d): 20 mm thickness completely vertical left side of the wall.

The shape of the left wall played a big role in controlling the flyer plate right tip, but with visible deformation on the plate. Relief of pressure behind the flyer plate was then examined. The problem was solved by re-introducing an exhaust port for HE product gases.
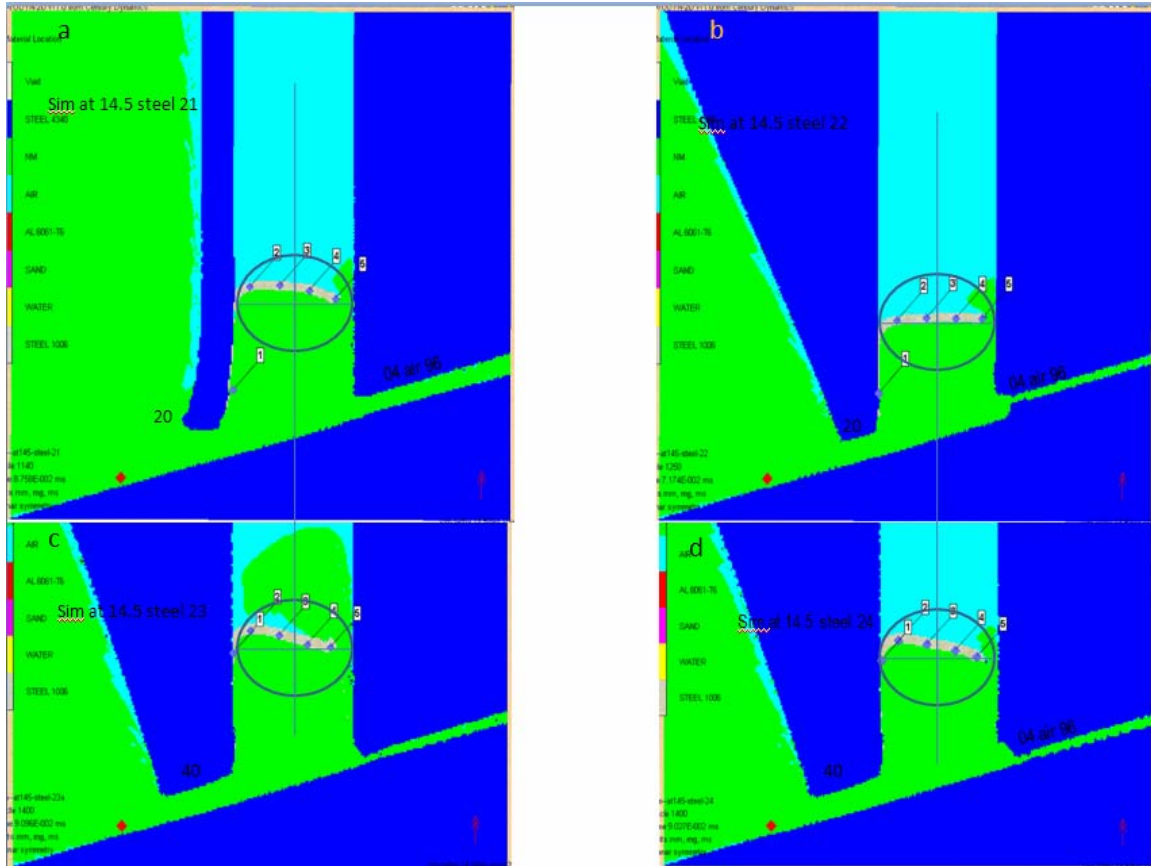
Figure 14.　　Simulations including exhaust tunnel for gases: (a): 10 mm, (b): 05 mm, (c): 05 mm thicker left wall, (d): same as (c) but increasing NM layer longitude.

As seen on Figure 14-b, a very flat profile was obtained, but there were still gases leaving the plate before it reaches its maximum velocity. The problem this time was solved by varying the position and dimension of the gases' exhaust tunnel and the shape of the container left wall. Reduction and a change in dimension of the main tunnel was also considered, as shown in Figure 15.
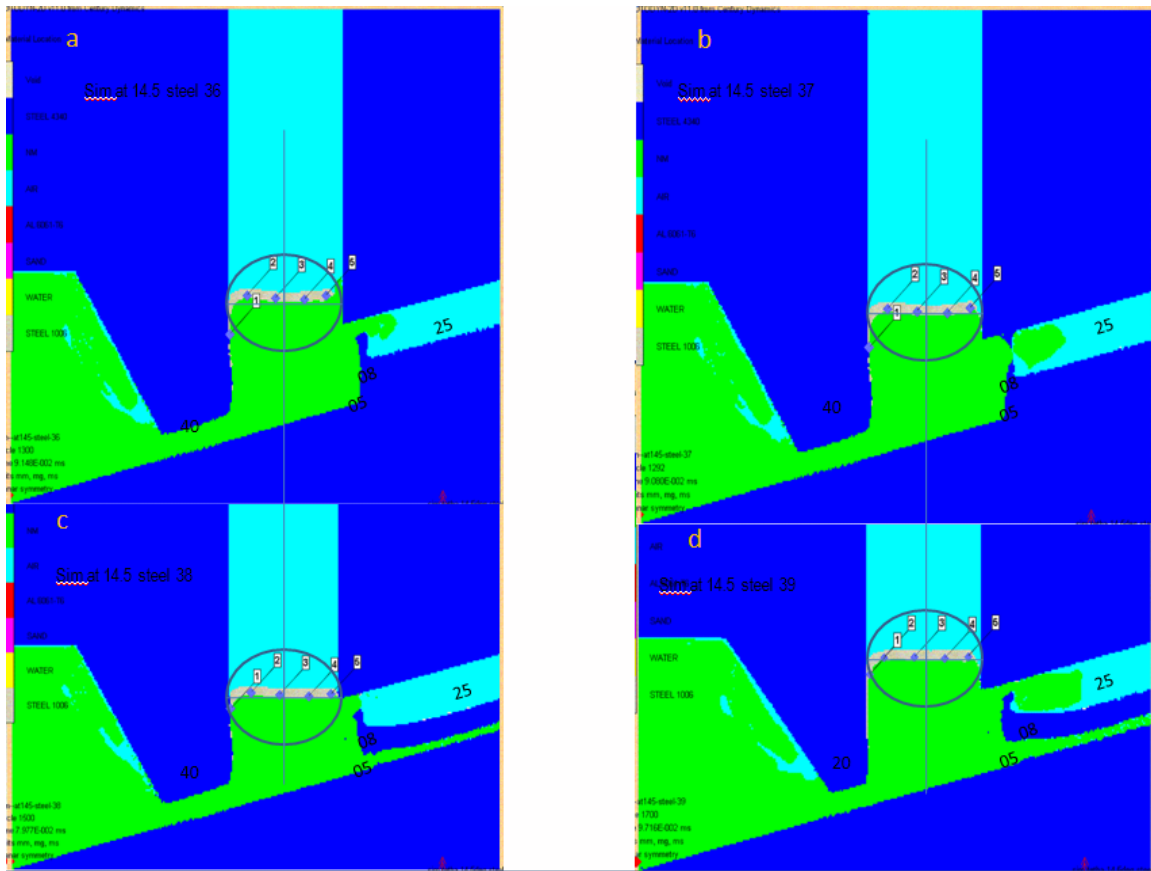
Figure 15.   Simulations varying tunnels' configuration: (a): 72 mm main tunnel 25 mm exhaust tunnel, (b): 70 mm main tunnel 25 mm exhaust tunnel, (c): 70 mm main tunnel 25 mm exhaust tunnel, 05 mm secondary exhaust tunnel (d): same configuration as (c), but reducing the thickness of the left wall.

A flat flyer plate profile was obtained at a run distance of 130 mm, but a minimum of 150 mm was required for the experiment. The next step was to make fine adjustments to maintain the flyer profile already obtained, but at a higher distance. Also, the secondary exhaust tunnel was deleted, the left wall thickness was changed; and an inclination angle at 49° with respect to the horizontal at point "h" was set. This is shown in Figure 16.
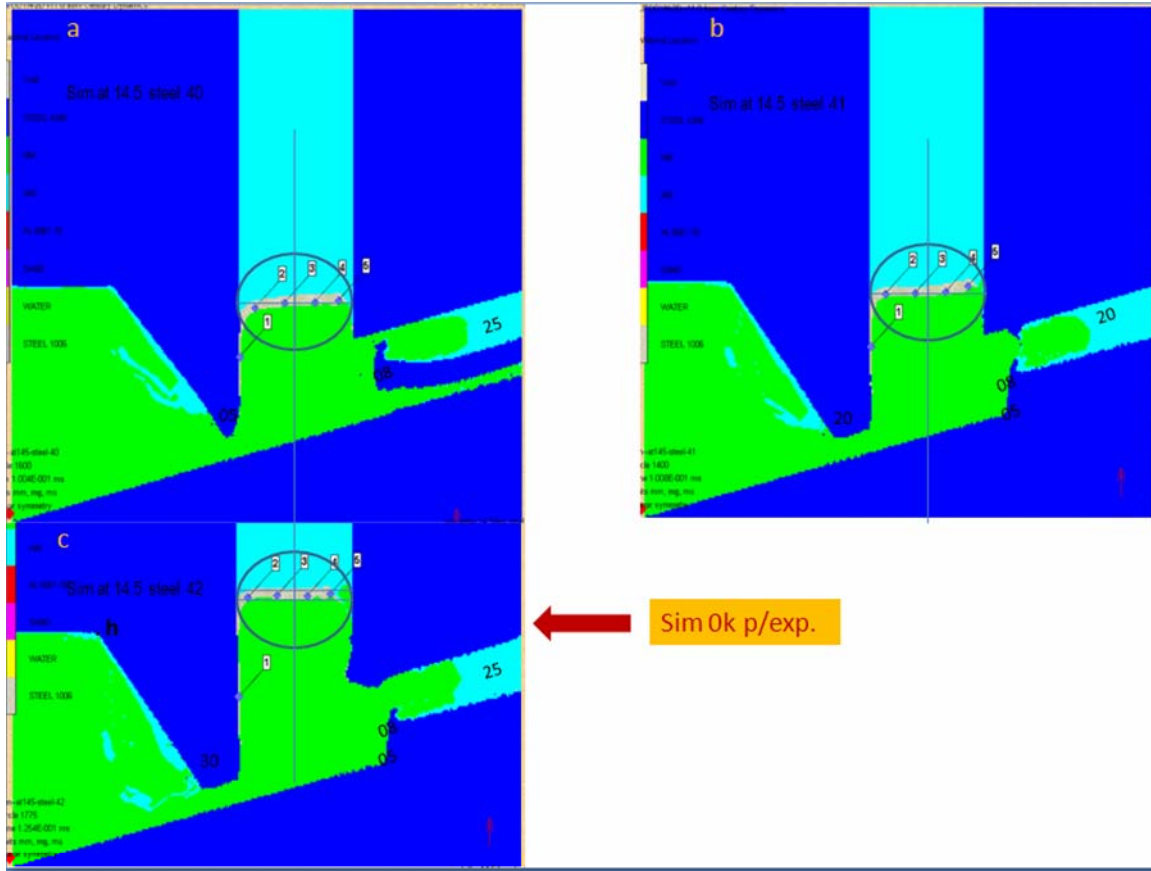
Figure 16.　　Simulations to reach 150 mm impact height: (a): 05 mm left wall tip, (b): 20 mm left wall tip with 20 mm exhaust tunnel and without secondary exhaust tunnel, (c): 30 mm left wall and 25 mm 14.5° inclination exhaust tunnel.

Once the correct profile and height were obtained, the next step was to include the layer sand on the simulation. In its final profile, the sand density from the simulation was different as the density of the real sand used in the experiments (Mil 7 Glass Bead, sieve: 60–80, microns: 250–298), but this silica glass beads have an homogeneous shape and dimensions and this characteristics are well accept for data analysis.
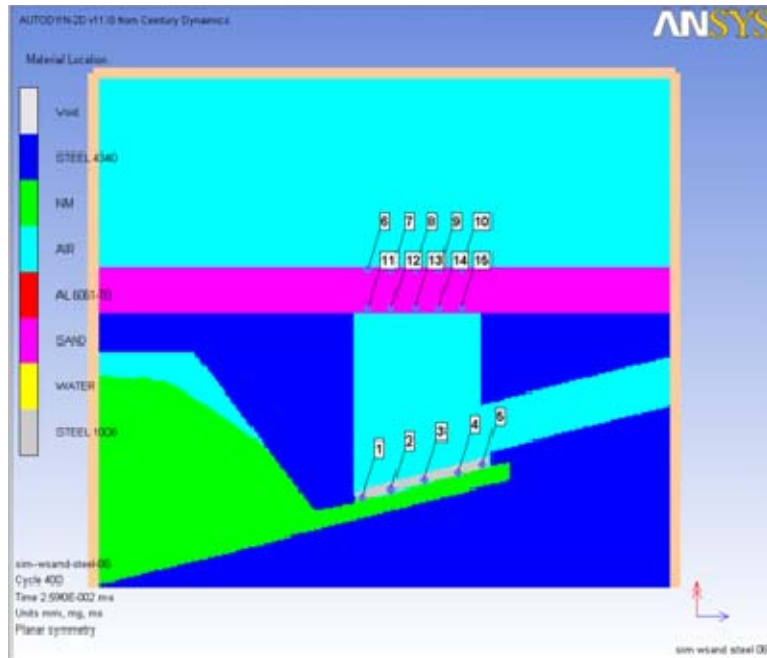
Figure 17.   Final configuration of the computational simulation. Gauges were set up on the flyer plate and in the target zone to measure the impact velocity as a function of propagation distance as a form of validation, color code read as follow: Cyan color indicates air at STP, Purple indicates steel 4340 or brass for the inertial confinement structure, Green color identifies NM-DETA explosive mixture as energetic material, Silver shows steel flyer plate, Pink was set for sand layer target.

Successful simulation required careful consideration and continued refinement of geometrical parameters. The computational simulation shown in Figure 17 represents a 25 mm thick layer of sand at the top in a pink color. The cyan color represents air at STP. Purple indicates steel or brass for the inertial confinement structure. The flyer plate is in grey and is located at an angle of 14.5 deg. Its dimensions are 75 mm square and 5 mm thick, made out of steel, which will be launched upwards by the detonation of the Nitromethane energetic material depicted in green. In this figure, the left side of NM has already detonated and the product gases can be seen expanding as green in color.

In Figure 18, the upper layer of sand starts to move upward with a flat profile, which is precisely what is desired experimentally.
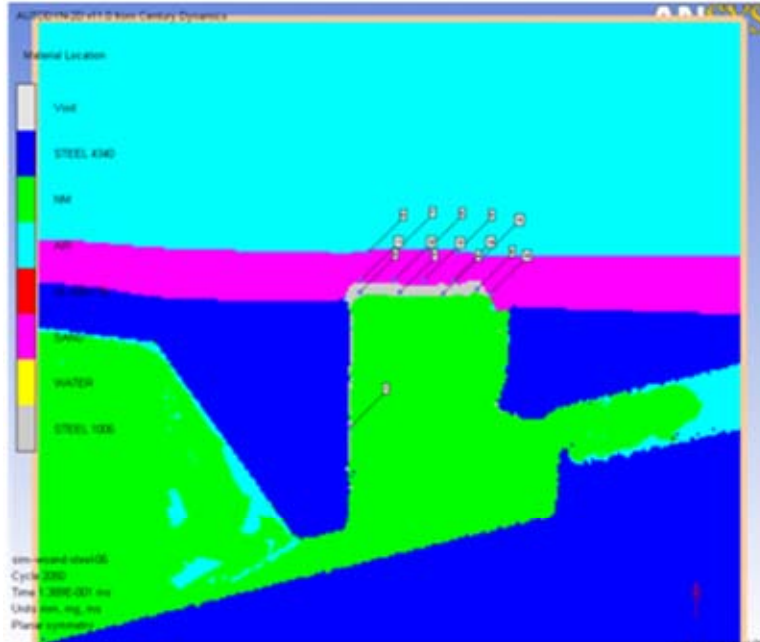
Figure 18.　　　　Upper layer of sand starts moving up with flat profile.

Figure 19 shows the absolute velocity versus time plot of the sand material at the various gauge locations.
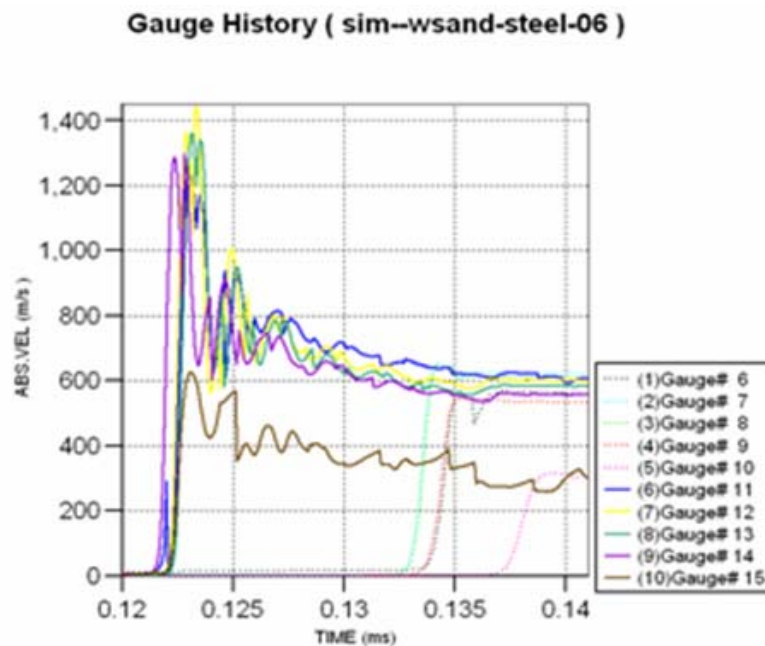
Figure 19.　　　　Bottom and Top sand layer velocity profile.

From this figure, we can clearly see that the shock wave takes about 10.65 µs to travel through the sand layer and cause sand particles to move upward. From these measurements, we can also compute the shock velocity traveling through the sand to be 2.35 km/s. Figure 19 also clearly indicates that the flyer plate velocity decreases as it hits the sand layer and this is the origin of the initial shock wave traveling upwards through the sand. As shown in Figure 20, the initial shock velocity impact at the interface between the FP and the sand layer recorded by gauges 01–10 was about 1,200 m/s.
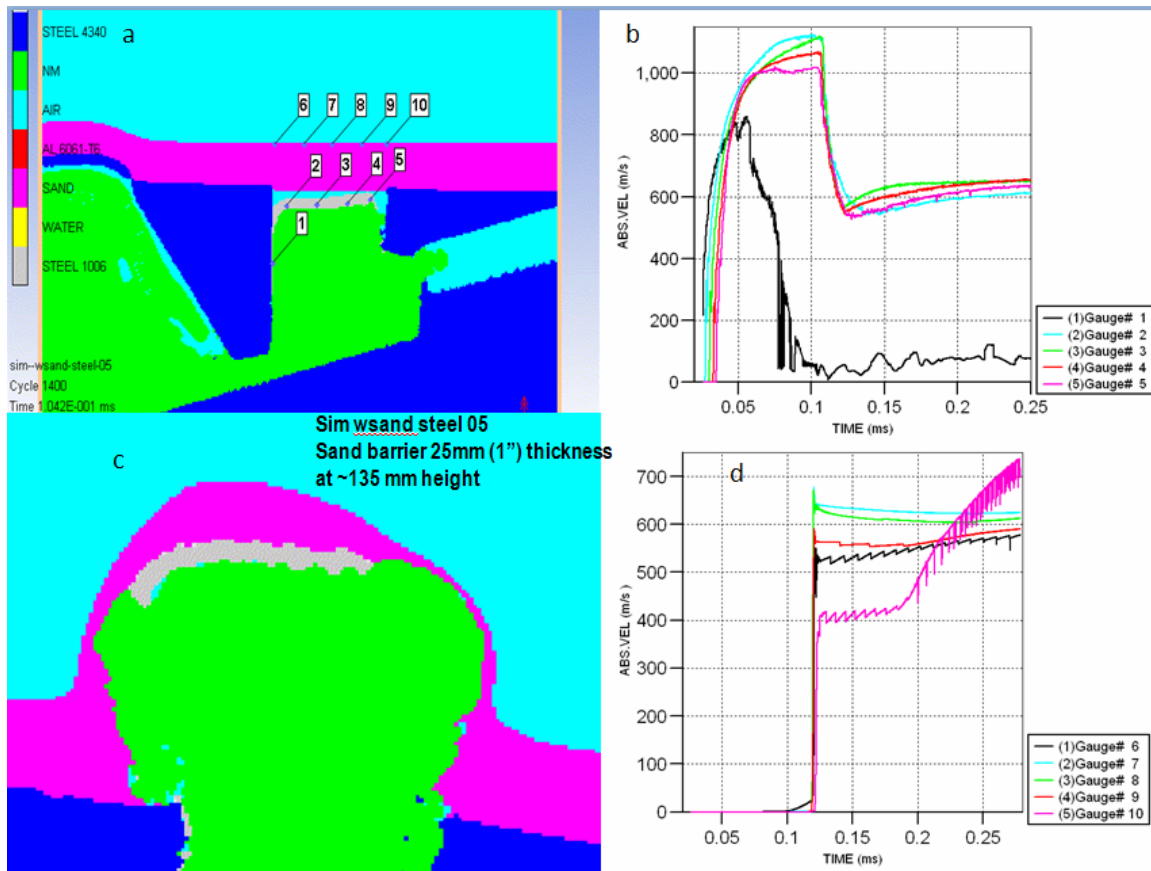
Figure 20.　　Computational simulations with sand layer at 135 mm height: (a): FP just before impacting sand layer, (b): graph showing data of absolute velocity versus time of the moment when FP hits the sand, (c): sand layer profile 132 µs after impact, (d): this graph (abs. vel. vs. time) shows the behavior of the sand layer and its final velocity.

The relevance of this simulation was to determine the angle of the NM case and flyer plate needed to achieve a flat flyer plate profile and, therefore, a flat HVSB profile.

2. Conical Charge

These simulations were performed on a horizontal view, as shown in Figure 21; however, as shown in the experimental section, all CC experimental tests were performed in a vertical arrangement.
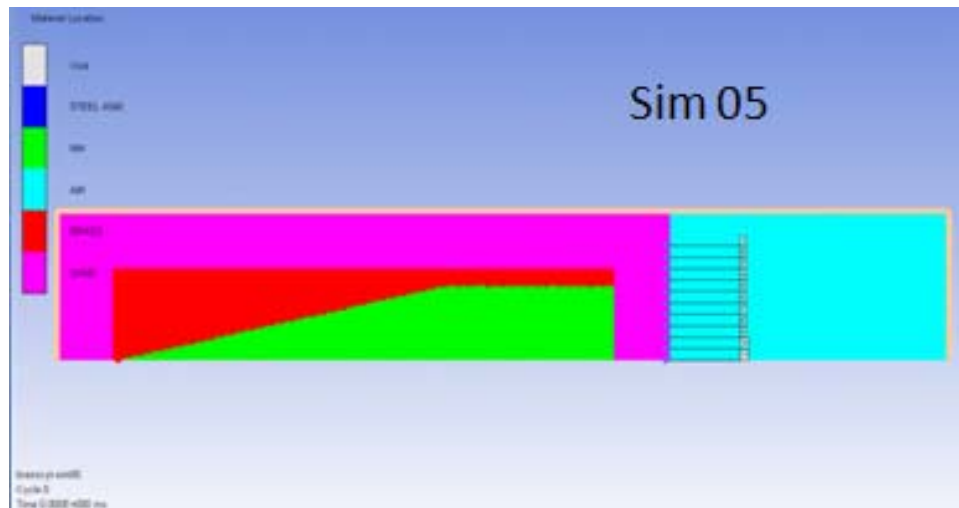
Figure 21.   CC simulation 1" thick sand layer.

By running the initial simulation, the sand profile was determined and changes were applied in subsequent simulations to improve its shape. Behavior of this simulation is predicted to work as a normal buried charge with spherical sand profile, as shown in Figure 22.
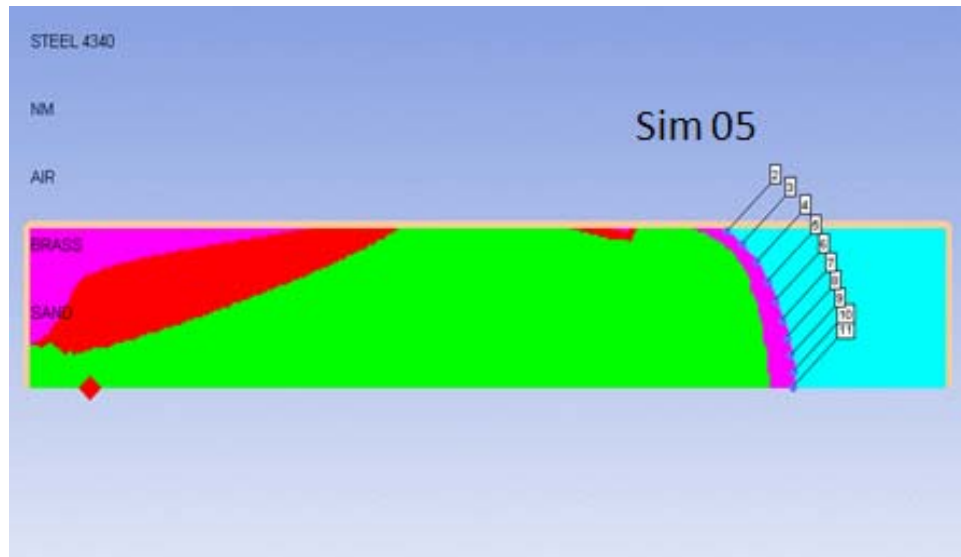
Figure 22.   CC simulation with spherical sand profile.

By introducing a FP method in the same geometrical design, this study looked for a final profile using a 25 mm layer of sand layer as target, as shown in Figure 23.
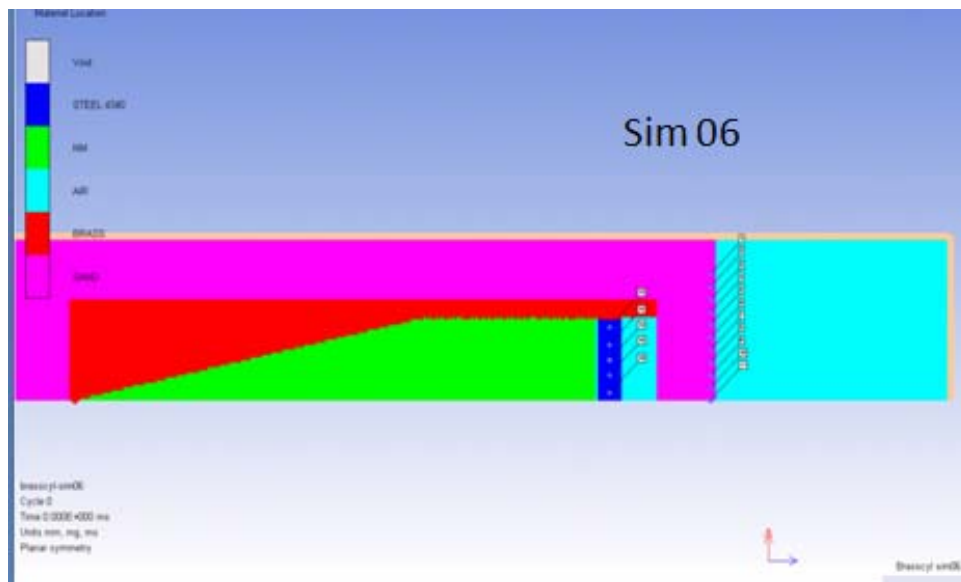
Figure 23.   Simulation of CC using FP method and 15 mm air gap.

An air gap of 15 mm in front of FP gave around 1.3 km/s velocity on FP registered by gauges 12–16 positioned on it, as shown in Figure 24.
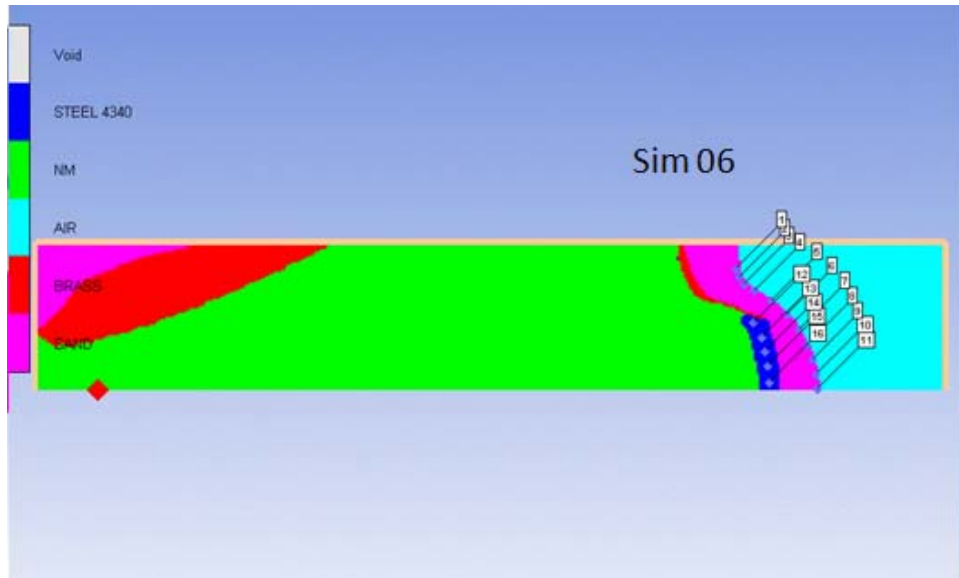
Figure 24.   Simulation using FP method and final sand profile.

An increase on air gap in front of the FP was applied and resulted in an improved profile, as seen in Figure 25.
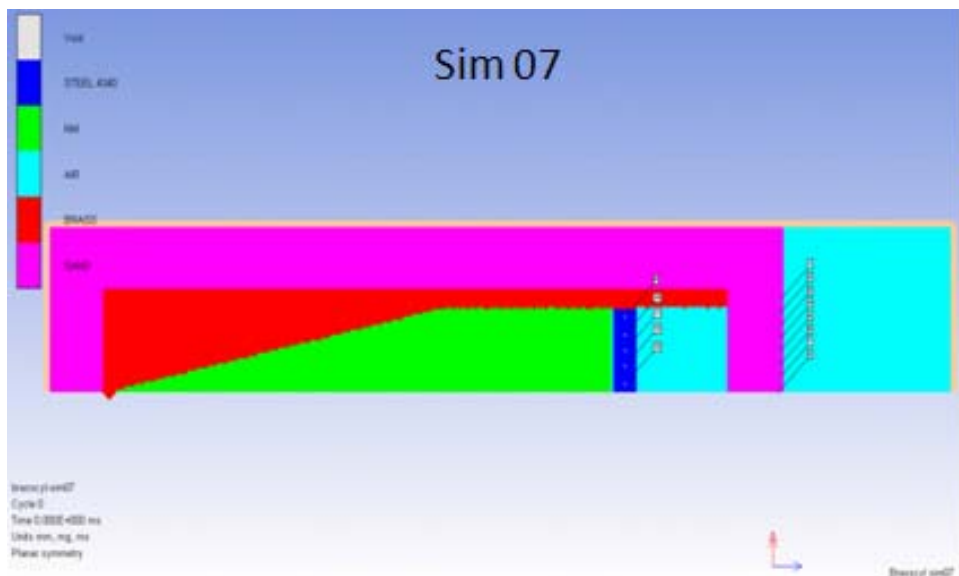
Figure 25.   Simulation with FP method, increasing air gap to 40 mm.

Flyer plate velocities up to 1.4 km/s average and sand velocities up to 1 km/s were obtained. The spherical shape of sand profile, however, remained the same. The final flyer plate simulation result is shown in Figure 26, and we were not able to improve on the curved (non-planar) impact conditions obtained.
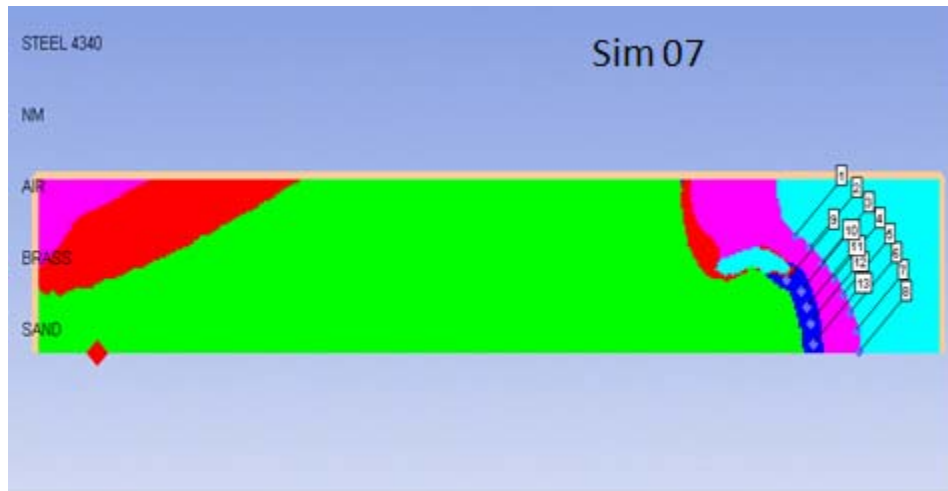
Figure 26.   Simulation of FP with 40 mm air gap and final sand profile.

Because the FP method was not useful for realizing flat impact conditions, no more simulations were performed using this method; instead, an attempt was made similar to the original design with the exception of a small modification—the removal of the flyer plate. This geometric arrangement is shown in Figure 27.
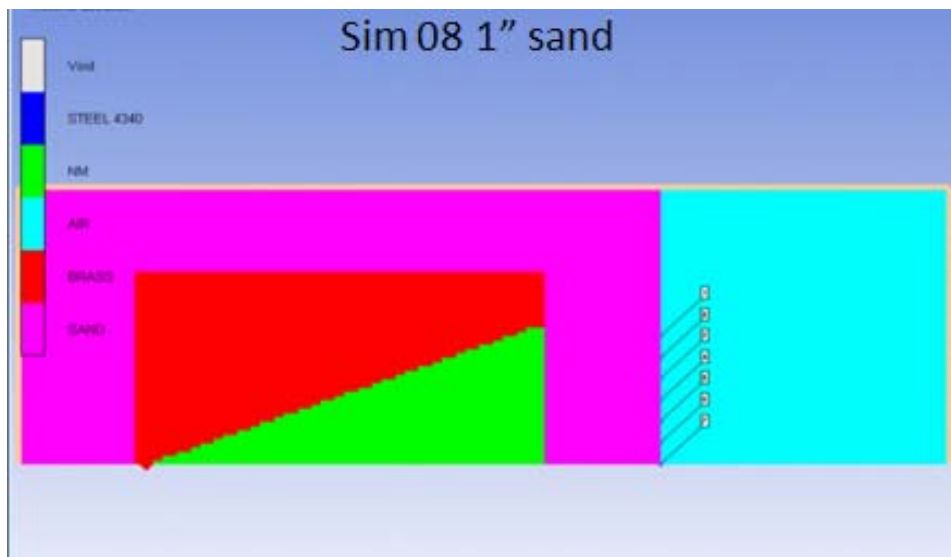
Figure 27.   CC simulation without FP.

The conical section was optimized and an angle of 20° was chosen. The sand layer used was 1 in thick, which should prove to delay the explosive gases from escaping through the sand layer prior to the sand reaching its target.

36
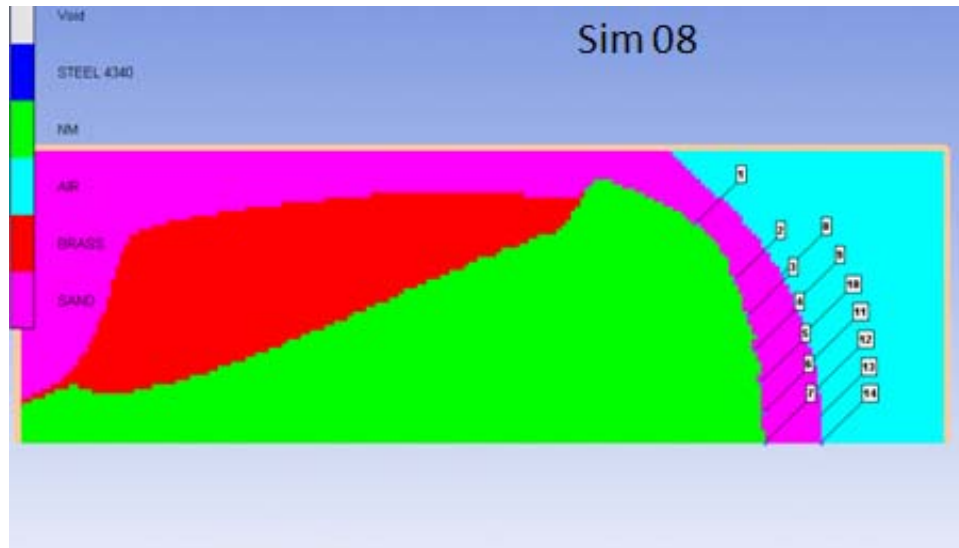
Figure 28.   CC simulation with triangular shape of 20° angle.

In this simulation, shown in Figure 28, a flat sand profile at velocities near 1.3 km/s was obtained with a radius of approximately 7.5 mm (15 mm diameter), which is important for the selection of target sizes in future work. The sand layer, without holding the profile for a large period of time however, broke up from the escaping gas effect. Since we wished to have a flat sand profile for a longer run distance, we chose to decrease the conical angle to 18° and to increase the thickness of the sand layer from one to two inches as shown in Figure 29.
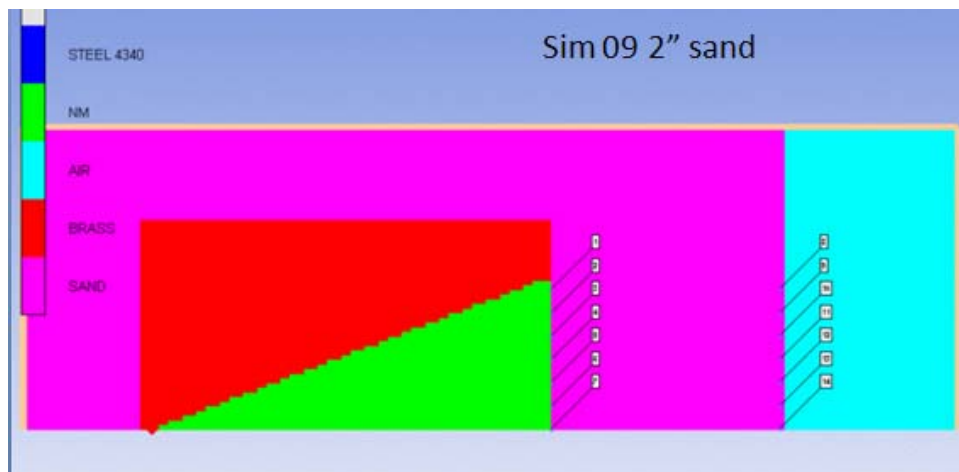
Figure 29.   CC simulation setup with 2" sand layer.

As shown in Figure 30, flat sand profile was obtained over a 20 mm diameter area, velocities reached were around 700 m/s. These results will be compared with the results obtained above with LSTF simulations.
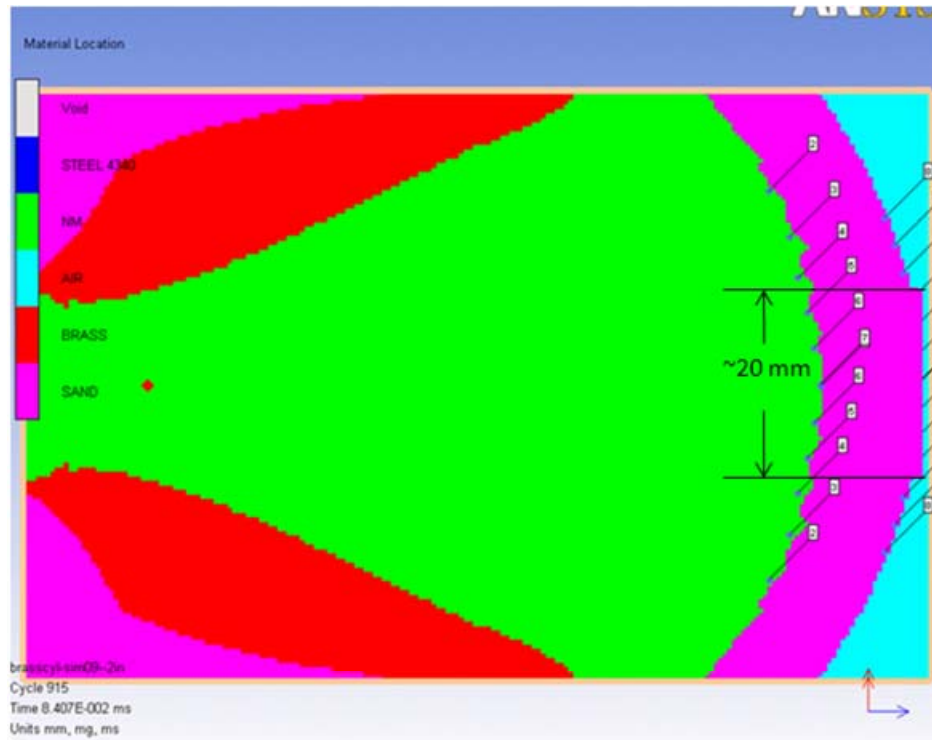
Figure 30.   Simulation using mirror in plane.

The simulation shown in Figure 31 represents an originally 50 mm thick layer of sand (shown in pink), that has been dynamically compressed to 25 mm under the shock loading. The brass used for the inertial confinement required for the detonation wave to survive the 18° expansion is shown in red. Nitromethane and its detonation product gases are depicted in green; and the cyan color represents air at STP.

Figure 31 shows the final configuration for the optimized charge—sand layer setup.
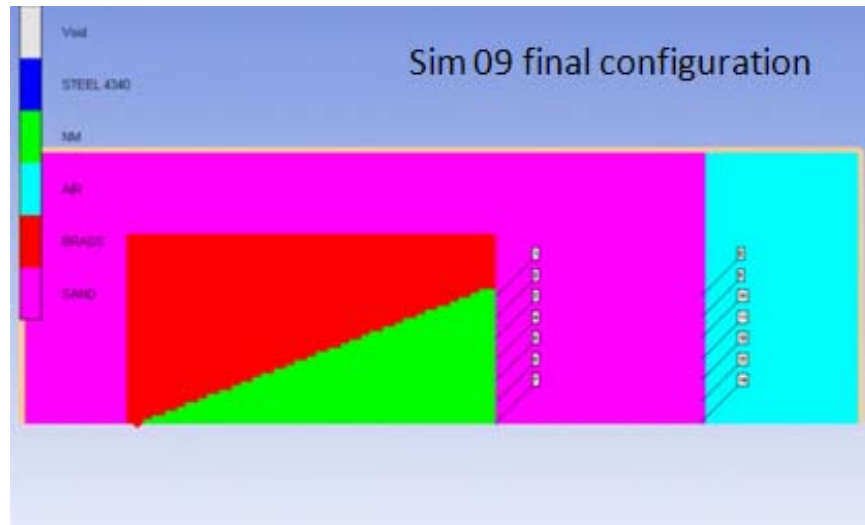
Figure 31.   CC final computational simulation configuration. Gauges were set up on the in the target zone (lower and upper sand layers) to measure the impact velocity as a function of propagation distance as a form of validation.

Figure 32 shows the absolute velocity versus time plot of the sand as it is accelerated by the passing shock wave propagating through the sand layer at the various gauge locations.

Gauge History (brasscyl-sim09--2in)
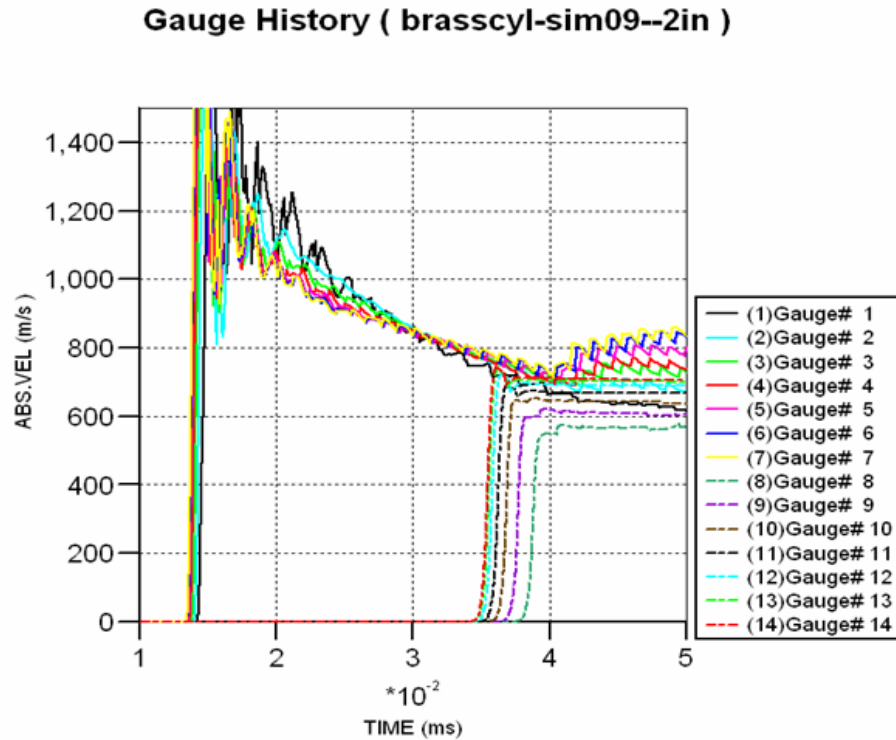
Figure 32.   Particle velocity profile as shock wave propagates through the sand layer.

The shock wave took about 21.25 μs to propagate through the sand layer (which indicates a similar shock velocity as in previous cases of 2.35 km/s), and it is clearly indicated in the plot that the sand velocity attenuates as the shock wave travels through the sand, due to conservation of momentum and due to work being done to compact the sand. The relevance of this simulation was to determine the angle of the CC needed to achieve a flat HVSB profile.

Figure 32 shows the initial impact of the detonation wave as the sand is quickly accelerated to over 1,400 m/s while the expanding explosive gases keep pushing the sand, the sand is being compacted and the particle velocity reduces to near 600 m/s when the top layer of sand is accelerated to this speed. Since there is no more sand to compact, conservation of momentum states that the velocities should remain constant at the free surface. On the inner surface, adjacent to the explosive gases, complex shock interactions continue on and yield the variations in particle velocities seen on this graph.

40

3. Summary

After performing all these simulations, we understand that the LSTF work requires a full 3D simulation to capture end-effects and we fully understand that by only considering 2D simulations for the LSTF configuration we expect that the simulations will over-predict the resultant velocities. However, we cannot calculate the amount of over-prediction until a set of experiments is preformed.

However, the main objective of the LSTF simulations was to predict the initial flyer plate angle required to obtain a flat plate at impact time. This was determined from the simulations described above. The next step is to obtain experimental validation of these results as a way of understanding how well these simulations represent reality.

The cylindrical charge simulations were performed in an axis-symmetric configuration and, therefore, take into account the symmetrical 3D effects encountered in such configuration. We will use these simulations to closely compare the experimental results and gauge the accuracy of our models. A slight variation is expected, due to the fact that the EOS for the sand used in our simulations is for generic sand; however, the sand used in the experiments was different.

The techniques used in this work made it possible to simulate the hypervelocity impact of small particles of sand debris with relative ease.

Results of this study were reported in this chapter and the relevance of these findings is discussed in Chapter VI.

THIS PAGE INTENTIONALLY LEFT BLANK

IV.   DESIGN AND CONSTRUCTION

The problem to be solved in the modeling efforts was that of obtaining a planar shock-wave to use to load sand and cause a well-defined cloud to be formed. This requirement, although simple to describe, is by no means trivial to achieve. Rather, at the small scales at hand, it is very hard to achieve. Simulation studies, nevertheless, as performed and described in the previous chapter, showed promising results in obtaining a flat sand profile traveling at around 600 m/s for the flat plate and up to 1.2 km/s for the cylindrical charge.

These results, and the individual properties of the various components, combined into a 3D design would ideally be integrated into a real LSTF using SolidWorks[2] 3D CAD software.

An extensive work of literature exists that deals with the investigation of buried mines. Most of this work, however, does not focus on the characterization of the blast output, which is essentially a flying cloud of sand. Rather, it focuses on cratering effects, with applications toward the survivability of structures subjected to near blasts or in the utilization of explosives for excavation or other industrial applications.

A.   DISCUSSION

A main issue to overcome is the fact that the proposed test facility in a university scale will have a relatively low value for the maximum allowed amount of High Explosive (HE) material that can be detonated at any one time. Therefore, the feasibility of building an explosive lens, which, at a minimum, would require hundreds of grams of HE, is not the most desirable solution. This study devised a solution in which a slanted flyer plate (FP), with an explosive layer underneath, which is detonated from one end, is accelerated and allowed to impact the material under investigation. As the detonation wave runs through the explosive layer, it pushes the FP. If the geometry is carefully designed and the

---

[2] The description of the SolidWorks 3D CAD software is taken from instructional tutorial furnished by SolidWorks Corporation 2008 SP5.0.

FP/explosive layers are precisely positioned, in theory, a flat FP that travels on the order of 1 to 2 km/s towards a layer of sand should be produced.

The second issue is the expense and danger of machining and/or pressing solid explosives to get the desired shape that will allow driving a FP. Previous research at NPS led this study's researchers to propose the use of a liquid explosive [5] so that no machining of reactive materials is required. This study selected Nitromethane (NM), which, in its pure form, is simply a solvent and not an explosive. NM; however, can be sensitized with the addition of diethylene-triamine (DETA) and results in a cap-sensitive mixture with detonation velocities near 6.2 km/s and detonation pressures near 12 GPa [6].

This type of system requires full 3D simulations, as there is no symmetry axis in such a configuration. As previously stated, our 2D simulations will tend to over-predict sand velocities; therefore, we also pursued a symmetric configuration that led to the design of our cylindrical charge—which will be used to measure the degree of accuracy of our predictive capabilities.

Some of the key problems related to these systems involve detonation growth and decay, due to the small volumes that exist in such a design and/or to the large expansion areas involved in this design. However, plans to introduce confinement in the form of high density materials, such as steel or brass, will help diminish or completely eliminate this problem.

B.   DESIGN

As the original design was conceived in 2D, the next step was to develop the same models, but in 3D, as follows:

Lay out the dimensions for the LSTF and CC elements as per the geometry used for the computational simulations. SolidWorks was the software chosen to improve the designs. Design schematics of these parts are reported in Appendix B.

Laying out the elements:

1. LSTF

There are six pieces that correspond to the LSTF main body, two pieces that make up the energetic material case holder, and one FP individual piece.

- For the top piece, as shown in Figure 33, a rectangle of 11.5″ x 5″ x 1″ with a square cut at 5.5″ from the back as escape tunnel for FP was designed.
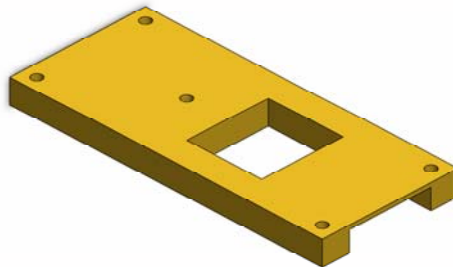

Figure 33.　　　3D CAD of top part.

- The sides (shown in Figure 34) are two rectangles 11.5″ x 5″ x 1″ dimensions using the short sides as the top and bottom.
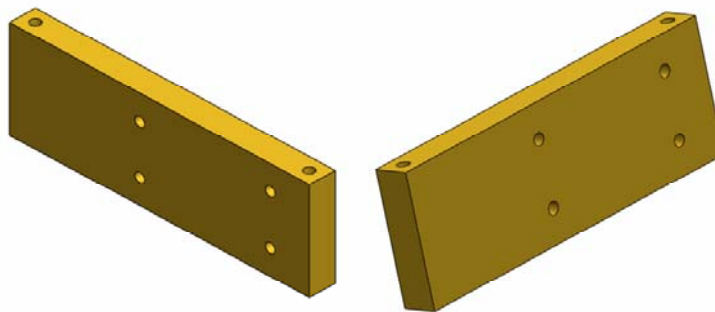

Figure 34.　　　3D CAD of left and right side parts.

- The bottom part had a ramp with an inclination of 14.5°, which will be the base for the NM case and flyer plate, as shown in Figure 36. The dimensions are 3″ x 2.77″ for the widest wedge dimension and 3″ x 0.47″ in the lowest with an overall length of 8.87 in, as shown in Figure 35.
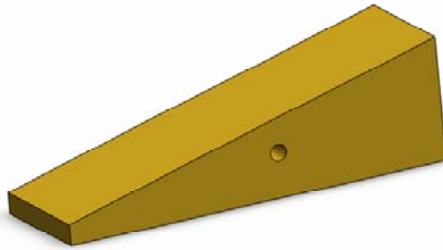
Figure 35.   3D CAD of bottom part with inclination ramp of 14.5°.

- An almost square solid piece was selected for the front part to form part of the HE product gas escape tunnel and exhaust duct with also 14.5° top side inclination, as shown in Figure 36.
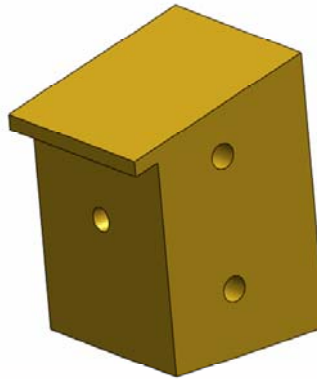
Figure 36.   3D CAD of front part.

- The back piece has two different inclination sides where one is 14.5° with respect the horizontal part of the main ramp where the NM case is set. The other side is 49° with respect to the top side and diverges out the main gases and shock wave from the initial detonation. This is shown in Figure 37.
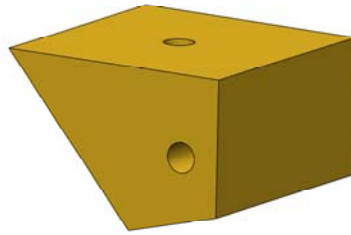
Figure 37.   3D CAD of back part.

- The FP is a 75 x 75 x 5 mm dimension plate made of steel, as shown in Figure 38.
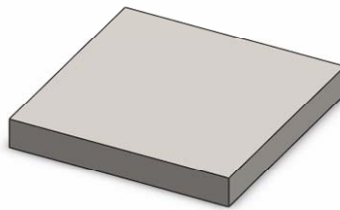
Figure 38.   3D CAD of FP.

- The NM case, with a rectangular shape of 2.95″ x 9.15″ and an interior pentagon cut-out of 0.31 in depth. It can hold 67 mL. of liquid explosive (NM synthesized). It is shown in Figure 39.
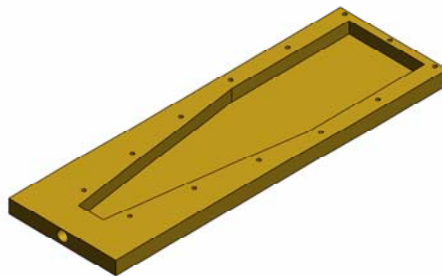
Figure 39.   3D CAD NM case.

- The NM case cover is a rectangular piece of plastic with the following dimensions: 2.95″ x 9.15″ x .06″, and is shown in Figure 40.
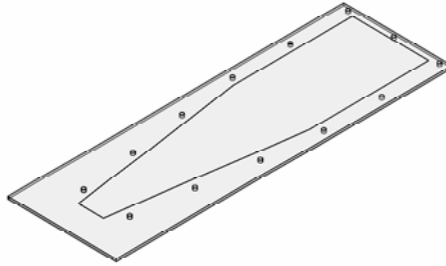
Figure 40.   3D CAD of NM case cover.

2.   Conical Charge

The simple design of the CC allows us to keep the number of parts to a minimum. The final assembly consisted of just 3 pieces:

- The main body is a cylindrical piece of brass 4.5 in high and 3.5 in diameter with an interior cone shape reaching from one end to the other. This conical volume holds 167 mL of liquid explosive (NM synthesized). In the bottom side, it had a seat diameter to place the detonator device (1/2-20 UNF-2A thread size). This piece is shown in Figure 41.
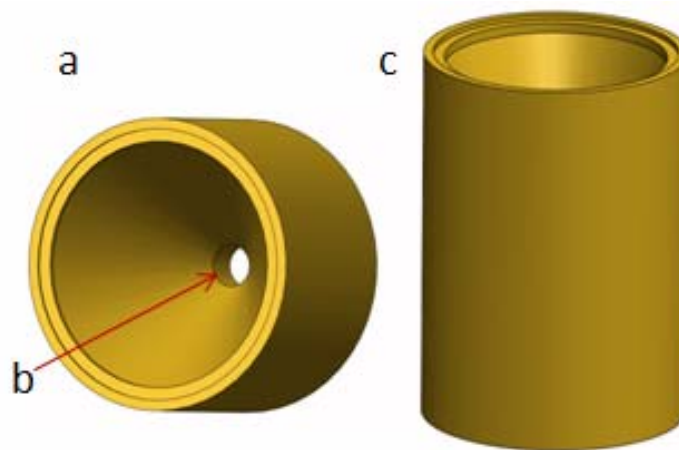
Figure 41.   3D CAD of main CC cylindrical body: (a): internal view showing the cone shape, (b) detonator seat, (c): external view.

- The second part is a threaded ring (3 1/2–16 UNF) as a cap, 4.0 in external diameter and 3.5 in internal diameter threaded on the inside. This is shown in Figure 42.
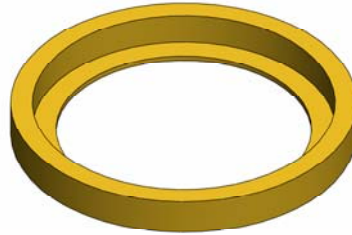
Figure 42.   3D CAD of top ring.

- The last part is a thin lid of Teflon 3.25 in diameter and 0.06 in thickness, as shown in Figure 43.

Figure 43.   3D CAD of cover lid.

3.   Test Chamber

The test chamber components are:

- The base is a 42 square inch steel plate, ¾ in thickness with 5/8 in through holes for bolts. This is shown in Figure 44.
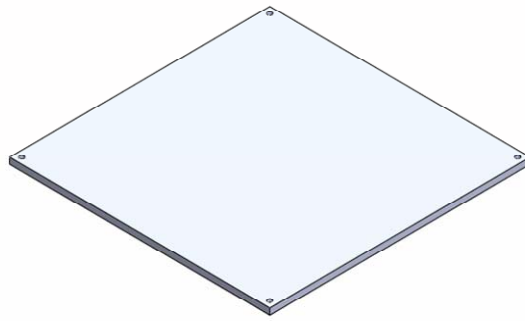
Figure 44.   3D CAD of test chamber base plate.

- The chamber is formed with a 24″ x 36″ diameter ¾ in thickness steel cylinder welded to the base plate. This part is shown in Figure 45.
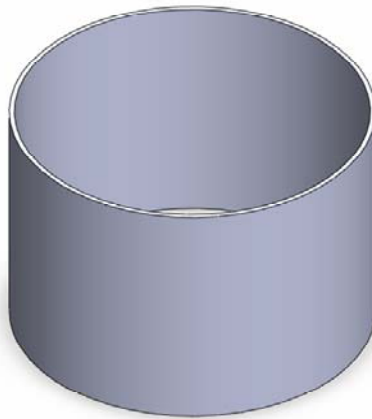
Figure 45.   3D CAD of cylinder that forms the main chamber.

- Outside of the external cylinder rim, there is a steel flange ¾ in thick with the same internal diameter as the external cylinder diameter and 40 in external diameter. An eight-hole pattern is drilled through at ¾ in. This is shown in Figure 46.
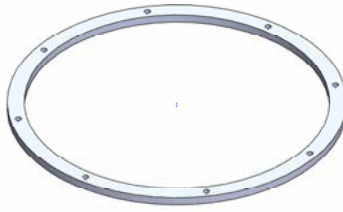
Figure 46.　　　　　3D CAD flange to secure test chamber cover.

- The cover for the chamber is a circular steel plate, 40 in diameter and ¾ in thickness with a 12 in hole in the center. The same eight-hole pattern is drilled through with ¾″ through holes.
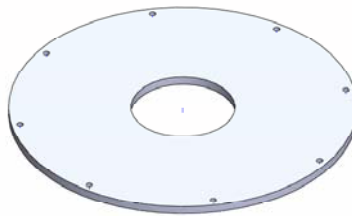
Figure 47.　　　　　3D CAD of top plate. Notice 12″ hole to allow interaction of HVSB and sensor instrumentation.

C.　CONSTRUCTION

1.　LSTF

The procedure used for the final assembly is given below:

- Attach the sides between the front and bottom parts using 6 x 7/16″ bolts. Be sure to accurately align the bottoms of the walls. Details are given in Figure 48.
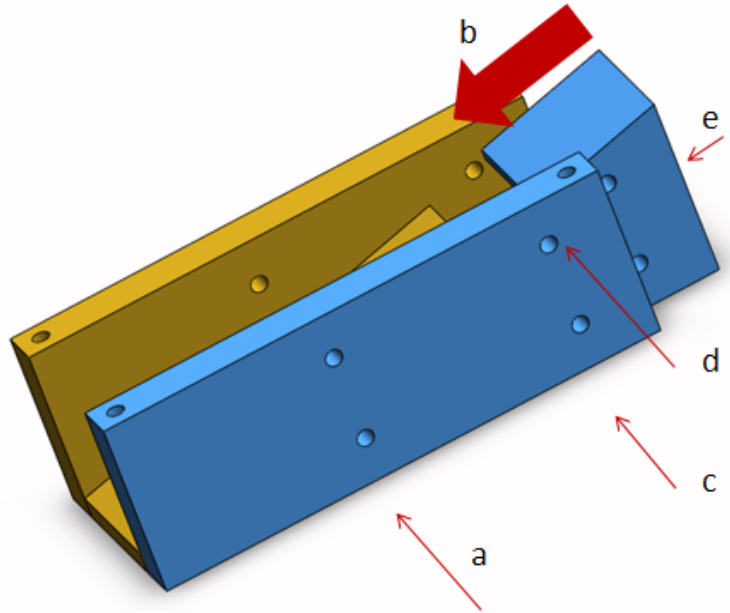
Figure 48.   3D bottom part assembly: (a): aligned left and right sides with bottom and place first bolt, (b): slide front part between the two sides until reach bottom part, (c, d) place next two bolts, (d): place last bolt to attach front to bottom part.

- Using 1 ½″ bolt, attach the back part to the bottom side of the top part, as shown in Figure 49
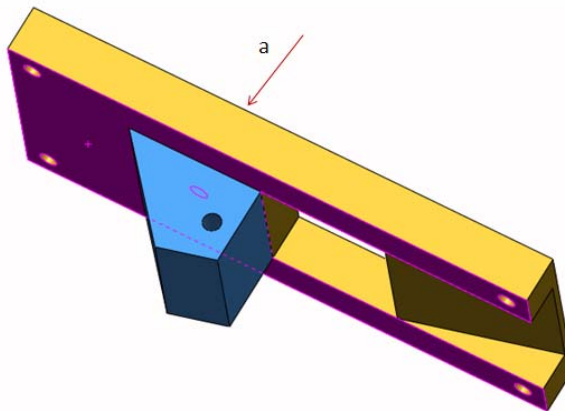
Figure 49.   3D top part assembly, (a): place bolt to secure top to back part.

- Attach the top part to the top side of the side pieces of the LSTF, as shown in Figure 50.
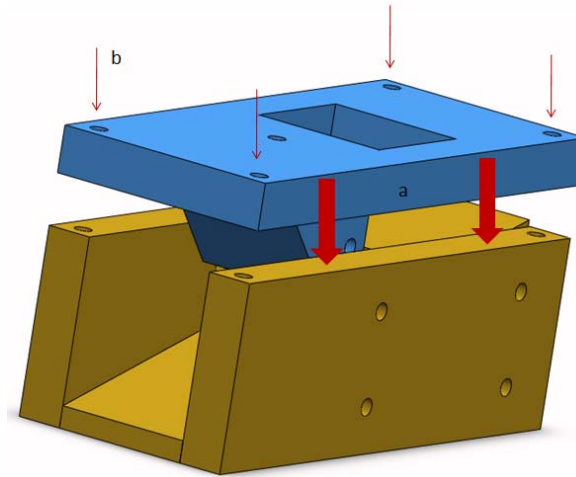
Figure 50.   3D top and bottom assembly: (a): slide top structure on top of the bottom structure, (b) place the four 1-1/2" bolts and tighten them to secure device.

- Place the NM case on a planar surface. Apply epoxy glue as a sealant to avoid liquid explosive leaks. Then, bolt the NM cover case in place. Finally, slide it in and out inside LSTF to be sure it fits smoothly. Shown in Figure 51.
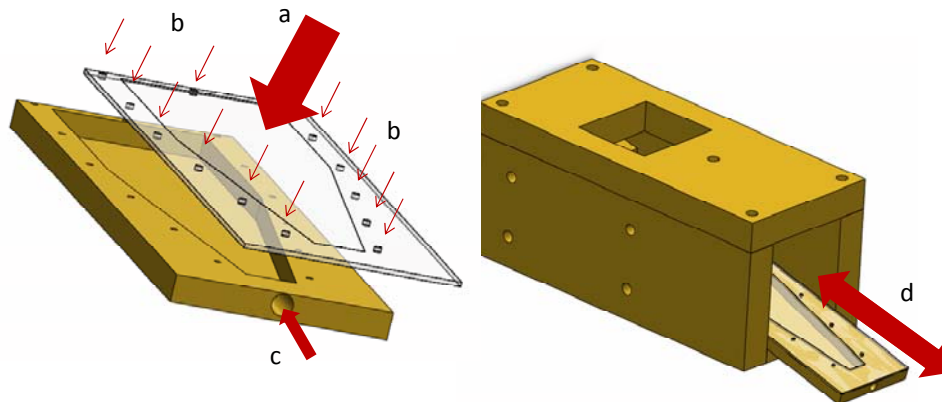
Figure 51.   3D NM case assembly: (a): place plastic cover in place over NM case, (b): bolt it and let epoxy dry, (c): keep this clean and clear for Detonator, (d): check that assembly fits well on LSTF.

- Finally carefully slide FP inside main tunnel on top part of LSTF, as shown in Figure 52.
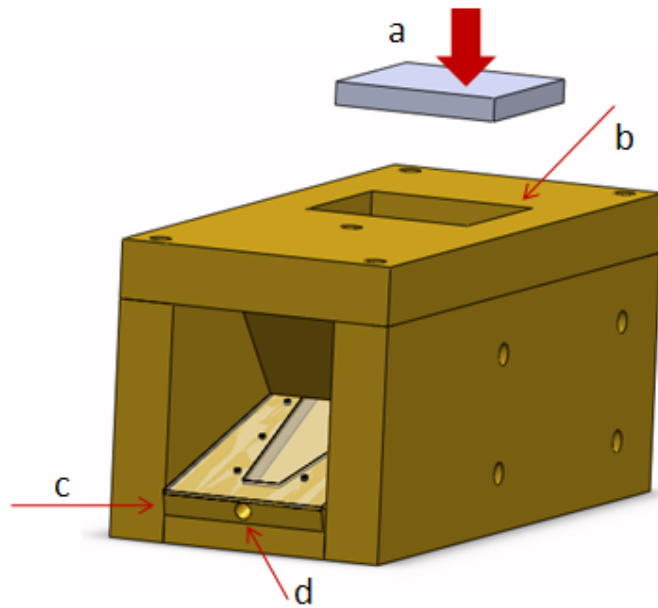
Figure 52.   LSTF 3D CAD assembly: (a): carefully slide FP inside escape tunnel, (b): main escape tunnel, (c) push NM case all the way in to final position, (d) keep detonator seat clear.

Shown in Figure 53, is a 3D CAD assembly of the explosively-driven flyer plate apparatus.
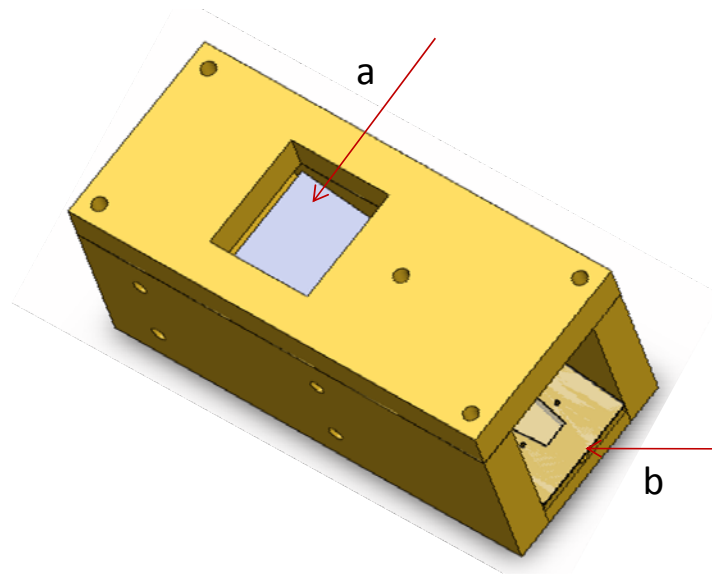
Figure 53.   3D CAD LSTF final assembly top view: (a): flyer plate sitting on top of NM case at the bottom of the escape tunnel, (b): NM case inside the LSTF.

Figure 54 shows a cross-sectional view of the assembly. The Nitromethane case is partially slid into place. The flat plate is depicted at its initial angle outside of the inertial confinement box.
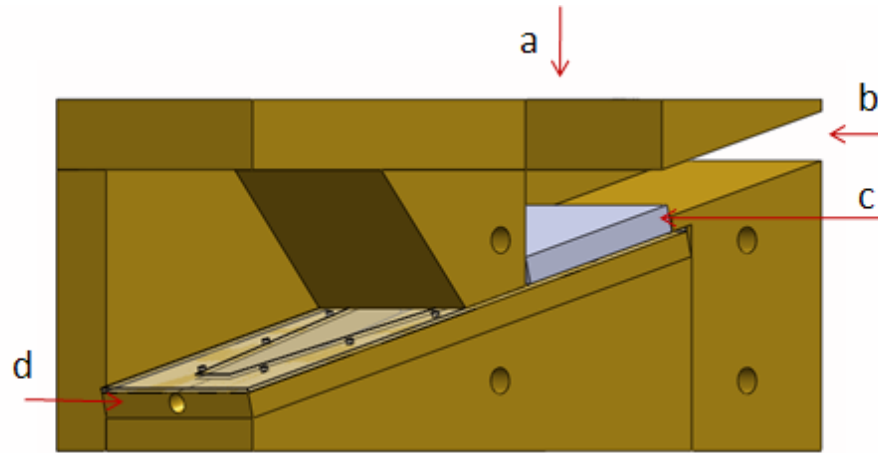
Figure 54.   Cross-sectional view of LSTF: (a): FP escape main tunnel, (b): gases exhaust tunnel, (c) FP seat in place, (d): NM case seat in place at slanted angle of 14.5°.

After the LSTF design was complete and the pieces manufactured, an inspection was done by removing each part. Because of the specially-prepared NM case assembly, further inspection of the energetic material charge volume was possible. The LSTF was found to be as satisfactory as possible according to the original sketch. The LSTF was assembled and then closed for storage and transportation purposes until experiments were conducted. Images of the assembly are shown in Figure 55.
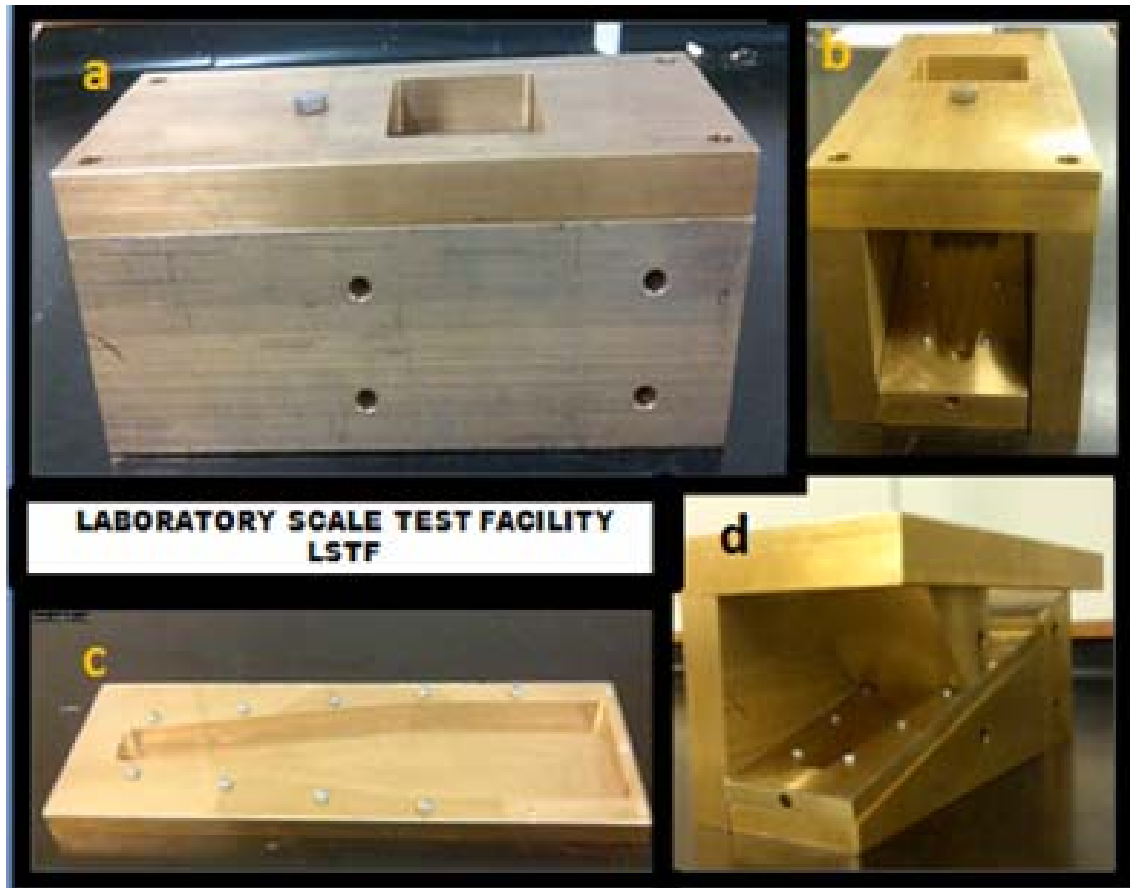
Figure 55.   Actual pictures of LSTF, (a): partial assembly of LSTF, (b): front view showing NM case position, (c): NM case assembly, (d): right wall removed to see internal configuration.

2.   Conical Charge

The procedure used for the final assembly is given below:

- Place the cylinder in vertical position, as shown in Figure 56.

Figure 56.   CC on vertical position.

- Place the Teflon lid on top of cylinder carefully. This is shown in Figure 57.
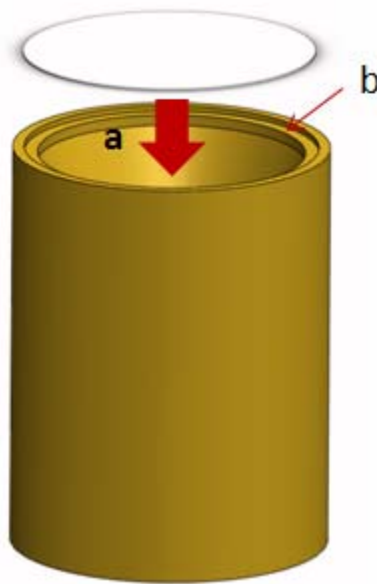
Figure 57.   CC 3D CAD (a): put Teflon lid on top of cylinder, (b): rim to hold Teflon lid.

- Put the cap screw in place and screw it tightly to the cylinder edge, as shown in Figure 58.
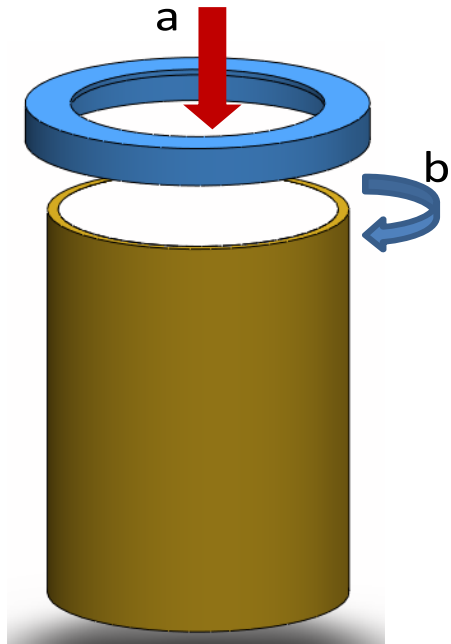
Figure 58.   CC 3D CAD, (a): put cap cylinder on top, (b): screw it tight CW.

Illustrated in Figure 59 is a 3D CAD assembly drawing of the CC explosive device.
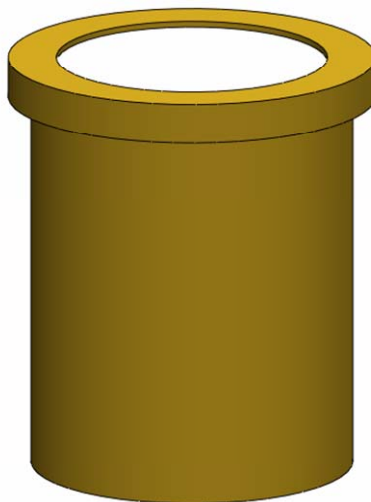
Figure 59.   CC 3D CAD final assembly.

Figure 60 shows a cross-sectional view of this assembly.
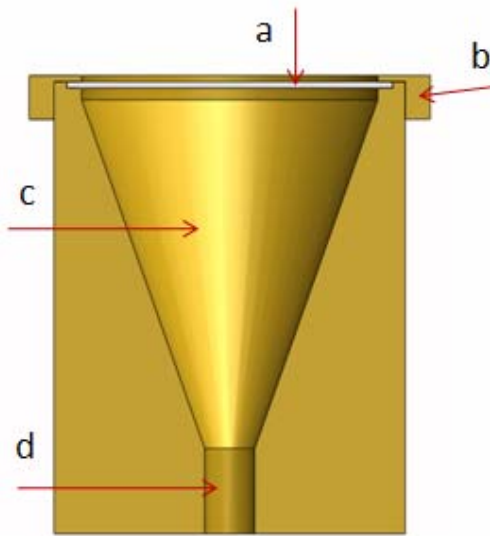
Figure 60.   Cross-sectional view of CC, (a): Teflon lid on place, (b): cap ring
well-tightened, (c): NM cone container, (d): detonator seat.

After the CC design was complete and the pieces manufactured, an inspection of it was made by removing each part. The CC was found to be as satisfactory as possible according to the original sketch. The CC was assembled and then closed for storage and transportation purposes until experiments were conducted. This is shown Figure 61.
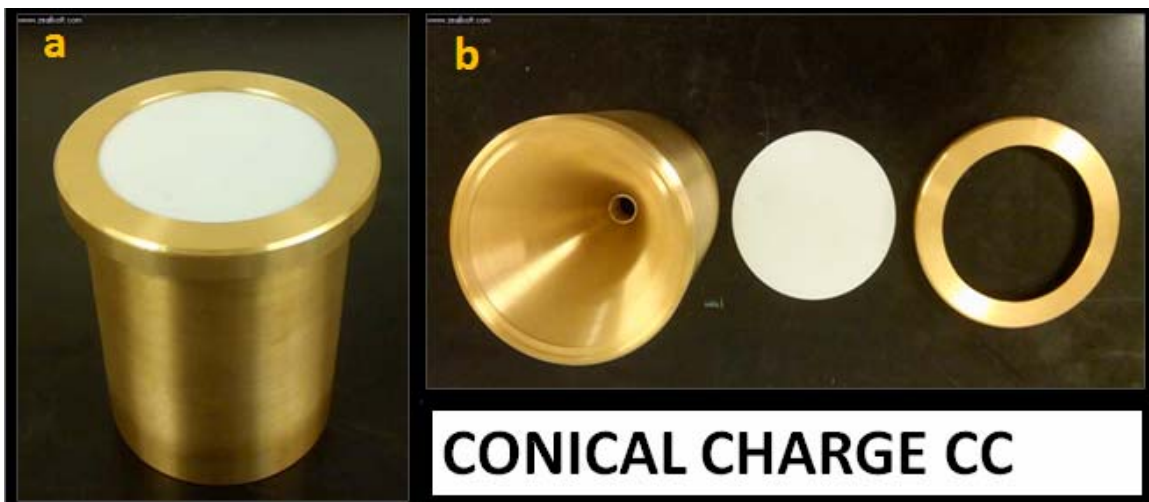
Figure 61.   Actual pictures of CC, (a): partial assembly of LSTF, (b): top
view showing CC main body with detonator seat at the bottom
Teflon lid and top cap ring.

3. Test Chamber

- Geometrically center the cylinder on top of base plate and weld them together, as shown in Figure 62.
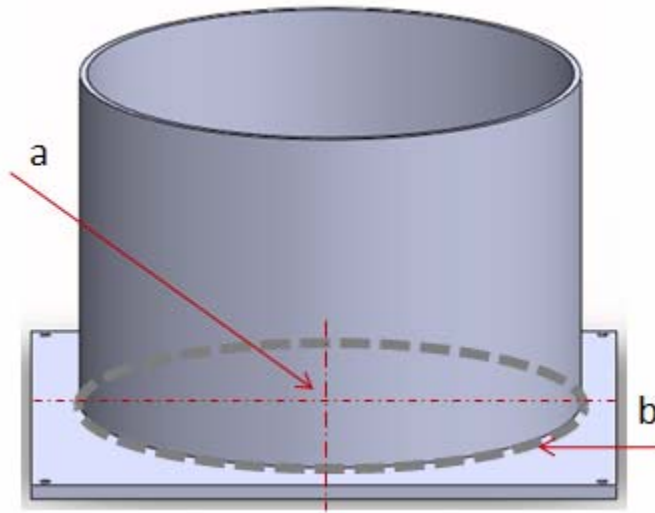
Figure 62.   3D CAD test chamber construction, (a): geometrical center, (b): welding line.

- Weld flange to the top of the cylinder. As shown in Figure 63.
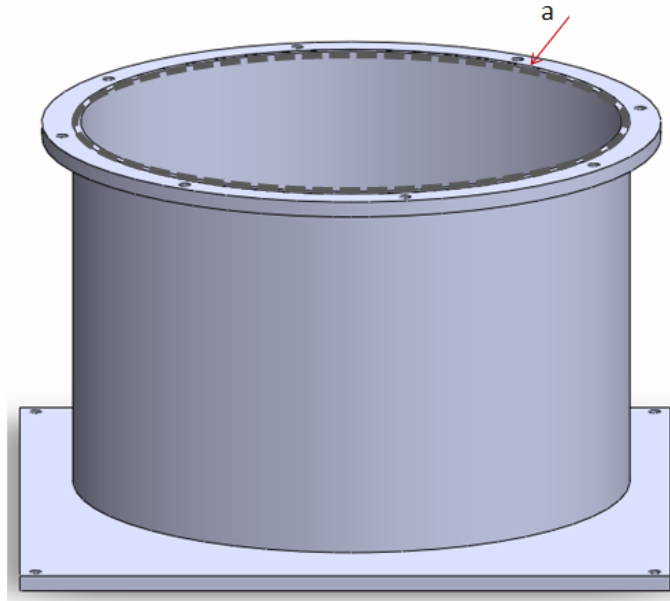
Figure 63.   3D CAD test chamber construction, (a): welding line.

- The cover plate is then bolted to the flange, as shown in Figure 64.
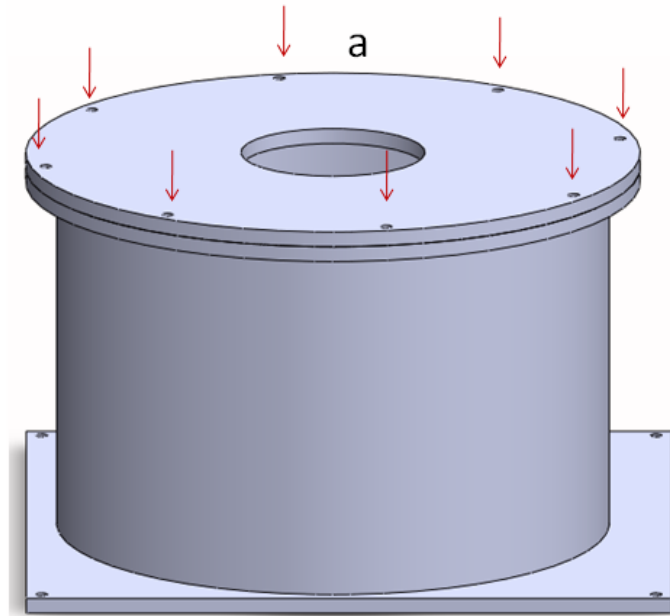
Figure 64.   3D CAD test chamber construction, (a): bolt cover with 5/8"
bolts.

Illustrated in Figure 65 is a 3D CAD assembly drawing of the test chamber.
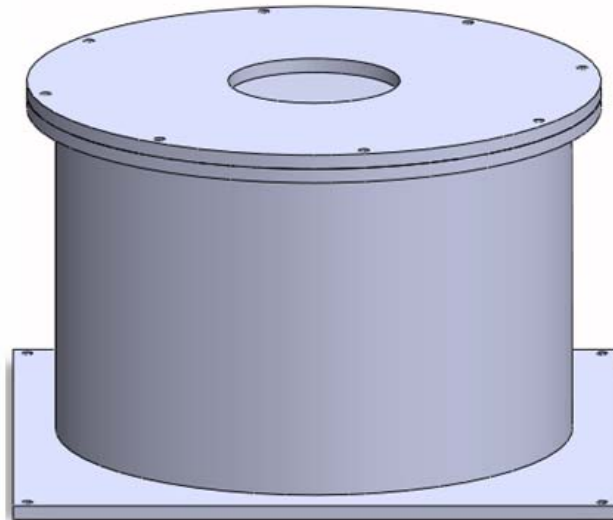
Figure 65.   3D CAD test chamber construction.

Figure 66 shows a cross-sectional view of the assembly.
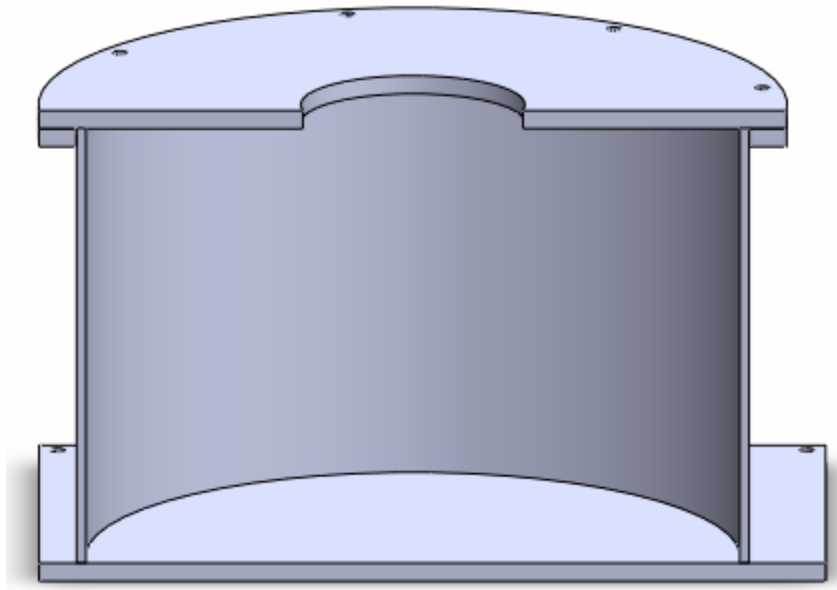
Figure 66.   3D CAD test chamber cross-sectional view.

The final dimension of the test chamber is observed in Figure 67, with an experiment set up inside.

Figure 67.   Actual view of the test chamber.

D.   PERFORMANCE

1.   Flyer Plate

The LSTF used Nitromethane (NM) as a propellant and 67 gr. of NM produced sand debris velocities up to 500-600 m/s. It works by producing high pressure gas from explosive products behind a steel-flyer plate into a vertical chamber (75 x 75 x 50 mm.). As the detonation is initiated, the FP is rapidly accelerated by the gaseous products of the explosion (1000–1200 m/s). Flyer plates 5 mm thick and with an area of 75 x 75 mm were accelerated at sand targets in the chamber at a fixed height.
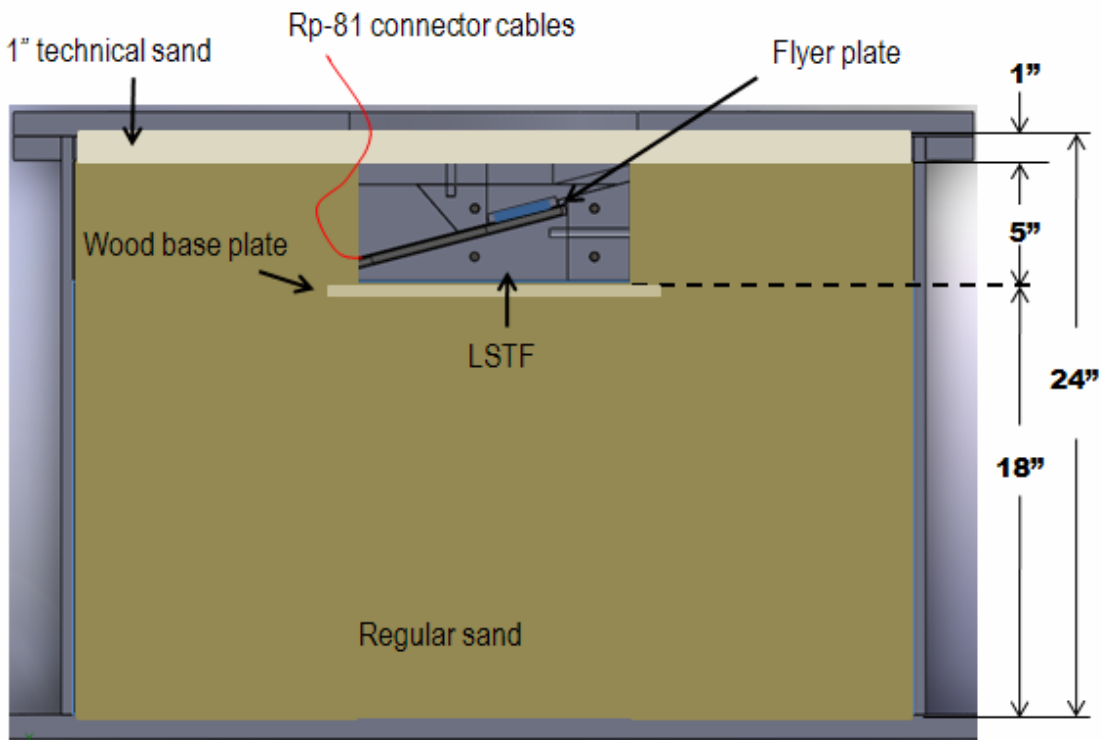
Figure 68.   LSTF final configuration inside test chamber.

In the configuration shown in Figure 68, the steel-flyer plate will strike the sand target with flat front profile perpendicular to the direction of flight. This will allow one to estimate accurately the momentum and energy deposited onto the target. Later, this information could enable the assessment of mass and velocity of the sand with the desired accuracy. It would also allow the evaluation of the effect of sand debris on targets.

2. Conical Charge

The CC used Nitromethane (NM) as propellant and 150 gr. of NM produces projectile (sand debris) velocities up to 650–750 m/s. It also works by producing high pressure explosive products gas behind a Teflon lid into a vertical conical chamber. As the detonation proceeds, the gaseous products of the explosion reach velocities of 1000–1600 m/s.
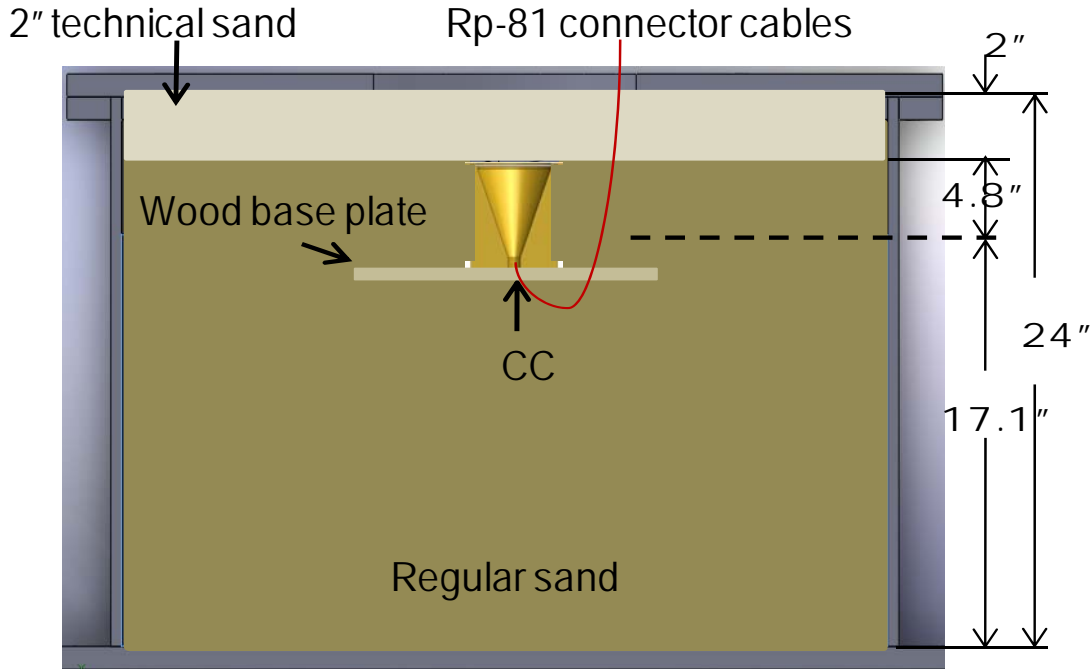
Figure 69.   CC final configuration inside test chamber.

In the configuration shown in Figure 69, NM gaseous products expanding upward produce HVSB with a flat profile. The information obtained from this experiment allows an assessment of the mass and velocity of sand with the desired profile and allows a comparison to be made with results obtained from the LSTF.

The flyer-plate technique used in this experiment had several advantages over conventional methods of producing high-velocity particles. The method was compact and fit conveniently into the test chamber. These relatively inexpensive laboratory experiments can then be used to scale HVSB experiments and to estimate full-scale results before conducting expensive full-scale experiments.

This chapter has presented the design of the laboratory-scale charges and their construction methodology. These, in conjunction with a set of well-known and controlled boundary conditions, are ideal for computational code validation. Chapter V will present the test procedure and will give a detailed description of the Standard Operation Procedure (SPO).

THIS PAGE INTENTIONALLY LEFT BLANK

V.   EXPERIMENTAL SETUP AND PROCEDURE

Initial experiments determined both the shape and velocity of the technical sand front and the ejecta thickness. The objective was to comprehensively characterize the sand profile and, thereby, calibrate and validate the dispersion aspects of the Deshpande, constitutive law used for the technical sand [7]. A high-speed camera recorded the technical sand profiles as they exited the blast chamber. Characterization of the sand profiles also served to fine-tune the details of detonation events, such as camera trigger timing and detonator placement.

A.   HIGH-SPEED VISION SYSTEM

A schematic view of the experimental setup is shown in Figure 70. The setup consists of two Digital power light PL2500DR monoligths and a Phantom V7.3 high-speed digital camera.

The optical arrangement used in the experiments has the following overall configuration:

    a.   Total intensity for the flashes 700 J.

    b.   Distance from the lens to the center of plate ~2m.

    c.   Feature spacing of the calibration grid z12 mm.

    d.   Lens F mount standard.

    e.   Maximum sensor resolution 800 x 600.

    f.   Maximum frame rate of 190,476 fps @ 32x8.

    g.   Image intensity quantization at 14 bits.

Since the Complementary metal–oxide–semiconductor (CMOS) array in the camera can be programmed to record at higher frame rates with lower inter-frame time using reduced image resolution, in this study the camera was operated at these settings: 256 x 256 array size, 13 µs and at 25 µs inter-frame times (equivalent to 76,923 and 40,000 fps, respectively). The camera and Digital

power lights were synchronized and triggered through an external TTL pulse. All the images were recorded digitally and stored with 12 bits of resolution.

B.   FIELD TEST

All experiments were performed at the explosive range facility operated by Pacific Scientific Energetic Materials Company (California), Inc. All testing was performed in the test chamber that contained the EVDs (LSTF or CC), standard sand (filling the cylinder), technical sand (Mil 7 Glass Beads sieve: 60–80, equivalent to microns: 250–298), and test recording equipment.
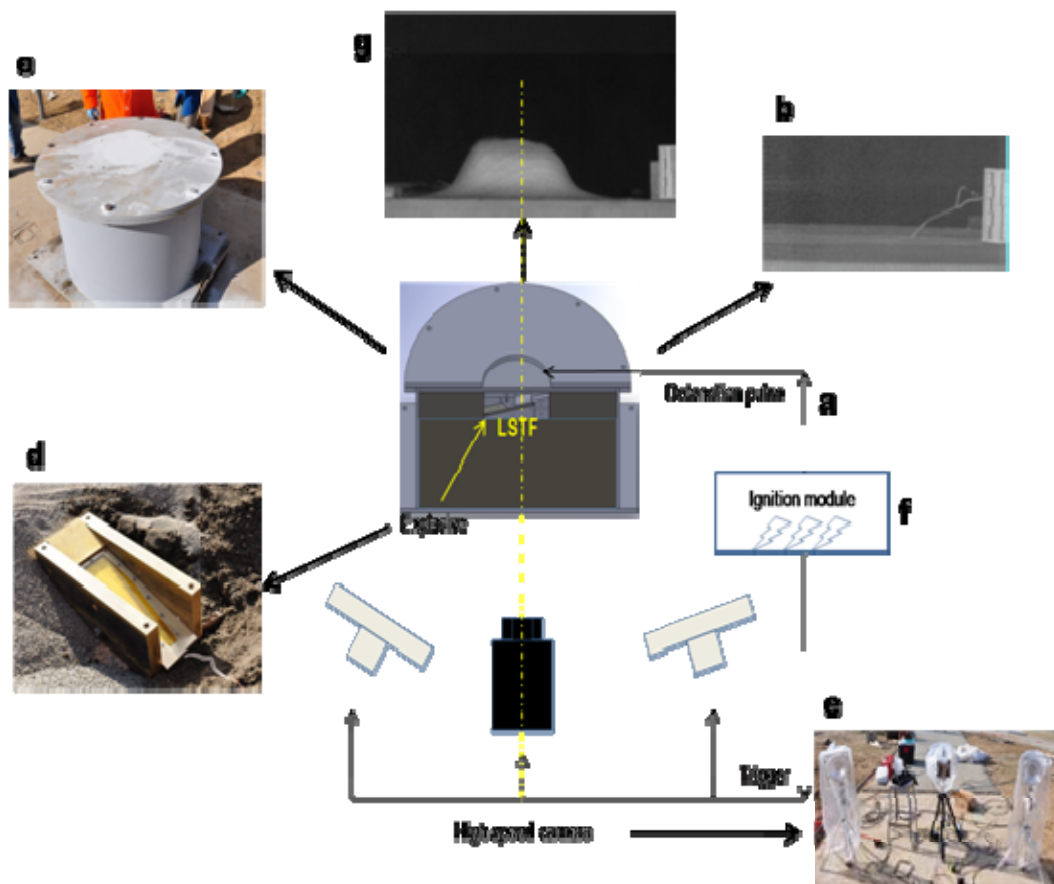
Figure 70.   Schematic (a): with photos of the experimental setup: top right (b): digital view of experimental setup showing setup just prior to blast loading; top left (c): sand filled steel test chamber serving as blast pit; bottom left (d): LSTF showing NM-DETA explosive mixture case; bottom right (e): two digital power lights and a high-speed and high-sensitivity Phantom V7.3 camera; (f): middle right ignition module; top center (g) flat sand profile from experiment.

C. EXPERIMENTAL PROCEDURE

The following procedure was used to perform the experiments (detailed SOP in Appendix E):

First, the NM and DETA explosive mixture was prepared in an assembly area, a detonator RP-81 was glued by 2-part epoxy and then the EVDs were filled with the mixture.

Second, the EVD case was placed close to the sand pit where the blast experiment is performed.

Third, the high-speed camera and the two Digital power lights were separated from the explosion site to avoid camera motion induced by the explosive blast loading. After mounting the camera outside the blast area, the high-speed camera was rotated and positioned to view the specimen and maximize the field of view on the test assembly.

Fourth, the two Digital power lights were set up at both sides of the test chamber and used to calibrate the vision system.

Fifth, the charge assembly used in the experiments (consisting of a high-energy NM-DETA explosive mixture and a detonator model RP-81) was placed in the sand pit inside the test chamber at a pre-determined depth of burial and high-voltage detonator cable was attached to the detonator on one end, and to the high-voltage source on the other end.

Sixth, the test chamber was closed, with the cover bolted tightly to the main body. The chamber then was filled with technical sand and leveled.

Seven, two simultaneous pulses were generated from the Ignition Module, one a 5 V camera trigger and the other a high-voltage (4000 V) detonation pulse.

As soon as the explosion was initiated, synchronized images with inter-frame times as low as 13 µs were recorded during the explosive HVSB.

During the experiments, a square section of the sand layer located exactly above the buried EVD and the geometrical center of the test chamber exhaust was observed with the high-speed camera. The field of view was around 8" x 4" (13 and 25 μs inter-frame time for the different tests) with the image size of 256 x 256. Results are shown in Figures 71–72. Test details are shown in Figure 73.
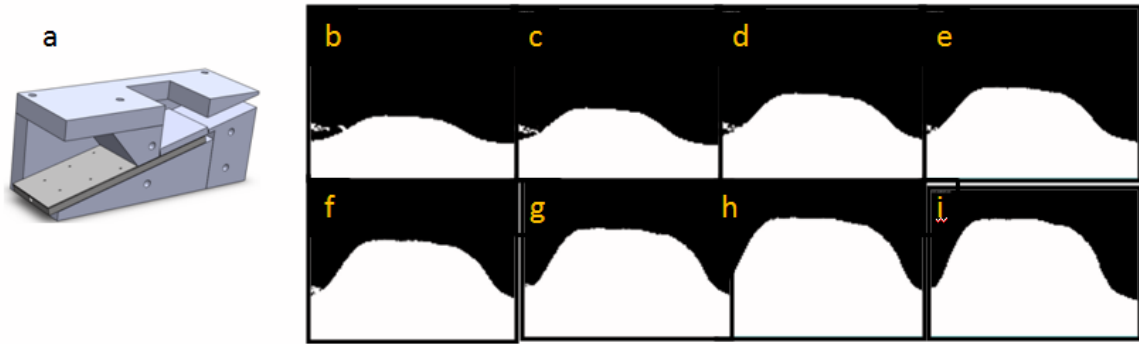

Figure 71.   (a): Configuration of LSTF experimental setup. (b)– (i): Sequence of first test high-speed images (25 μs) obtained during tests.
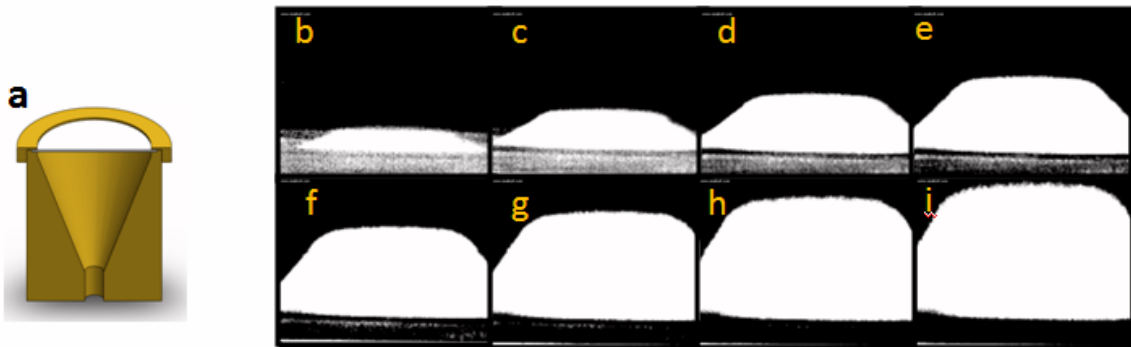

Figure 72.   (a): Configuration of CC experimental setup. (b)– (ii): Sequence of first test high-speed images (13 μs) obtained during tests.

70
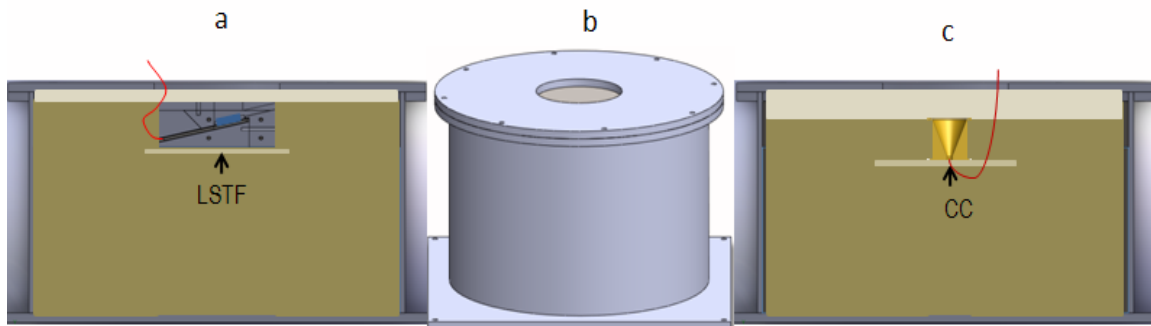
Figure 73.   Test chamber assembly, (a): LSTF setup, (b): note that a 12"
diameter opening was left open at the top to allow for the sand
to interact with target plates and vertical pendulum systems,
(c): CC setup.

In this chapter, the experimental procedure was established. Experiments produced images of sand velocity and showed the sand dispersion from planar shock waves.

Plots from Chapters III and V will be compared in Chapter VI. The differences may determine how useful these techniques are in the simulation of buried mines and/or IEDs debris damage. They will also be used for code validation purposes.

THIS PAGE INTENTIONALLY LEFT BLANK

VI.   RESULTS AND DISCUSSION

The flyer plate technique (LSTF) resulted in a 40% difference in sand velocities between experiments and simulations, as shown in Figure 74. As predicted, the simulations overestimated the sand velocities and this was mainly due to omitting 3D effects in the simulations. The experimental results were obtained from image analysis of the high-speed video recording. The resolution of each image was 256 x 256 pixels, the field of view was represented to be 1.38 mm/pixel.   The frames were taken at 40,000 fps, which would yield a velocity resolution of 57 m/s per pixel. This explains that the oscillations in Figure 74b indicate a velocity of 350 m/s ± 57m/s are due to 1 pixel variations.
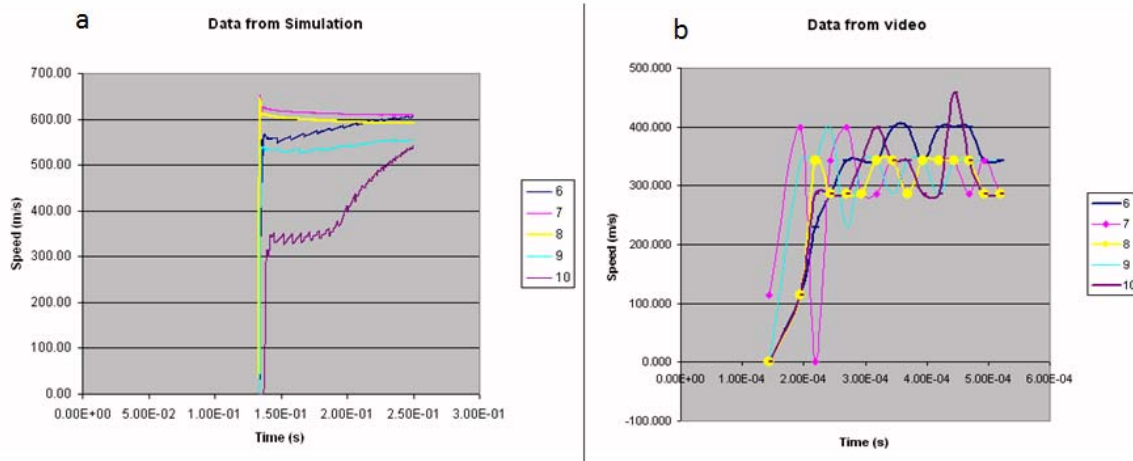

Figure 74.   Velocity of gauge number 8 (depicted in yellow) shows the characteristic velocity of the HVSB with a difference of 40% between simulations and experiments: (a): data from simulations, (b): data from experiments.

The conical charge (CC) experimental results showed better agreement, within about 10% of the simulation's predicted sand velocities. The small difference in results is probably due principally to the difference on sand density between the computational default sand density (1.674 g/cc) and the experimental density from technical sand (1.513 g/cc).
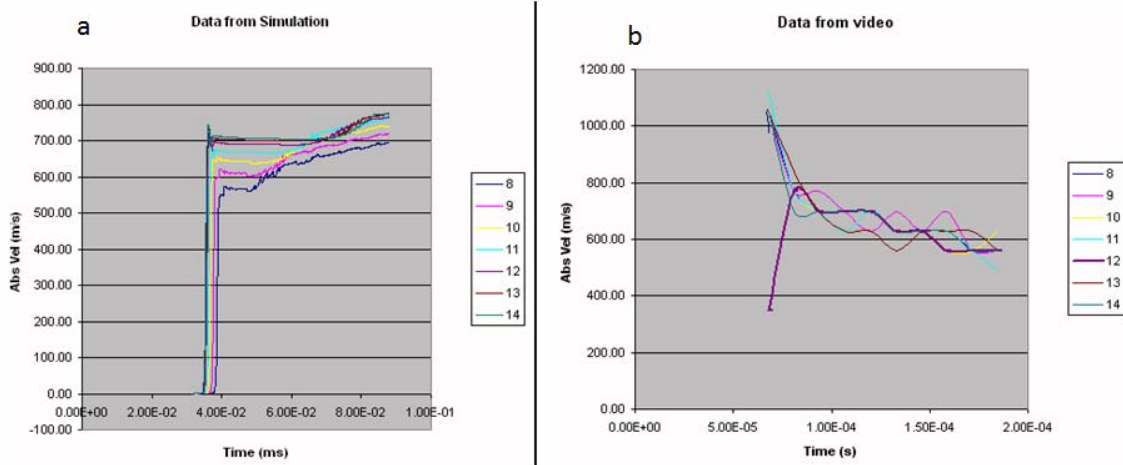
Figure 75.   Velocity of gauge number 11 depicted in light blue shows the
characteristic velocity of the HVSB with a difference of 10%
between simulations and experiments:(a): data from
simulations, (b): data from experiments.

The sand density utilized for the experiments was obtained from
laboratory measurements as shown on Table 1.

Test #	Volume (cc) ± 1 cc	Mass (gr) ± 0.1 gr.	ρ (g/cc)	Mass 33% water	ρ 33% water (g/cc)	Mass 66% water	ρ 66% water (g/cc)	Mass 100% Saturated sand	ρ 100% water (g/cc)
1	10	15	1.500	16.6	1.660	17.8	1.780	18.6	1.860
2	20	30	1.500	32.4	1.620	34.8	1.740	37.2	1.860
3	30	45.4	1.513	48.8	1.627	52	1.733	56.6	1.887
4	40	61.1	1.528	64.6	1.615	69	1.725	75.8	1.895
5	50	76.2	1.524	81.5	1.630	86.8	1.736	94.3	1.886
6	60	90.7	1.512	97.1	1.618	104.2	1.737	112.8	1.880
7	70	106	1.514	112.9	1.613	121	1.729	131.7	1.881
8	80	120.3	1.504	127.3	1.591	136.7	1.709	149.2	1.865
9	90	134.3	1.492	143.2	1.591	153.6	1.707	166.7	1.852
10	100	148	1.480	158.7	1.587	170	1.700	185	1.850

Table 1.   Density measurements from technical sand obtained on laboratory.

Error analysis indicates less than 1.5% total error in dry sand density
measurements, for wet sand the estimate error is less than 3%.
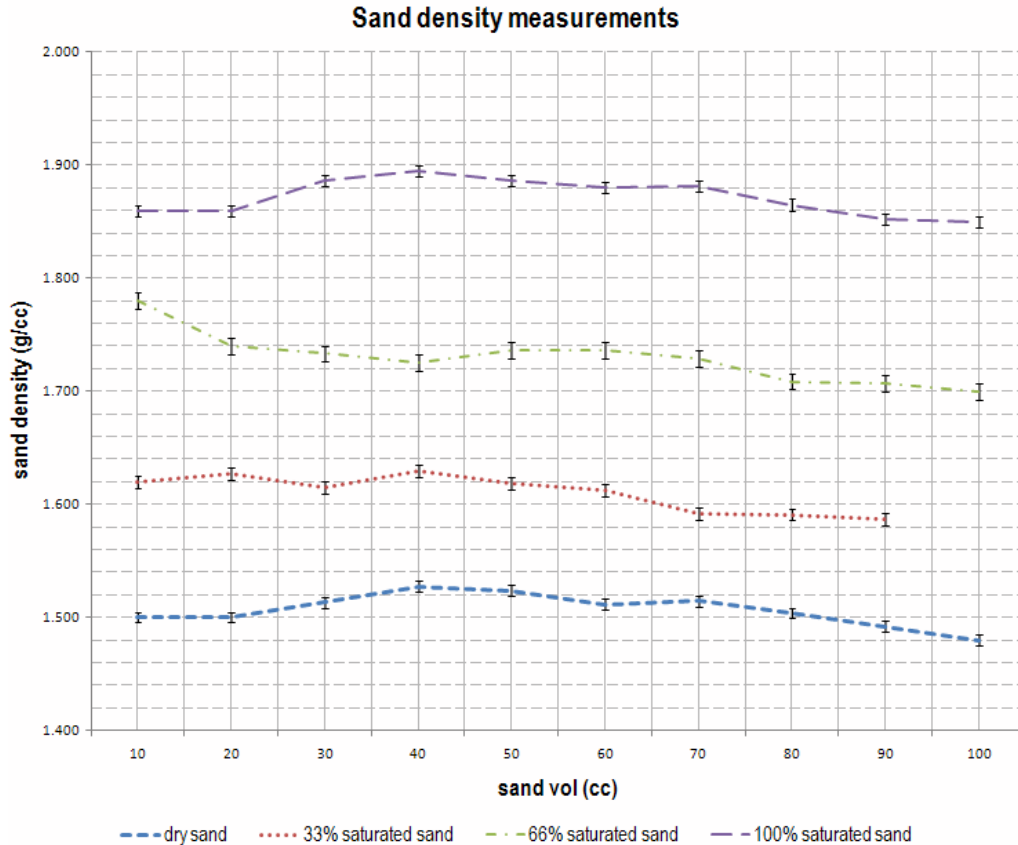
Figure 76.   Sand density from measurements on laboratory.

Experimental laboratory techniques were used to measure the density of technical sand (Mil 7 Glass Bead, sieve: 60–80), with measurements conducted with dry sand and water-saturated sand at different percentages of water. The technical sand was composed of 250–298 micron diameter glass spheres saturated with distilled water. The beads were sorted using a 150 mL beaker. The mass of the dry spheres was measured; distilled water was then added through the sample and then allowed to rest to dissolve trapped air bubbles.

Since the goal of this work was to investigate the effect of HVSB, we chose to achieve homogeneous sediment at the expense of simplicity in the density data analysis.

$$\rho \text{ ratio} = \rho_{experiments} / \rho_{simulations} = 1.513 \text{ g/cc} / 1.674 \text{ g/cc}$$

$$\rho_{experiments} = 0.9 \, \rho_{simulations}$$

The original compaction parameters for sand on simulation were then modified by multiplying the sand density by 0.9 factor.

VII. CONCLUSIONS AND RECOMMENDATIONS

This chapter presents conclusions and recommendations for follow-up work. The main objectives of this thesis were to design, build, and test the Laboratory-scale Test Facility and the Cylindrical Charge; test results confirm that these objectives were met.

A. CONCLUSIONS

Testing confirmed that controlled detonation and use of a slanted flyer plate allows a flat ejected sand profile to be achieved. Although simulations over-predicted sand velocities by up to 40%, the trends and flat sand profiles were captured correctly. The results of this study show that:

- A small-scale test environment for armor systems was designed for future work against buried explosive threats.

- Detailed results support the need for validation data for ongoing modeling efforts in these areas for cellular composite structures for advanced armor designs.

- In addition, the design of an axis-symmetric charge (CC) configuration allowed for a good comparison between experiments and simulations, and resulted in agreement to within 10% in sand velocities.

B. RECOMMENDATIONS

Finally, armor design optimization research may be carried out by a clever combination of analytical, numerical, and experimental methods.

This laboratory-scale approach to materials blast testing and research can be used in various ways to extend the current understanding of HVSB. Future simulations would include the replication of simulations, in full 3D, that more accurately represent experimental work.

- Data can then be introduced into the constitutive equations being used by hydrocodes for a reliable simulation of mine survivability phenomena.

- Appropriate equations of state for the technical sand are required in order to reduce the 10% error found in the CC experiments. Perhaps the inclusion of a p-alpha model for the technical sand in question is required. Such work will be required to take place in a light gas gun facility, such as the one in operation at NPS' Spanagel Hall Room 027.

APPENDIX A. CONFIGURATION OF SIMULATIONS IN AUTODYN

A.   LABORATORY-SCALE TEST FACILITY SIMULATIONS

Symmetry: 2D Axial.
Units: Length mm, mass mg, time ms.
      Origin of the Coordinate System: Located in the left wall of the LSTF.
      Boundaries Type: Flow-out (Euler), Preferred Material: All Equal, I and J lines located at the edge of the grids.
      Solver: Euler, 1 cells per mm^2.
      Joins: Parts Joined.
      Detonation: 2D point, Initiation time: 0, Range of Influence: Unrestricted.

B.   MATERIAL PARAMETERS FOR SIMULATIONS

Table 2.   Material parameters for simulations.

ANSYS AUTODYN

Material Name - STEEL 4340:

Equation of State	Linear
Reference density	7.83000E+00 (g/cm3)
Bulk Modulus	1.59000E+08 (kPa)
Reference Temperature	3.00000E+02 (K)
Specific Heat	4.77000E+02 (J/kgK)
Thermal Conductivity	0.00000E+00 (J/mKs)
Strength	Johnson Cook
Shear Modulus	8.18000E+07 (kPa)
Yield Stress	7.92000E+05 (kPa)
Hardening Constant	5.10000E+05 (kPa)
Hardening Exponent	2.60000E-01 (none)
Strain Rate Constant	1.40000E-02 (none)
Thermal Softening Exponent	1.03000E+00 (none)
Melting Temperature	1.79300E+03 (K)
Ref. Strain Rate (/s)	1.00000E+00 (none)

Strain Rate Correction	1st Order
Failure	None
Erosion	None
Material Cutoffs	-
Maximum Expansion	1.00000E-01 (none)
Minimum Density Factor	1.00000E-04 (none)
Minimum Density Factor (SPH)	2.00000E-01 (none)
Maximum Density Factor (SPH)	3.00000E+00 (none)
Minimum Soundspeed	1.00000E-06 (m/s)
Maximum Soundspeed	1.01000E+20 (m/s)
Maximum Temperature	1.01000E+20 (K)
Reference:	Engng. Frac. Mech. Vol 21. No. 1. pp 31-48. 1985 Johnson & Cook

Material Name – NM:

Equation of State	JWL
Reference Density	1.12800E+00 (g/cm3)
Parameter A	2.09250E+08 (kPa)
Parameter B	5.68900E+06 (kPa)
Parameter R1	4.40000E+00 (none)
Parameter R2	1.20000E+00 (none)
Parameter W	3.00000E-01 (none)
C-J Detonation Velocity	6.28000E+03 (m/s)
C-J Energy/Unit Volume	5.10000E+06 (kJ/m3)
C-J Pressure	1.25000E+07 (kPa)
Burn on Compression Fraction	0.00000E+00 (none)
Pre-burn Bulk Modulus	0.00000E+00 (kPa)
Adiabatic Constant	0.00000E+00 (none)
Auto-convert to Ideal Gas	Yes

Additional Options (Beta)	None
Strength	None
Failure	None
Erosion	None
Material Cutoffs	-
Maximum Expansion	1.00000E-01 (none)
Minimum Density Factor	1.00000E-06 (none)
Minimum Density Factor (SPH)	2.00000E-01 (none)
Maximum Density Factor (SPH)	3.00000E+00 (none)
Minimum Soundspeed	1.00000E-06 (m/s)
Maximum Soundspeed	1.01000E+20 (m/s)
Maximum Temperature	1.01000E+20 (K)
Reference:	"LLNL Explosives Handbook," Dobratz B.M & Crawford P.C., UCRL-52997 Rev. 2 January 1985

Material Name – AIR:

Equation of State	Ideal Gas
Reference Density	1.22500E-03 (g/cm3)
Gamma	1.40000E+00 (none)
Adiabatic Constant	0.00000E+00 (none)
Pressure Shift	0.00000E+00 (kPa)
Reference Temperature	2.88200E+02 (K)
Specific Heat	7.17600E+02 (J/kgK)
Thermal Conductivity	0.00000E+00 (J/mKs)
Strength	None
Failure	None
Erosion	None

Material Cutoffs	-
Maximum Expansion	1.00000E-01 (none)
Minimum Density Factor	1.00000E-04 (none)
Minimum Density Factor (SPH)	2.00000E-01 (none)
Maximum Density Factor (SPH)	3.00000E+00 (none)
Minimum Soundspeed	1.00000E-02 (m/s)
Maximum Soundspeed	1.01000E+20 (m/s)
Maximum Temperature	1.01000E+20 (K)
Reference:	"Thermodynamic and Transport Properties of Fluids, SI Units," GFC Rogers, YR Mayhew

Material Name - BRASS

Equation of State	Shock
Reference Density	8.45000E+00 (g/cm3)
Gruneisen Coefficient	2.04000E+00 (none)
Parameter C1	3.72600E+03 (m/s)
Parameter S1	1.43400E+00 (none)
Parameter Quadratic S2	0.00000E+00 (s/m)
Relative Volume, VE/V0	0.00000E+00 (none)
Relative Volume, VB/V0	0.00000E+00 (none)
Parameter C2	0.00000E+00 (m/s)
Parameter S2	0.00000E+00 (none)
Reference Temperature	0.00000E+00 (K)
Specific Heat	0.00000E+00 (J/kgK)
Thermal Conductivity	0.00000E+00 (J/mKs)
Strength	None

Failure	None
Erosion	None
Material Cutoffs	-
Maximum Expansion	1.00000E-01 (none)
Minimum Density Factor	1.00000E-04 (none)
Minimum Density Factor (SPH)	2.00000E-01 (none)
Maximum Density Factor (SPH)	3.00000E+00 (none)
Minimum Soundspeed	1.00000E-06 (m/s)
Maximum Soundspeed	1.01000E+20 (m/s)
Maximum Temperature	1.01000E+20 (K)
Reference:	LA-4167-MS. May 1 1969. Selected Hugoniots

Material Name – SAND:

Equation of State	Compaction
Reference Density	2.6410E+00 (g/cm3)
Density #1	1.6740E+00 (g/cm3)
Density #2	1.7395E+00 (g/cm3)
Density #3	1.8738E+00 (g/cm3)
Density #4	1.9970E+00 (g/cm3)
Density #5	1.1438E+00 (g/cm3)
Density #6	2.2500E+00 (g/cm3)
Density #7	2.3800E+00 (g/cm3)
Density #8	2.4850E+00 (g/cm3)
Density #9	2.5850E+00 (g/cm3)
Density #10	2.6713E+00 (g/cm3)
Pressure #1	0.00000E+00 (kPa)
Pressure #2	4.57700E+03 (kPa)
Pressure #3	1.49800E+04 (kPa)
Pressure #4	2.91510E+04 (kPa)

Pressure #5	5.91750E+04 (kPa)
Pressure #6	9.80980E+04 (kPa)
Pressure #7	1.79443E+05 (kPa)
Pressure #8	2.89443E+05 (kPa)
Pressure #9	4.50198E+05 (kPa)
Pressure #10	6.50660E+05 (kPa)
Unloading Method	Linear
Density (Soundspeed) #1	1.6740E+00 (g/cm3)
Density (Soundspeed) #2	1.7456E+00 (g/cm3)
Density (Soundspeed) #3	1.08630E+00 (g/cm3)
Density (Soundspeed) #4	1.1468E+00 (g/cm3)
Density (Soundspeed) #5	2.3000E+00 (g/cm3)
Density (Soundspeed) #6	2.5720E+00 (g/cm3)
Density (Soundspeed) #7	2.5980E+00 (g/cm3)
Density (Soundspeed) #8	2.6350E+00 (g/cm3)
Density (Soundspeed) #9	2.6410E+00 (g/cm3)
Density (Soundspeed) #10	2.8000E+00 (g/cm3)
Soundspeed #1	2.65200E+02 (m/s)
Soundspeed #2	8.52100E+02 (m/s)
Soundspeed #3	1.72170E+03 (m/s)
Soundspeed #4	1.87550E+03 (m/s)
Soundspeed #5	2.26480E+03 (m/s)
Soundspeed #6	2.95610E+03 (m/s)
Soundspeed #7	3.11220E+03 (m/s)
Soundspeed #8	4.60000E+03 (m/s)
Soundspeed #9	4.63400E+03 (m/s)
Soundspeed #10	4.63400E+03 (m/s)
Strength	MO Granular
Pressure #1	0.00000E+00 (kPa)

Pressure #2	3.40100E+03 (kPa)
Pressure #3	3.48980E+04 (kPa)
Pressure #4	1.01324E+05 (kPa)
Pressure #5	1.84650E+05 (kPa)
Pressure #6	5.00000E+05 (kPa)
Pressure #7	0.00000E+00 (kPa)
Pressure #8	0.00000E+00 (kPa)
Pressure #9	0.00000E+00 (kPa)
Pressure #10	0.00000E+00 (kPa)
Yield Stress #1	0.00000E+00 (kPa)
Yield Stress #2	4.23500E+03 (kPa)
Yield Stress #3	4.46950E+04 (kPa)
Yield Stress #4	1.24035E+05 (kPa)
Yield Stress #5	2.26000E+05 (kPa)
Yield Stress #6	2.26000E+05 (kPa)
Yield Stress #7	0.00000E+00 (kPa)
Yield Stress #8	0.00000E+00 (kPa)
Yield Stress #9	0.00000E+00 (kPa)
Yield Stress #10	0.00000E+00 (kPa)
Density #1	1.67400E+00 (g/cm3)
Density #2	1.74570E+00 (g/cm3)
Density #3	2.08630E+00 (g/cm3)
Density #4	2.14680E+00 (g/cm3)
Density #5	2.30000E+00 (g/cm3)
Density #6	2.57200E+00 (g/cm3)
Density #7	2.59800E+00 (g/cm3)
Density #8	2.63500E+00 (g/cm3)
Density #9	2.64100E+00 (g/cm3)
Density #10	2.80000E+00 (g/cm3)

Yield Stress #1	0.00000E+00 (kPa)
Yield Stress #2	0.00000E+00 (kPa)
Yield Stress #3	0.00000E+00 (kPa)
Yield Stress #4	0.00000E+00 (kPa)
Yield Stress #5	0.00000E+00 (kPa)
Yield Stress #6	0.00000E+00 (kPa)
Yield Stress #7	0.00000E+00 (kPa)
Yield Stress #8	0.00000E+00 (kPa)
Yield Stress #9	0.00000E+00 (kPa)
Yield Stress #10	0.00000E+00 (kPa)
Density #1	1.67400E+00 (g/cm3)
Density #2	1.74570E+00 (g/cm3)
Density #3	2.08630E+00 (g/cm3)
Density #4	2.14680E+00 (g/cm3)
Density #5	2.30000E+00 (g/cm3)
Density #6	2.57200E+00 (g/cm3)
Density #7	2.59800E+00 (g/cm3)
Density #8	2.63500E+00 (g/cm3)
Density #9	2.64100E+00 (g/cm3)
Density #10	2.80000E+00 (g/cm3)
Shear Modulus #1	7.69000E+04 (kPa)
Shear Modulus #2	8.69400E+05 (kPa)
Shear Modulus #3	4.03170E+06 (kPa)
Shear Modulus #4	4.90690E+06 (kPa)
Shear Modulus #5	7.76900E+06 (kPa)
Shear Modulus #6	1.48009E+07 (kPa)
Shear Modulus #7	1.65710E+07 (kPa)
Shear Modulus #8	3.67180E+07 (kPa)
Shear Modulus #9	3.73470E+07 (kPa)

Shear Modulus #10	3.73470E+07 (kPa)
Failure	Hydro (Pmin)
Hydro Tensile Limit	-1.00000E+00 (kPa)
Reheal	Yes
Crack Softening	No
Stochastic Failure	No
Erosion	Geometric Strain
Erosion Strain	2.00000E+00 (none)
Type of Geometric Strain	Instantaneous
Material Cutoffs	-
Maximum Expansion	1.00000E-01 (none)
Minimum Density Factor	1.00000E-04 (none)
Minimum Density Factor (SPH)	2.00000E-01 (none)
Maximum Density Factor (SPH)	3.00000E+00 (none)
Minimum Soundspeed	1.00000E-06 (m/s)
Maximum Soundspeed	1.01000E+20 (m/s)
Maximum Temperature	1.01000E+20 (K)
Reference:	Laine L. Sandvik A., "Derivation of Mechanical Properties for Sand," 4th SILOS, CI-Premier LTD, pp 361 -367

THIS PAGE INTENTIONALLY LEFT BLANK

APPENDIX B. DRAWINGS

A.   LSTF TOP PART

B. LSTF LEFT SIDE PART

NAVAL POSTGRADUATE SCHOOL

TITLE:
Part2 Left side

SIZE A DWG. NO. 07-2009-P2 REV

SCALE: 1:3 WEIGHT: SHEET 2 OF 14

φ.38 thru holes
4 x typ

φ.38 ⊽ 0.75
TAP for 3/8-16
2 x typ

4.00
11.50
5.00
1.50
1.00
1.00
1.00
.50
.50
4.00

UNLESS OTHERWISE SPECIFIED:
DIMENSIONS ARE IN INCHES
TOLERANCES:
FRACTIONAL±
ANGULAR: MACH±   BEND ±
TWO PLACE DECIMAL ±
THREE PLACE DECIMAL ±

INTERPRET GEOMETRIC TOLERANCING PER:

MATERIAL
Brass

FINISH

NAME DATE
DRAWN FJDH
CHECKED JOS
ENG APPR.
MFG APPR.
Q.A.
COMMENTS:

NEXT ASSY USED ON
APPLICATION

C.   LSTF RIGHT SIDE PART

Ø .38 thru holes
4 x Typ

11.50

5.00

1.50

1.00

1.00

1.00

4.00

1.00

1.00

Ø .38 ▽ 0.75
TAP for 3/8-16
2 x Typ

.50

.50

NAVAL POSTGRADUATE SCHOOL

TITLE:
Part3 Right side

SIZE DWG. NO.
A   07-2009-P3   REV

SCALE:1:3   WEIGHT: SHEET 3 of 9

UNLESS OTHERWISE SPECIFIED:

DIMENSIONS ARE IN INCHES
TOLERANCES:
FRACTIONAL±
ANGULAR: MACH±   BEND ±
TWO PLACE DECIMAL   ±
THREE PLACE DECIMAL ±

INTERPRET GEOMETRIC
TOLERANCING PER:

MATERIAL

FINISH

DO NOT SCALE DRAWING

	NAME	DATE
DRAWN	FJGH	
CHECKED	JOS	
ENG APPR.		
MFG APPR.		
Q.A.		
COMMENTS:		

NEXT ASSY   USED ON
APPLICATION

5   4   3   2   1

91

D. LSTF FRONT PART

E. LSTF BOTTOM PART

F.   LSTF BACK PART

G. LSTF FLYER PLATE PART

Drawing title block:

NAVAL POSTGRADUATE SCHOOL

TITLE: Part9 flyer plate

SIZE: A
DWG. NO.: 07-2009-P9
REV

SCALE: 1:1 WEIGHT: SHEET 9 of 14

Dimensions: 2.95, 2.95, .39, .39

MATERIAL: Brass
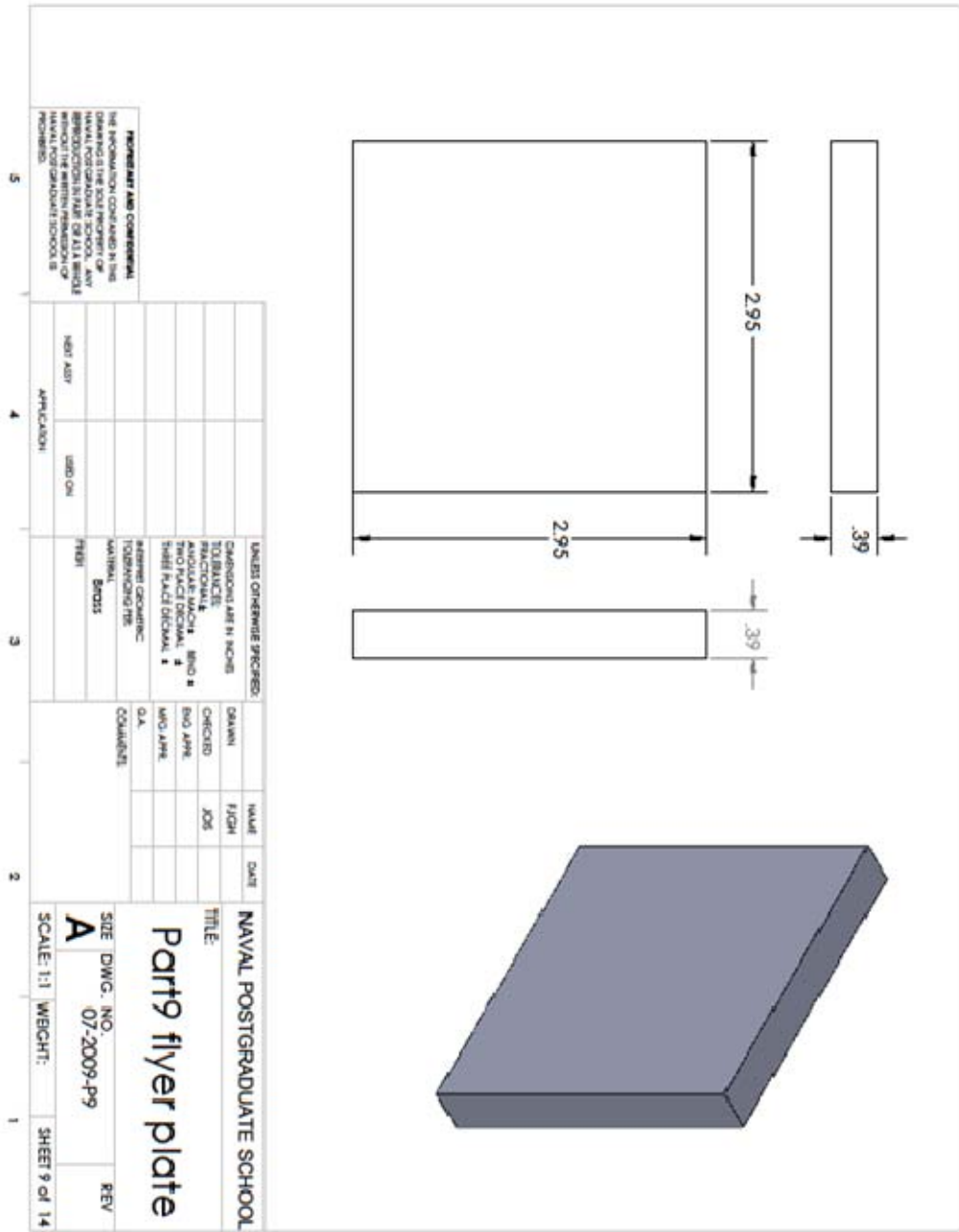
H. LSTF FINAL ASSEMBLY
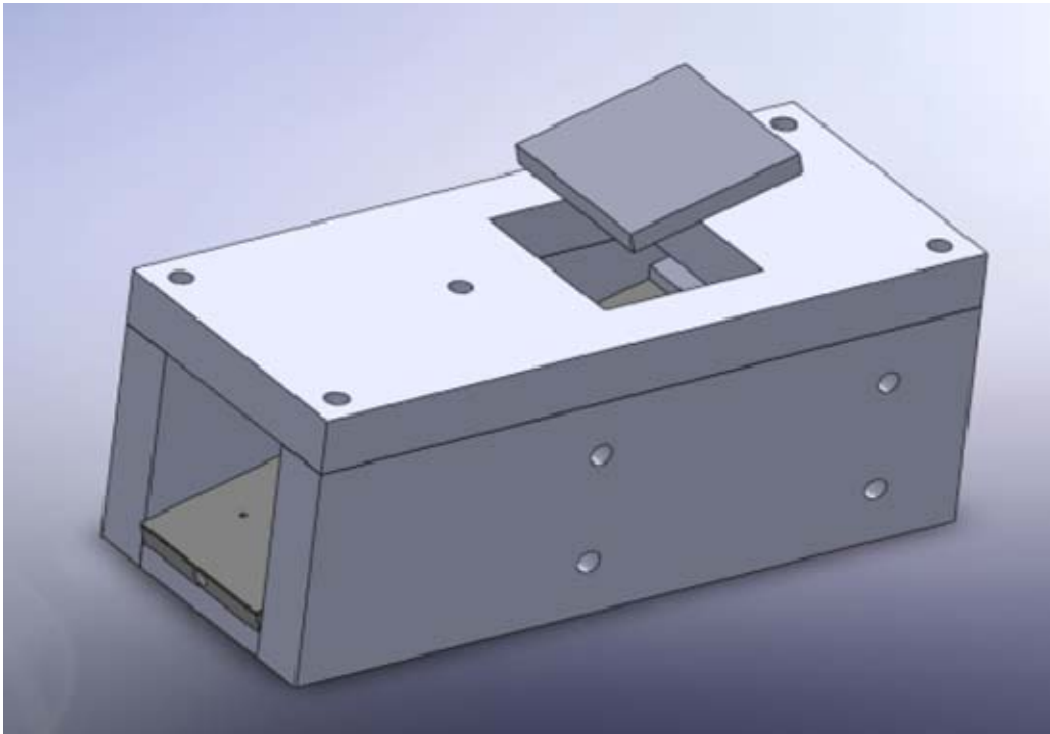
I. NITROMETHANE CASE BOTTOM PART
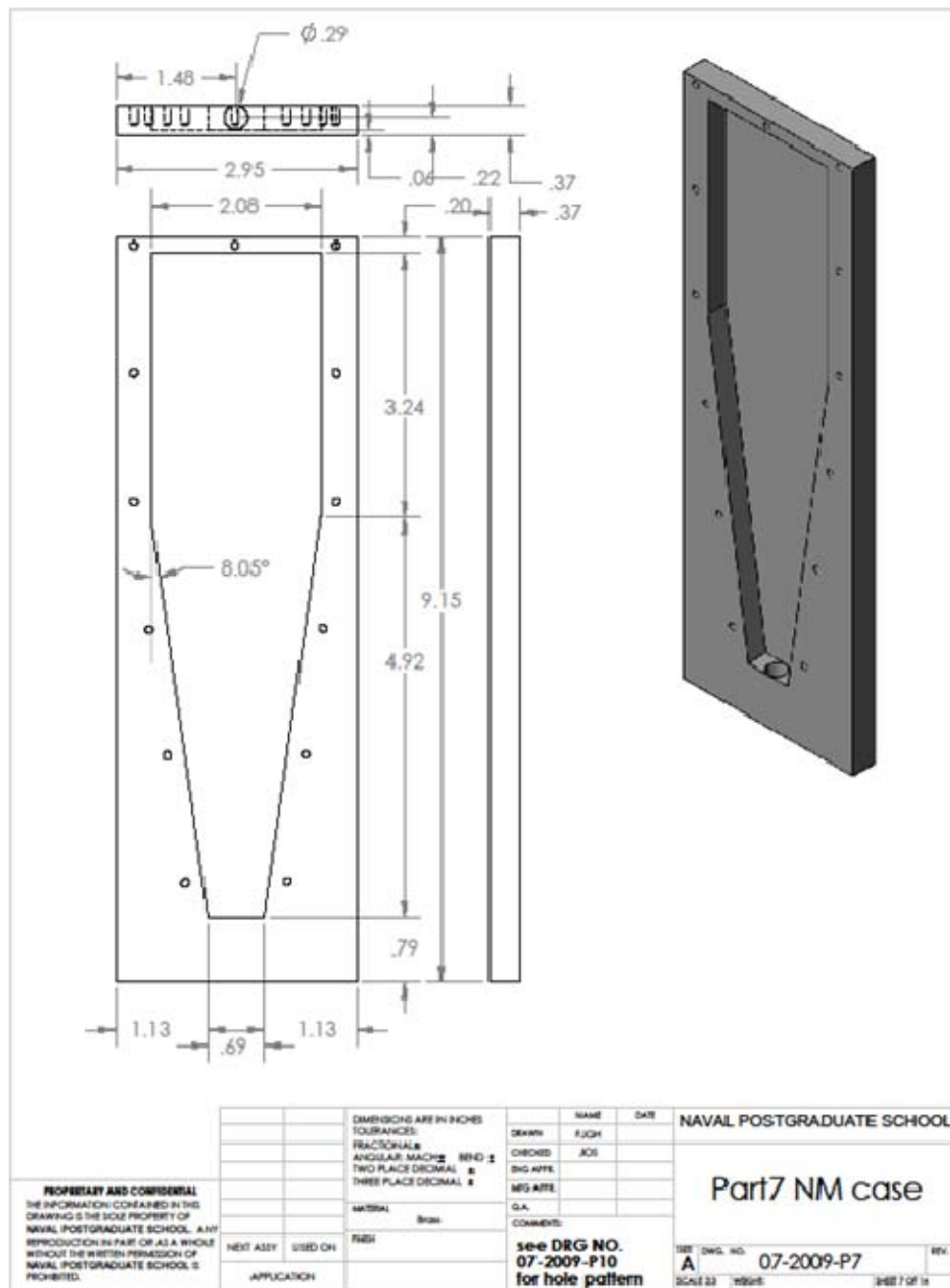
J.   NITROMETHANE CASE TOP PART
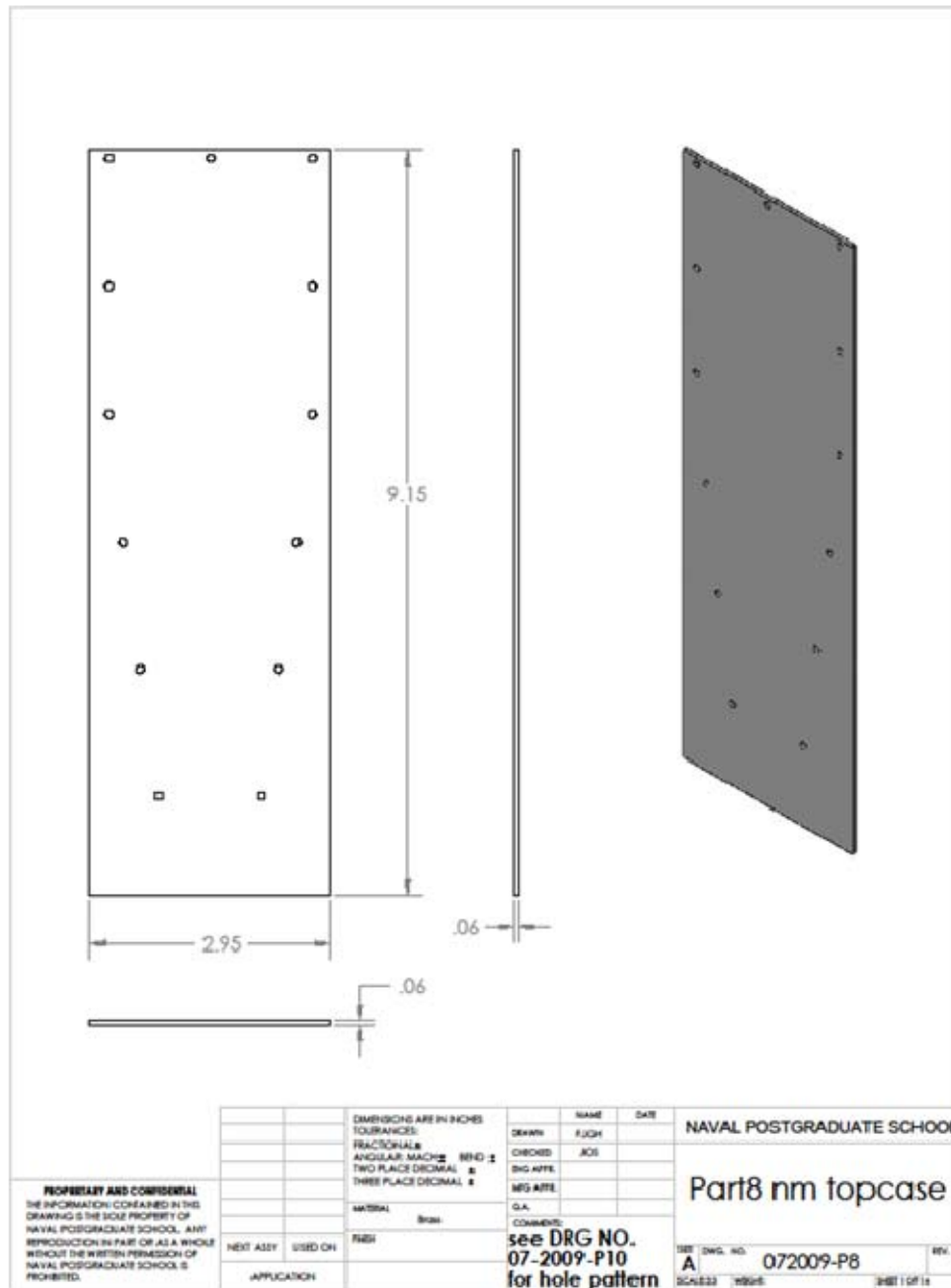
K. NITROMETHANE CASE HOLE PATTERN
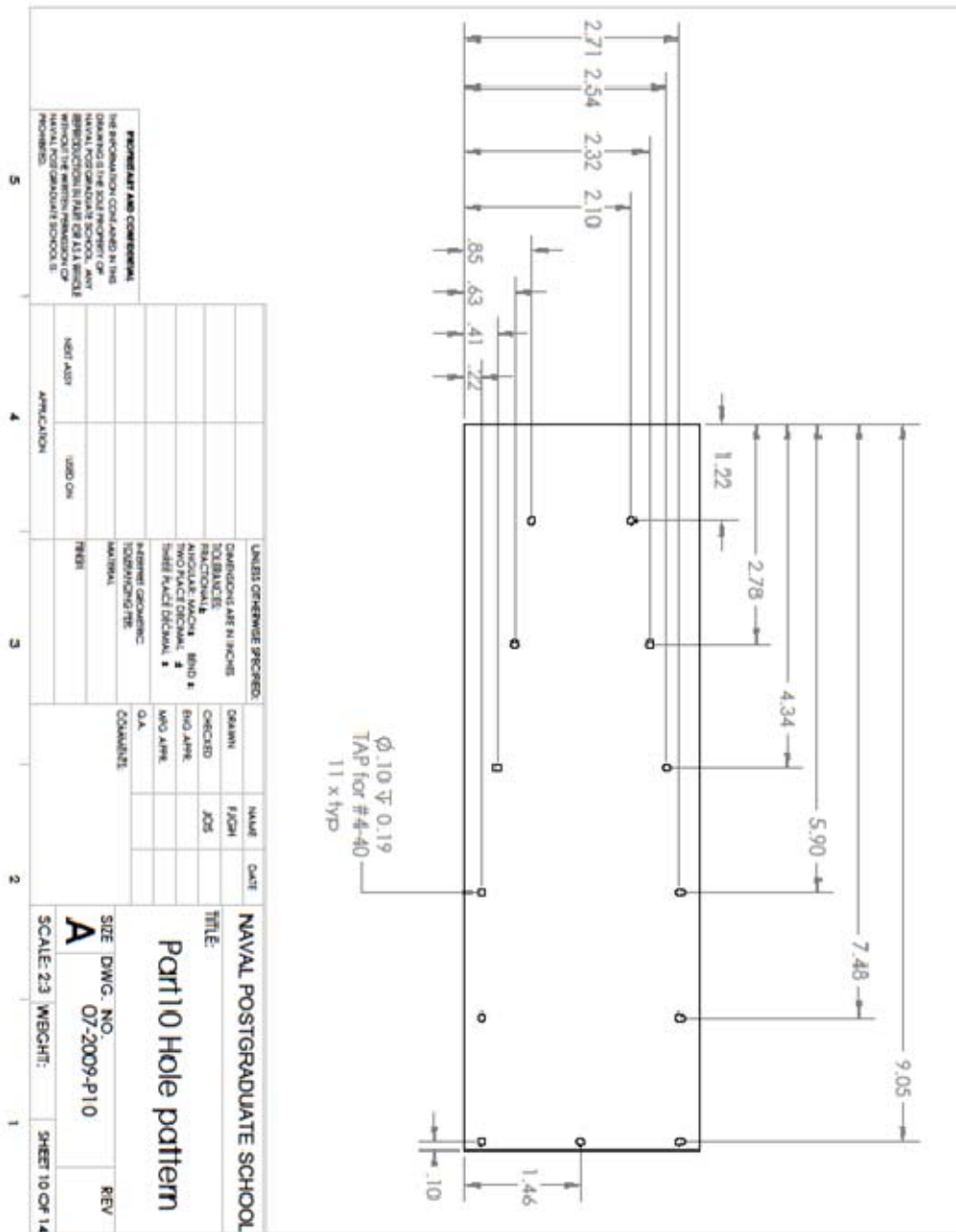
L. NITROMETHANE CASE FINAL ASSEMBLY

M.   TEST CHAMBER BASE PLATE

N.   TEST CHAMBER CYLINDER

NAVAL POSTGRADUATE SCHOOL

TITLE:
Part12 test chamber cylinder

SIZE **A**   DWG. NO.   07-2009-P12   REV

SCALE: WEIGHT: SHEET 12 OF 14

UNLESS OTHERWISE SPECIFIED:

DIMENSIONS ARE IN INCHES
TOLERANCES:
FRACTIONAL±
ANGULAR: MACH±   BEND ±
TWO PLACE DECIMAL   ±
THREE PLACE DECIMAL ±

INTERPRET GEOMETRIC
TOLERANCING PER:

MATERIAL
Steel

FINISH

DO NOT SCALE DRAWING

	NAME	DATE
DRAWN	IFJGH	
CHECKED	JOE	
ENG APPR.		
MFG APPR.		
Q.A.		
COMMENTS:		

NEXT ASSY   USED ON
APPLICATION

Φ35.00
Φ36.00

24.00

O. TEST CHAMBER FLANGE

Ø.75
8 x typ
thru holes

Ø36.00

Ø40.00

1.00

NAVAL POSTGRADUATE SCHOOL

TITLE:
Part13 test chamber flange

SIZE: A

DWG. NO. 07-2009-P13

REV

SCALE: WEIGHT: SHEET 13 OF 14

UNLESS OTHERWISE SPECIFIED:

DIMENSIONS ARE IN INCHES
TOLERANCES:
FRACTIONAL
ANGULAR: MACH   BEND
TWO PLACE DECIMAL
THREE PLACE DECIMAL

MATERIAL
Steel

FINISH

DO NOT SCALE DRAWING

NEXT ASSY   USED ON
APPLICATION

P.   TEST CHAMBER TOP PLATE

Ø12.00
thru hole

Ø.75
8 x typ
thru holes

40.00

1.00

NAVAL POSTGRADUATE SCHOOL

TITLE:
Part14 test chamber top

DWG. NO. 07-2009-P14

SIZE A

SHEET 14 OF 14

Q.   TEST CHAMBER FINAL ASSEMBLY
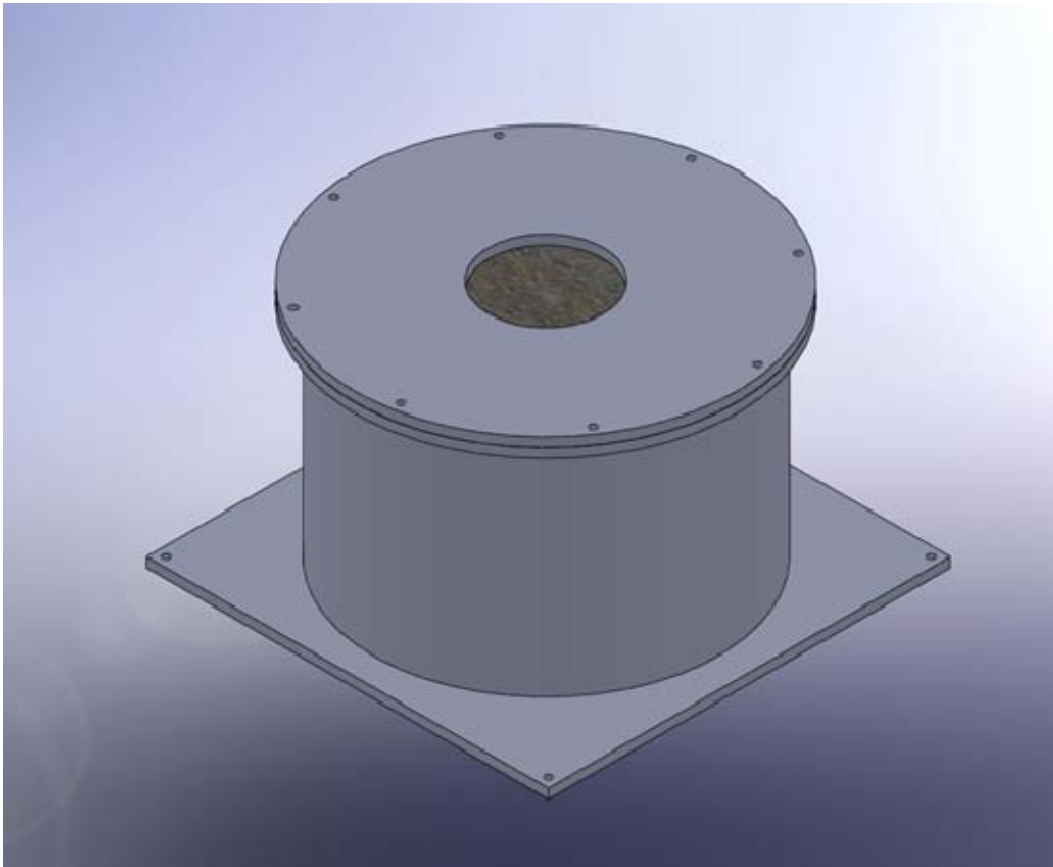
THIS PAGE INTENTIONALLY LEFT BLANK

APPENDIX C. HAZARD SUMMARIES OF CHEMICALS

A. HAZARD SUMMARY FOR NM

- NM can affect you when breathed in.
- NM should be handled as a CARCINOGEN WITH EXTREME CAUTION.
- Contact can irritate the skin and eyes.
- Breathing NM can irritate the nose, throat and lungs causing coughing, wheezing and/or shortness of breath.
- Exposure to NM can cause loss of appetite, nausea, vomiting and diarrhea.
- NM may cause headache, weakness, loss of coordination and seizures.
- High levels can interfere with the ability of the blood to carry Oxygen, causing headache, fatigue, dizziness, and a blue color to the skin and lips (methemoglobinemia). Higher levels can cause trouble breathing, collapse and even death.
- NM may damage the liver and kidneys.
- Repeated or prolonged contact with NM can cause dry, cracked skin.
- NM is a HIGHLY FLAMMABLE and REACTIVE chemical and a DANGEROUS FIRE and EXPLOSION HAZARD.

B. HAZARD SUMMARY FOR DETA

- DETA can affect you when breathed in and by passing through your skin.
- DETA is a CORROSIVE CHEMICAL and contact can severely irritate and burn the skin and eyes with possible eye damage.
- Breathing DETA can irritate the nose and throat, causing coughing and wheezing.
- DETA may cause a skin allergy. If allergy develops, very low future exposure can cause itching and a skin rash.
- DETA may cause an asthma-like allergy. Future exposure can cause asthma attacks with shortness of breath, wheezing, cough, and/or chest tightness.

THIS PAGE INTENTIONALLY LEFT BLANK

APPENDIX D. HANDLING AND USE OF NITROMETHANE

Recommendations for storage, handling and use of Nitromethane [8]:

- Store in original drums in a cool place away from hazardous conditions or transfer to an underground or barricaded storage tank.
- Protect storage and processing vessels from high-energy objects with a suitable barricade.
- Ordinary steel, aluminum, and stainless steel are satisfactory materials of construction. Formulations employing NM should not be exposed to brass, bronze, or copper unless tests have shown them to be inert. Lead, such as terne plate, is not satisfactory with NM.
- NM is combustible. Its fires can be extinguished with CO_2 or water.
- Do not expose NM to dry caustic.
- Do not sell empty NM drums to reconditioners unless they have first been well rinsed with water.
- Do not allow solutions of NM and bases to become dry.
- Certain mixtures of NM and amines are sensitive to a No. 8 cap. Thus, if such mixtures are required in a process, they should be diluted with an inert material or should be protected from severe shock.
- Some ternary mixtures of NM, amines, and heavy metal oxides can be very hazardous.
- Like other organic compounds, NM may form a sensitive explosive mixture with strong oxidizing agents, such as nitrogen tetroxide.
- Liquid NM should not be processed or handled in high pressure equipment, which would permit elevated pressures and temperatures.
- NM should be protected from all possible sources of adiabatic compression.
- Detonation traps should be installed at each end of lines of ½ - inch diameter or more from storage processing.

THIS PAGE INTENTIONALLY LEFT BLANK

APPENDIX E. STANDARD OPERATING PROCEDURES FOR HVSB TESTS USING LABORATORY-SCALE TEST FACILITY

A. NON-EXPLOSIVE OPERATIONS

NAVAL POSTGRADUATE SCHOOL PHYSICS DEPARTMENT LABORATORY-SCALE TEST FACILITY PSEMC TEST SITE				
DATE: OCTOBER-2009	ID #: NPS-ED-HVSB TEST-01	PAGE		
		1	OF	1
This document contains Standard Operating Procedures (SOPs) for HVSB TESTS using LABORATORY-SCALE TEST FACILITY (LSTF).				
RESPONSIBLE	No.	ACTIVITY (DESCRIPTION)		
NON-EXPLOSIVE OPERATIONS				
Lab Engineer	01	-Keep the test site ready to use. This includes making sure the test site is clear for testing.		
	02	-Make sure the neighboring area designed to prepare mixtures is clear to prepare Nitromethane mixtures and no obstacles exist between here and test site.		
	03	-Set up cameras and sensors.		
	04	-Run all cables and proper focusing as required.		
	05	-Test to make sure data is recorded and that the triggering is properly set up.		
	06	-Run detonator high-voltage cables between test cell and control room.		
	07	-Measure connections' resistance and then proceed to short the wires prior to connecting to high voltage power supply.		
Assistant	01	-Remove the chamber top plate. The preferred method is by using a forklift. However, if necessary, a 2, 3 or 4-man operation can be conducted to lift it manually. First, make sure all bolts and nuts have been removed.		
	02	-Fill the test chamber with sand 18″. Using shovels, or by opening new sand bags into the test chamber, fills up to the 18″ mark.		
	03	Level the base plate. Place the base plate on top of the sand, as close to the center of the chamber as possible. Use a level to make sure it is properly leveled.		
Author:	Felipe Garcia _____		Approved:	Prof. Jose O. Sinibaldi _____

B.   EXPLOSIVE OPERATIONS

NPS	NAVAL POSTGRADUATE SCHOOL PHYSICS DEPARTMENT LABORATORY-SCALE TEST FACILITY PSEMC TEST SITE		
DATE: OCTOBER-2009	ID #: NPS-ED-HVSB TEST-01	PAGE	
		1 OF 3	
This document contains Standard Operating Procedures (SOPs) for: HVSB TESTS USING LABORATORY-SCALE TEST FACILITY (LSTF).			
RESPONSIBLE	No.	ACTIVITY (DESCRIPTION)	
EXPLOSIVE OPERATIONS			
Supervisor	01	Set up the test article:	
	02	Go to explosive Magazine in control room. Locate RP-81 detonators and remove one (1). Close magazine and install lock making sure it is safely locked.	
	03	Take detonator to the neighboring area designed to prepare mixtures.	
	04	Take a new 100 mL. bottle of 99.9% pure Nitromethane from solvent storage locker and place on operation table.	
	05	Take a new 25 mL. bottle of 99.95% pure diethylene-triamine (DETA) from the corrosive's storage locker and place on operation table.	
	06	Locate a clean 100 mL. glass graduated cylinder with 1mL. marks and place it on operation table and label "Sensitized NM."	
	07	Locate a clean 10 mL. glass graduated cylinder with 0.1mL marks and place it on operation table and label "DETA."	
	08	Locate 2 glass or plastic beakers (100 mL size) and place on operation table and label "Diluted Sensitized NM Waste" and "Diluted Solvent Waste."	
	09	Locate a 100 mL. Acetone bottle and place on operation table.	
	10	Locate a clean glass dropper and place on operation table.	
	11	Prepare Sensitized NM mixture:	

	12	Fill about 2/3 of the 10 mL. cylinder with DETA directly from DETA bottle.
	13	Pull in one full load of DETA into dropper by pressing the rubber suction cup; then inserting into DETA filled graduated Cylinder; then releasing the rubber suction cup.
	14	Calibrate dropper by counting drops required to fill 1 mL. of the 10 mL. cylinder. Repeat 3 times and take average. Record the number of drops required.
	15	Fill the 100 mL. graduated cylinder about 1/2 way with NM. Then add the number of drops of DETA required adding 1mL into the 100 mL. cylinder half filled with NM.
	16	Finish filling the cylinder with NM up to the 100 mL. mark. You now have 100 mL. of sensitized NM.
	17	Fill energetic driving package.
	18	Using the sensitized NM mixture. Fill up the assembled energetic component package. Care must be taken to prevent any bubbles from remaining inside. This can be visualized by inspecting through the clear lexan top. Shake carefully to loosen any bubbles trapped from surface tension.
	19	Seal energetic package.
	20	Use the 5 minute epoxy bottle to expose only a few drops. Apply these drops onto detonator body and insert onto energetic package until the detonator comes to a stop. Add additional epoxy to the edges outside the detonator.
	21	Wait 5 minutes to make sure the epoxy is fully cured.
Supervisor and Assistant	01	Set up LSTF:
	02	Place the sensitized NM filled energetic package inside the LSTF assembly.
	03	Fix the remainder LSTF components to LSTF as required.
	04	Place the LSTF inside the test chamber on top of the leveled base plate.
	05	Verify Connect end is shorted. Connect lead wire to detonator leads.
Assistant	01	Cover experimental set-up with homogeneous sand until top of LSTF

	02	Fill the test chamber with technical sand.
	03	Level sand surface with sand leveling tool.
	04	Install the chamber top-plate using the test cell hoist and ensure all bolts are installed.
Lab Engineer	01	Perform visual inspection of test cell, diagnostics, cameras,
	02	Check all personnel return to the control room.
	03	Inside the control room:
	04	Verify completion of site checklist, signatures of on-site personnel
	05	Roll Call.
	06	Verify 120AC is disconnected from the power outlet.
	07	Re-verify gates are closed and yellow lights are "ON"
	08	Verify all cell phones are off.
Firing Tech	01	Goes to wing wall, verifies safe/arm plug installed in safe socket
	02	Turn ON red lights at wing wall.
	03	Verify shunt is in place and if applicable connect firing leads to detonator.
	04	Remove shunt and connect connector to firing unit.
	05	Verify Firing Unit is "ON" position.
	06	Removes safe/arm plug from safe socket.

Author:	Felipe Garcia _____	Approved:	Prof. Jose O. Sinibaldi _____

C. POST-DETONATION OPERATIONS

	NAVAL POSTGRADUATE SCHOOL PHYSICS DEPARTMENT LABORATORY-SCALE TEST FACILITY PSEMC TEST SITE			
	DATE: OCTOBER-2009	ID #: NPS-ED-HVSB TEST-01	PAGE	
			1 OF 1	
This document contains Standard Operating Procedures (SOPs) for: HVSB TESTS USING LABORATORY-SCALE TEST FACILITY (LSTF).				

RESPONSIBLE	No.	ACTIVITY (DESCRIPTION)
POST-DETONATION OPERATIONS		
Firing Tech	01	Insert safe/arm plug in safety console arm socket - horn sounds.
	02	Plug-in 120 ac.
	03	Scan Road and verify is safe to proceed.
	04	Verify all equipment is set and triggers are ready.
	05	Start Countdown: 5, 4, 3, 2, 1, Fire.
Supervisor	01	Wait 5-10 minutes before sending anyone outside of the control room. Disconnect 120ac power from outlet.
	02	Check the list of Laboratory staff.
	03	During those 5-10 minutes, review test cell camera footage for any safety issues during and/or after intentional detonation event.
Lab Engineer	01	Check data collection.
Supervisor	01	Analysis of data.
Assistant	01	Clean up the cell (site) test using vacuum cleaner and broom.
Supervisor and Firing Tech	01	In case of a "Hang Fire," wait 20 minutes. Supervisor and Firing Tech assess the area.
	02	Disconnect 120 AC.
Author: Felipe Garcia _____		Approved: Prof. Jose O. Sinibaldi _____

THIS PAGE INTENTIONALLY LEFT BLANK

LIST OF REFERENCES

[1] AUTODYN TM Theory Manual Revision 4.3, Concord, CA: Century Dynamics, Inc., 2003.

[2] Defense and Veterans Brain Injury Center, 2009, Blast Injuries, http://www.dvbic.org/TBI---The-Military/Blast-Injuries.aspx (accessed November 6, 2009).

[3] M. Grujicic, B. Pandurangan, G. M. Mocko, S. T. Hung, B. A. Cheeseman, W. N. Roy, and R. R. Skaggs, "A combined multi-material euler/lagrange computational analysis of blast loading resulting from detonation of buried landmines," Department of Mechanical Engineering Clemson University, Clemson, SC 29634, Army Research Laboratory – Survivability Materials Branch Aberdeen, Proving Ground, MD 21005-5069.

[4] M. Grujicic, B. Pandurangan, I. Haque, B. A. Cheeseman, W. N. Roy, and R. R. Skaggs. "Computational analysis of mine blast on a commercial vehicle structure". Department of Mechanical Engineering Clemson University, Clemson SC 29634. Army Research Laboratory – Survivability Materials Branch Aberdeen, Proving Ground, MD 21005-5069.

[5] G. Serrano, "Potential utility of Nitromethane for explosive ordnance disposal," Master's thesis, Naval Postgraduate School, Monterey, CA, 2005.

[6] S.A. Sheffield, L.L. Davis, and R. Engelke, "Detonation Properties of Nitromethane, Deuterated Nitromethane and Bromonitromethane," Los Alamos National Laboratory, LA-UR-99-3283, 1999.

[7] V.S. Deshpande, R.M. McMeeking, H.N.G.Wadley, and A.G. Evans, "Constitutive model for predicting dynamic interactions between soil ejecta and structural panels," Department of Mechanical Engineering, University of California, Santa Barbara, CA 93106, USA Materials Department, University of California, Santa Barbara, CA 93106, USA cDepartment of Materials Science and Engineering, University of Virginia, Charlottesville, VA 22904, USA.

[8] Commercial Solvents Corporation, Storage and Handling of NITROMETHANE, NP Series, TDS No. 2, January 1961.

THIS PAGE INTENTIONALLY LEFT BLANK

INITIAL DISTRIBUTION LIST

1.   Defense Technical Information Center
      Ft. Belvoir, VA

2.   Dudley Knox Library
      Naval Postgraduate School
      Monterey, CA

3.   General Staff of the Mexican Navy
      Mexican Navy Headquarters
      México, DF
      México

4.   Centro de Estudios Superiores Navales
      Mexican Navy
      México, DF
      México

5.   Dr. Jose O. Sinibaldi
      Naval Postgraduate School
      Monterey, CA.

6.   Dr. Robert S. Hixson
      Naval Postgraduate School
      Monterey, CA